MASTER THESIS

DEVELOP AND IMPROVE MODELLING CAPABILITIES OF REACTOR VESSEL INTERNALS USING ANSYS

SAJEED DAFEDAR

(S2163225)

Faculty of Engineering and Technology

EXAMINATION COMMITTEE

Chairman:

Prof. Dr. Ir. Leo van Dongen

Chair of Maintenance Engineering

Department of Design, Production and Management

UT Supervisor:

Dr. Ir. Alberto Martinetti

Department of Design, Production and Management

UT External Member:

Dr. Ir. Peter Chemweno

Department of Design, Production and Management

Company Supervisors:

Ir. Ciska de Haan -de Wilde

Ir. Peter Baas

Asset Integrity Team

Nuclear Research and Consultancy Group (NRG)

Date: 15 December 2020

DPM 1761

NRG Nuclear. For life.

UNIVERSITY OF TWENTE.

Author:

Sajeed Dafedar

University of Twente

Student number: S2163225

Graduation Committee:

Prof. Dr. Ir. Leo van Dongen

University of Twente

Faculty of Engineering Technology (ET)

Department of Design, Production and Management

Dr. Ir. Alberto Martinetti

University of Twente

Faculty of Engineering Technology (ET)

Department of Design, Production and Management

Dr. Ir. Peter Chemweno

University of Twente

Faculty of Engineering Technology (ET)

Department of Design, Production and Management

Ir. Ciska de Haan - de Wilde

Nuclear Research and Consultancy Group

Manager Asset Integrity

Ir. Peter Baas

Nuclear Research and Consultancy Group

Consultant Asset Integrity

Acknowledgements

This report has been written to fulfil the graduation process of the master Mechanical Engineering at the University of Twente. This report presents the process and results of my graduation project, which I have executed for the company Nuclear Research and Consultancy Group (NRG).

I am thankful to the University of Twente and Nuclear Research and Consultancy Group for providing me with a challenging project. This thesis work would not have been possible without the help and encouragement of many people. First, I would like to convey my heartfelt thanks to my supervisor professor, Dr. Alberto Martinetti, who made this master assignment available to me and whose support, availability and willingness to provide feedback and help with questions helped me immensely during the entire span of my master thesis. Your support has been hull of my ship, protecting me from the waves and supporting me from shore to shore.

During the research, I have got to know this great company and many of its professional and inspiring employees. By working at NRG office at Petten and executing this research, I learned a lot about the nuclear subject, and how one of the best nuclear-based firms operates in the country. I want to express my sincere gratitude to this great company and all its employees who made me feel welcome and supported. I would especially like to thank Peter Baas and Ciska de Haan -de Wilde; they consistently showed me the direction throughout the thesis work. They helped me with their technical advice and insights on the nuclear process. I am thankful for their kind attention and support they gave, especially during my clueless period, to make this an enjoyable journey. Both their support and advice has been the rig and sails that have brought the ship forward.

I would like to thank the Maintenance Engineering and Operations department of the University of Twente and its chairman, Prof. dr. ir. Leo van Dongen who he has been one of the driving forces behind this research. I would also like to thank Dr. ir. Peter Chemweno for accepting to be the external member of UT graduation committee. As for my colleagues, Lorenzo Stefanini, Casper Versteylen, Luca Ratti, Antonio Graziano, and many others; I am sincerely grateful to all your help and support whenever I needed it, not just at work but also making it a lot enjoyable at the office.

Lastly, I want to express my deepest gratitude to my family and friends who have always believed in me. Their continued support is invaluable to me.

I hope you will enjoy reading this thesis.

Sajeed Dafedar

Abstract

Nuclear reactors present a unique challenge to researchers interested in building new ones or even just making existing reactors more efficient. By their very nature, it is challenging to observe what is happening in an operating reactor directly. Modelling and simulation provide the ability for scientists and engineers to understand what is happening in the reactor. Predictive simulations have always been one of the backbones of nuclear reactor safety. Being able to monitor the state of reactors while they are running at nominal conditions is hugely advantageous. The early detection of anomalies gives the possibility for the utilities to take proper actions before such problems lead to safety concerns or impact plant availability.

This thesis deals with developing and improving the modelling capabilities for simulations of the reactor vessel core. It was done in collaboration with Nuclear Research and Consultancy Group (NRG).

First, the thesis deals with improving the modelling capabilities of Pressurized Water Reactor (PWR) by considering transient thermal simulations. Transient analysis is an essential tool when designing nuclear reactors since they predict the behaviour of a reactor during changing conditions, such as a control-rod movement, induced by an operator, or an accident scenario. The approach to simulate the transient analysis was to find the start-up loading conditions of the pressurized water reactor and apply these as a loading conditions in ANSYS to get the thermal distribution in the reactor vessel. The applied start-up loading condition was supported by importing heat generation and reference temperatures. The verification of these transient thermal simulations was done based on the thermal heat capacity of the reactor. Later, the modelling capabilities of the SALIENT experiments, which is one of the supporting experiments of the “Dutch Molten-Salt Program” was to be improved. The current model of the SALIENT experiment was unable to find an accurate and stable solution in recent version of APDL due to highly distorted elements. Hence, specific hypotheses were carried out to improve the modelling capabilities for it to converge in latest APDL versions.

Improving the modelling capabilities of reactor pressure vessel will further help to efficiently use the reactor core and conduct research to develop new type of reactor. In the end, the thesis is concluded with a discussion, conclusion, and finally recommendations were given.

Disclaimer

During this thesis, the COVID-19 (Coronavirus) virus spread in the Netherlands, resulting in a closure of the NRG office at Petten. Due to the lockdown, the model in which the work was to be performed was not accessible for most of the period. Hence, the thesis assignment had to be slightly altered because there was no Virtual Private Network (VPN) access for personal computer, as the use of VPN is only for permanent employee of the company. ANSYS Student license from the University of Twente was used which limited the count of elements. Therefore, the results and conclusions from this report are limited.

Contents

Acknowledgements iii

Abstract iv

Disclaimer v

List of Figures ix

List of Tables x

List of Acronyms xi

1 Introduction 2
- 1.1 Introducing Company . . . 2
- 1.2 Work Process of the Company . . . 3
- 1.3 Problem Definition . . . 4
- 1.4 Thesis Motivation . . . 4
- 1.5 Research Objectives . . . 5
- 1.6 Research Question . . . 5
- 1.7 Thesis Outline . . . 5

2 Literature Review 7
- 2.1 Nuclear Energy . . . 7
  - 2.1.1 Basic Nuclear Principle . . . 7
- 2.2 Nuclear Reactor . . . 8
  - 2.2.1 Parts in the Nuclear Reactor . . . 9
  - 2.2.2 Types of Nuclear Reactor . . . 13
    - 2.2.2.1 High Flux Reactor (HFR) . . . 13
    - 2.2.2.2 Molten Salt Reactor (MSR) . . . 14
  - 2.2.3 Reactor Pressure Vessel (RPV) . . . 15
- 2.3 Theory for Pressurized Water Reactor . . . 17
  - 2.3.1 Laminar and Turbulent flow . . . 17
  - 2.3.2 Reynolds Number and Boundary layer . . . 18
  - 2.3.3 Conservation of Mass . . . 18
  - 2.3.4 Convective Heat Transfer . . . 19

2.4 Finite Element Method Software: ANSYS 20

3 Modelling and Thermal Analysis of the Pressurized Water Reactor 24
3.1 Model 25
3.2 Mesh 26
3.3 Material 31
3.4 Approach 32
3.5 Boundary Condition 33
3.6 Results 39
3.6.1 Result Validation 43

4 Convergence in SALIENT Experiment Model 45
4.1 SALIENT Experiment Model 45
4.2 Limitation in the current model 50
4.2.1 Requirements for the solution 52
4.3 Tried Hypothesis and Results to Solve for Convergence 53
4.3.1 Manual Mesh Rezoning 54
4.3.2 Mesh Adaptability 59
4.3.3 Transient Analysis 61
4.3.4 Element type PLANE222 63

5 Discussion 65
5.1 Modelling and thermal analysis of the PWR 65
5.2 Convergence in SALIENT Experiment Model 65

6 Conclusions and recommendations 68
6.1 Conclusions 68
6.2 Recommendations 69
6.2.1 Recommendations based on literature 69

Bibliography 70

Appendices

A Snippet Code 76

B Pressurized Water Reactor (PWR) 77

C Small Portion of Code for Manual Mesh Rezoning 79

List of Figures

1.1 High Flux Reactor In Petten . . . 3
1.2 Work Process of AIS Department . . . 3
1.3 Thesis Report Workflow . . . 6

2.1 Nuclear Fission Process . . . 8
2.2 Nuclear Fuel Cycle . . . 10
2.3 Fuel Assembly . . . 11
2.4 Moderator Slowing Neutron to Create more Fission Events . . . 11
2.5 Schematic showing the change of power output about the position of control rod . . . 12
2.6 Containment Building . . . 13
2.7 Isometric View of Petten High Flux Reactor . . . 14
2.8 Reactor Pressure Vessel Internals . . . 15
2.9 Coolant Flow Path in the reactor pressure vessel . . . 17
2.10 Laminar Flow . . . 18
2.11 Turbulent Flow . . . 18
2.12 Sketch of mass flow through area A in a flow field . . . 19

3.1 Initial Design Methodology . . . 25
3.2 Geometry of RPV . . . 25
3.3 Nodes in SOLID90 Element . . . 27
3.4 Common types of Meshing . . . 27
3.5 Mesh: Core Barrel . . . 28
3.6 Mesh: Baffle . . . 29
3.7 Mesh: Former . . . 29
3.8 Mesh: M12 Bolt . . . 30
3.9 Mesh for the Geometry . . . 30
3.10 Approach to Model . . . 32
3.11 Thermal Boundary Conditions . . . 33
3.12 Part of 3D ASCII table in excel . . . 34
3.13 Imported Heat Generation . . . 35
3.14 PWR Start-Up Condition Graph . . . 35
3.15 PWR Start-Up condition in ANSYS Tabular Data . . . 36
3.16 Convection Boundary on Core Barrel . . . 37
3.17 Temperature as a function of time and height boundary condition for baffle . . . 38

3.18 Representation of boundary condition for baffle . . . 38
3.19 Temperature Distribution of the Model . . . 39
3.20 Temperature distribution of formers . . . 40
3.21 Temperature distribution of Core Barrel . . . 40
3.22 Temperature distribution of baffle . . . 41
3.23 Temperature distribution of bolts . . . 41
3.24 Maximum temperature distribution in a single bolt. . . . 42

4.1 Three main configurations for in-core irradiation channel at the HFR . . . 46
4.2 TRIO-131 set up in the in-core facility for the experiment . . . 46
4.3 SALIENT-03 experiment setup design . . . 47
4.4 Transverse model of SALIENT-03 experiment . . . 48
4.5 Position of Gas Gaps . . . 49
4.6 1/3rd of the whole model . . . 50
4.7 PLANE223 Element . . . 51
4.8 Mid-side PLANE223 nodes: a) Aligned b) misaligned (highly distorted) during analysis in higher version of APDL . . . 52
4.9 A converged solution in ANSYS APDL V14 using PLANE223 . . . 53
4.10 Not converged solution in ANSYS APDL V20 using PLANE223 . . . 54
4.11 The time point where the solution does not converge in higher version of ANSYS APDL 55
4.12 The time and temperature value at the point of not converged solution in higher version of APDL . . . 55
4.13 Iteration time, and convergence after rezoning . . . 56
4.14 Partial convergence plot at TIME=0.706 . . . 56
4.15 A solid model containing gas gaps in between . . . 57
4.16 Not converged results of the model before manual mesh rezoning . . . 58
4.17 Converged solid model after rezoning in higher version of APDL with gas gaps . . . 58
4.18 Initial mesh during analysis . . . 59
4.19 Final mesh after rezoning . . . 59
4.20 2D Geometry in workbench . . . 60
4.21 Converged solution in workbench . . . 61
4.22 Contact in between elements . . . 62
4.23 The converged solution of transient analysis of SALIENT-03 model in APDL V20 . . . 62
4.24 PLANE222 element type . . . 63
4.25 The converged solution in V20 just by changing from PLANE223 to PLANE222 . . . 64

A.1 Snippet code for height, time, and temperature . . . 76

B.1 Pressurised Water Reactor . . . 78

C.1 Portion of Mechanical APDL code . . . 79

List of Tables

3.1 Parameters for the PWR 26
3.2 Mesh Details 31
3.3 Temperature-dependent properties of AISI 347 31
3.4 Temperature-dependent properties of AISI 316Ti 32
3.5 Thermal Boundary Conditions 33

List of Acronyms

NRG	Nuclear Research and Consultancy Group
GWe	Gigawatt electrical
IEA	International Energy Agency
GFR	Gas-cooled Fast Reactor
HFR	High Flux Reactor
MW	Megawatt
AIS	Asset Integrity Service
FEM	Finite Element Method
CFD	Computational Fluid Dynamics
RPV	Reactor Pressure Vessel
MSR	Molten Salt Reactor
CS	Consultancy and Services
PWR	Pressurized Water Reactor
APDL	ANSYS Parametric Design Language
FEA	Finite Element Analysis
ASME	American Society of Mechanical Engineering
NQA-1	Nuclear Quality Assurance - 1
ISO-9001	International Organization for Standardization
ANSI	American National Standards Institute
NRC	Nuclear Regulatory Commission
DOF	Degrees of Freedom
AISI 347	American Iron and Steel Institute

KTA Kerntechnischer Ausschuss

DIN Deutsches Institut für Normung

HTC Heat Transfer Coefficient

MCNP Monte Carlo N-Particle Transport Code

RCS Reactor Coolant System

ASCII American Standard Code for Information Interchange

NSSS Nuclear Steam Supply System

JRC Joint Research Centre

“Now I know what the atom looks like”

- Ernest Rutherford

(1871-1937)

Chapter 1

Introduction

The theory of the atom started many centuries ago. However, we only latterly began to understand the immense power incorporated in the tiny mass. The first nuclear chain reaction occurred at the University of Chicago in 1942. During the 1940s the atomic research was primarily focused on developing defence weapons. Later, atomic energy was used in the generation of electricity. Recently nuclear power is applied to medical and other industrial purposes [1].

Today there are around 440 nuclear power reactors. Most of them generate a combined electricity of 400 Gigawatt electrical (GWe). According to the International Energy Agency (IEA), nuclear energy has a growth of 15 percent from 2018 to 2040 [2]. Nuclear power is currently a sustainable energy source, and therefore, a nuclear reactor is becoming increasingly important [3].

In the nuclear industry, scientific knowledge and technology are continually developing. Nuclear reactors are classified into four series of generation: I, II, III+, which are currently existing ones, and IV for the future ones. The IV generation nuclear plants are expected to be made known into the market in about 25 years. The future reactors will concentrate on sustainability, safety and reliability and economy. Some of the future reactor under study are Gas-cooled Fast Reactor (GFR), which uses gases like helium to cool the reactor [4].

1.1 Introducing Company

NRG was started in the 1960s as a research centre to explore the future of nuclear technologies. NRG is the global market leader in the supply of medical isotopes and focuses on the development of new uses of medical isotopes to treat life-threatening diseases. NRG also provides services in the field of radiation protection, provides consultation in the area of reliability and safety of a nuclear installation, and also performs nuclear technological research [5].For nuclear research, a High Flux Reactor (HFR) was built in 1961. The High Flux Reactor (HFR) in Petten is one of the most robust beneficial material testing reactors in the world. HFR in Petten is a light water-cooled and moderate reactor operated at 45 Megawatt (MW) [6]. The reactor is the property of the European Commission and operated by NRG. Besides the nuclear energy research centre, it is also used for different commercial applications like the production of medical radio-isotopes for the treatment of cancer. The medical radio-isotopes that are produced by the HFR are used to treat more than 30.000 patients every day [7]. The 60-year-old HFR in Petten is expected to remain functional until 2024 when it is replaced by a new high flux reactor

(Pallas) in Petten [8].

Figure 1.1: High Flux Reactor In Petten [9]

1.2 Work Process of the Company

Different departments are working together in NRG. Before continuing with the explanation of the company work process, It must be mentioned that the scope of this project is related to the Asset Integrity Service (AIS) team at NRG. Hence, Other department's work process is neglected. In Figure 1.2 the work process of the department is shown.

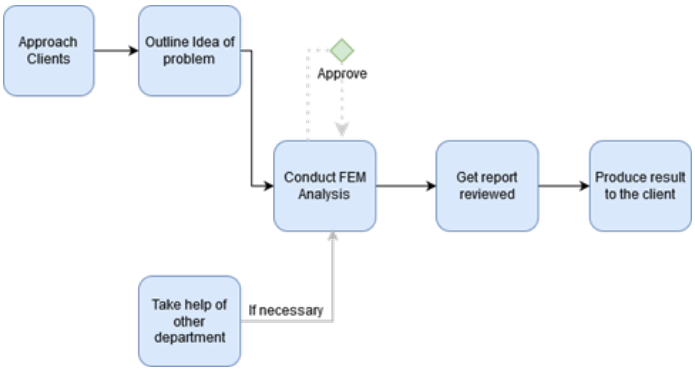

Figure 1.2: Work Process of AIS Department

The process starts as soon as the client approaches the problem related to thermo-mechanical. The outline of the issues like input data or constraints are noted. Later the problem is solved using the Finite Element Method (FEM). Simultaneously, other departments like Computational Fluid Dynamics (CFD) or Material are integrated if necessary, for assessing the problem. Finally, the result obtained by analysis is written down as a report and reviewed and approved by the manager, and is handed over to the client.

1.3 Problem Definition

A key challenge of nuclear reactor design and analysis is the system complexity, which arises from a wide range of multi-physics phenomena being important across multiple length scales. In recent years, a modelling approach for reactor internals has been developed within NRG to create models for the assessment of the Reactor Pressure Vessel (RPV). Along with reactor pressure vessel internals, several models based on Molten Salt Reactor (MSR) are also being analysed by Asset integrity team of the Consultancy and Services (CS) unit of NRG. These models are complex and highly interdisciplinary. It is typical in the nuclear industry to perform simulations mirroring the current state of the plant, and to simulate the future behaviour of the reactor. With this goal, NRG always tends to improve their modelling capabilities every year to achieve accurate nuclear plant calculation results. With the help of these accurate calculations, better service can be provided to the end-user. At NRG improving the model may include several phenomena like core physics, thermo-mechanical analysis, fuel thermal performance, chemistry, structural integrity, and physical or mesh quality of the model. In this assignment, the modelling capabilities of the Pressurized Water Reactor (PWR) and MSR at NRG are to be improved while including phenomena like mesh quality, thermal analysis, and convergence of model.

1.4 Thesis Motivation

A reactor core in a nuclear power plant is the crucial part as the hot source with radioactivity nuclear fuel, which possesses security risks and economic potential. Incapacity of a nuclear power plant to carry out desired control of its core can result in either higher operating costs or a reduction in system security and reliability, and the implementation of desirable control for the core can improve security and effectiveness of the nuclear power plant. The reactor is readily affected by a flow-induced thermal distribution that can cause the component inside the reactor to fail due to high temperatures. Hence, it is necessary to predict converged temperature distribution result in the nuclear core so that analysis such as thermo-mechanical stress can be done based on these predicted result. Over the decades, continuous work has been devoted to research and to make the nuclear plant calculations accurate. However, it is challenging to observe what is happening in an operating reactor directly. Hence, improvement in modelling and simulation provides the ability to not only understand what is happening but how it is happening in those environments and to predict results.

1.5 Research Objectives

This thesis is aimed at understanding the concept and process of nuclear energy and nuclear reactors. With this concept, a thermal distribution in the reactor pressure vessel and convergence of the experiment model is studied. The overall thesis objective is summarized in the following statement:

To develop and improve the modelling capabilities of reactor pressure vessel internals by using ANSYS.

1.6 Research Question

The research objective is achieved by framing the research question with several sub research questions. They are formulated as:

1. How to improve the modelling capabilities of reactor pressure vessel internals using Ansys?.
    - How can the solid model be created in a refined way using Ansys?
    - How is the transient thermal condition applied to a real-life pressurized water reactor?
    - How to validate the results of transient thermal with real-life pressurized water reactor?
    - How to solve the convergence issue of highly deformed elements using a higher version of Ansys?
    - How solving the solution convergence of highly distorted elements will help to improve the model?

1.7 Thesis Outline

This thesis project aims to provide the readers with the overview of thermal distribution in the reactor pressure vessel and convergence of the solution during analysis. The technical feasibility is demonstrated with a workflow illustrated in figure 1.3

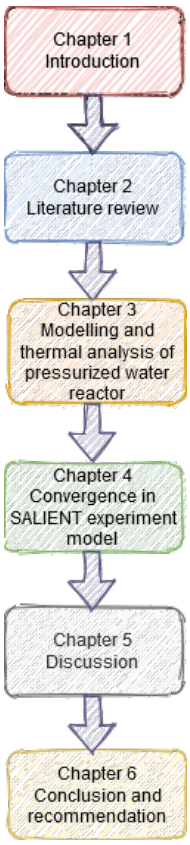

Figure 1.3: Thesis Report Workflow

- **Chapter 1: Introduction**
  This chapter describes the company where the thesis is done, the work process of the company, problem definition, thesis motivation, research objective and research questions are framed.
- **Chapter 2: Literature review**
  This chapter describes all the relevant literature to a nuclear reactor and nuclear energy.
- **Chapter 3: Modelling and thermal analysis of a pressurized water reactor**
  This chapter describes the reactor pressure vessel internals of the a nuclear plant and describes the thermal transient analysis and temperature distribution overview.
- **Chapter 4: Convergence in SALIENT experiment model**
  This chapter describes the SALIENT experiments conducted in the reactor and the convergence issue with the experimental model in higher version of ANSYS Parametric Design Language (APDL).
- **Chapter 5: Discussion**
  This chapter discusses the outcomes of the results got by the previous chapters
- **Chapter 6: Conclusion and recommendation**
  It is the final chapter with reports the conclusion and recommendation for future work.

Chapter 2

Literature Review

This chapter comprises of all fundamental theory and literature which will be later used in the consecutive chapters. It begins with a review of nuclear energy with basic nuclear principle and continues with the nuclear reactor and parts in a nuclear reactor. Types of the nuclear reactor and reactor pressure vessel are discussed briefly. Later some theory and formulas for PWR are described, and at last, some literature on ANSYS is defined.

2.1 Nuclear Energy

2.1.1 Basic Nuclear Principle

Atoms are constructed as a scale-down solar system. At the centre of the atom is the nucleus. Revolving around the nucleus are the electrons. The nucleus is composed of protons and neutrons, that are densely packed collectively [10]. Many elements occur in nature with a mixture of isotopes. Most of the component found in nature are stable, but a lot, counting Uranium 238 (^{238}U) are not stable; hence they are called radioactive elements [11]. Nuclear energy is determined by how it propagates. Nuclear power is produced by radioactive decay, fission, and fusion. Radioactive decay occurs naturally by breaking down of unstable atoms over a long period [12]. Energy is produced in a nuclear power plant when highly unstable nuclei, for example, if a ^{235}U nucleus consumes an extra neutron, it undergoes nuclear fission and splits into two or more fragments with gamma (γ) radiation as seen in Figure 2.1.The neutrons produced in a fission process are absorbed by other ^{235}U nucleus, and the process can continue in self-sustaining chain reaction depending on the quantity of uranium fuel left [11]. Majority of the commercial nuclear plants today use nuclear fission process to generate energy, whereas combining two fragments of nuclei to form a massive core (nuclear fusion) is still under research.

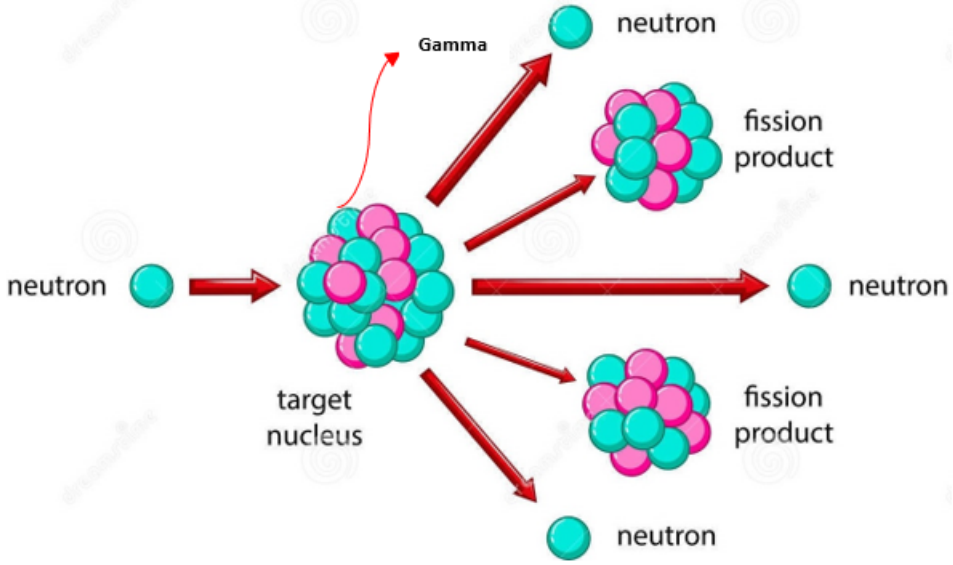

Figure 2.1: Nuclear Fission Process [13]

2.2 Nuclear Reactor

A nuclear power plant is an industrial site that generates electricity from thermal energy produced by the nuclear fission chain reaction in the vessel of a nuclear reactor [14]. A nuclear reactor is the heart of the nuclear power plant which contains nuclear fuel and has systems to start and stop the nuclear reaction in a controlled manner. The nuclear reactor generated electricity for the first time in September 1948 at X-10 Graphite reactor in Oak Ridge [15]. Nuclear plant act in a similar manner to a conventional coal plant, in which the coal is burnt to boil the water and produce steam and then drive the turbine to produce electricity. The only difference from the conventional power plant is that nuclear plant uses fission as a source of heat [11].

The nuclear reactor is directed by the splitting of atoms (fission) where a neutron is fired at the atom which releases additional neutrons. The fission process with neutrons can be summed up as follows:

$$^{235}U + n(\rightarrow)Fissionproduct + vn$$

For each neutron absorbed by the atom, on the even out approximately 2.5 (v=2.5) neutrons are released. The new neutrons can be used to bombard other ^{235}U nuclei leading to release of more neutron, forming a nuclear chain reacting system [16]. The fissioning of the atom in the chain reaction releases a large measure of kinetic energy as heat. This heat is used to generate steam to drive the turbine and to produce electricity. The generated heat in the reactor is kept in check by moving coolant, typically water. To establish the nuclear reaction takes place at the accurate speed, the nuclear plant has a system that quicken, stops, or slows down the heat produced by the nuclear reaction [17]. This process is ordinarily done by using control rods which are made from material such as cadmium,

hafnium, or boron.

$$E = mc^2 \tag{2.1}$$

In equation (2.1),E is energy, m is the mass of an atom, and c is the speed of light. This equation depicts the basic idea behind nuclear power as there are billions of atoms in a tiny amount of matter which can be converted into lots of energy [18].

In nature, just making something scorching by itself is not helpful to produce electricity. The absolute ultimate measure of energy that can be derived from a temperature difference is given by the Carnot equation [19].

$$Efficiency = \frac{T_H - T_C}{T_H} \tag{2.2}$$

In this equation, T_C is the absolute temperature of the cold side, T_H is the hot side. We can soon see that if the cold-side temperature were zero, the efficiency would be 1, engineer express for ideal conditions. Unfortunately, that temperature is absolute - We would need to make the cold side colder than the temperature of exterior space. On earth we can only certainly hope to cool object down to a slight over room temperature; 300 K. This essentially hinders the efficiency of a thermal, and we want that hot end of the engine to become as hot as possible to get the most electricity out of the heat. Equation (2.2) can be applied to calculate efficiency of the nuclear power plant, which has pressurised water at 325 ^oC. Heat transferred is a complex system in the reactor, producing steam which is used to drive the generator. At some point, the water is at 27 ^oC and then heated to have a maximum theoretical efficiency of 49.8 percent. On an average, a typical nuclear power plant actual efficiency is about 35 percent [20].

2.2.1 Parts in the Nuclear Reactor

There are several components familiar to most types of reactor:

1. Fuel
2. Moderator
3. Control Rods
4. Coolant
5. Turbines
6. Generator
7. Containment

These components will be explained in detail as follows:

1. **Fuel**
   The fissionable material used in the reactor to produce heat to power turbine is called as fuel. Low -Enriched Uranium (U-238, U-235) is the most used fuel in reactors because of its high melting point, but few reactors use Plutonium (Pu-236) and Thorium (Th-232) [15].

Uranium is one of the least sufficient minerals in the earth's crust, but because of its radioactivity, it is a plentiful supply of energy. One pound of uranium has as much energy as three million pounds of coal. Uranium has a half-life of 4.5 billion years where it gradually decays and drops its radioactivity. Uranium is found in several geological formations, as well as seawater. To be mined as a fuel, however, it must be adequately concentrated, making up at least one hundred parts per million (0.01 per cent) of the rock it is in. The mining process is like coal mining, with both open pit and underground mines. Once mined, the uranium ore is dispatched to a processing plant to be concentrated into usable fuel. Most uranium concentrate is made by leaching the uranium from the ore with acids. When completed, the uranium ore is turned into UO_2, the fuel form of uranium, and shaped into small pellets. After being used in the reactor, it can be cautiously waste deposited, or a part can be reprocessed [10].

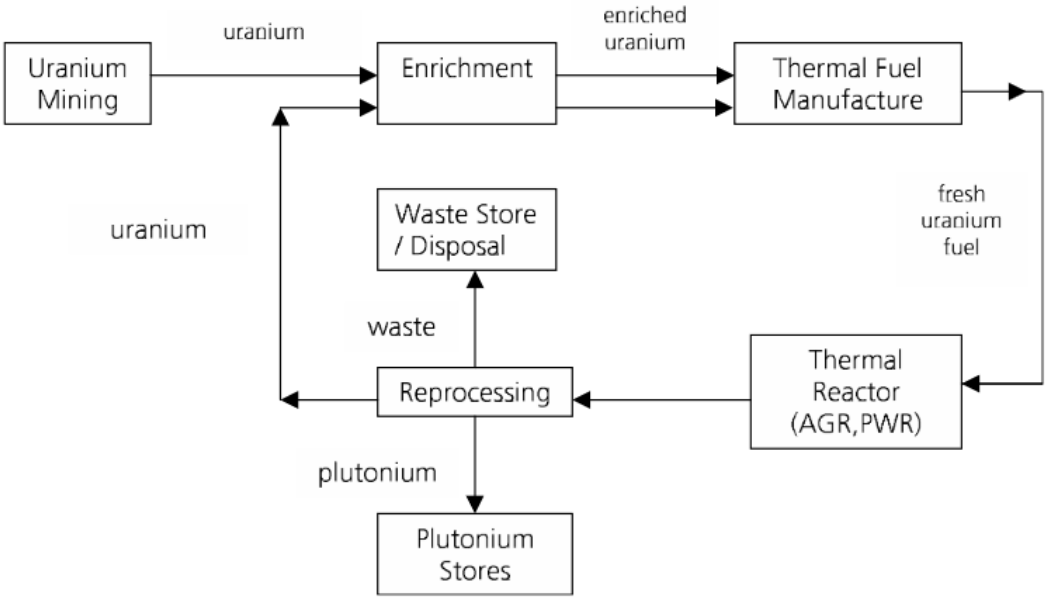

Figure 2.2: Nuclear Fuel Cycle

How is the fuel set up in the reactor? The fuel must be held in a powerful physical form adequate to sustain high operating temperature and an excessive radiation surrounding. Fuel framework needs to preserve its shape and integrity for several years. The reactors use uranium fuel in the form of uranium dioxide (UO_2). This UO_2 is pressed into pellets; these pellets are sintered into the thin-walled metal tube called cladding, as shown in figure 2.3. The cladding is then loaded and encapsulated in the fuel rod, which is made of zirconium alloy. The set of fuel rod are bundled together and is known as fuel assembly (figure 2.3) [21].

The space between pellet and cladding is filled with helium gas to boost the conduction of heat. Generally, the fuel assembly is about 4-metre-long and 25 cm wide, and about 179-264 fuel rods are placed in each fuel assembly. A typical nuclear reactor contains 157 fuel assemblies and energy for approximately four years of operation at full power [21]. The control rods are directly inserted into fuel assembly through the top.

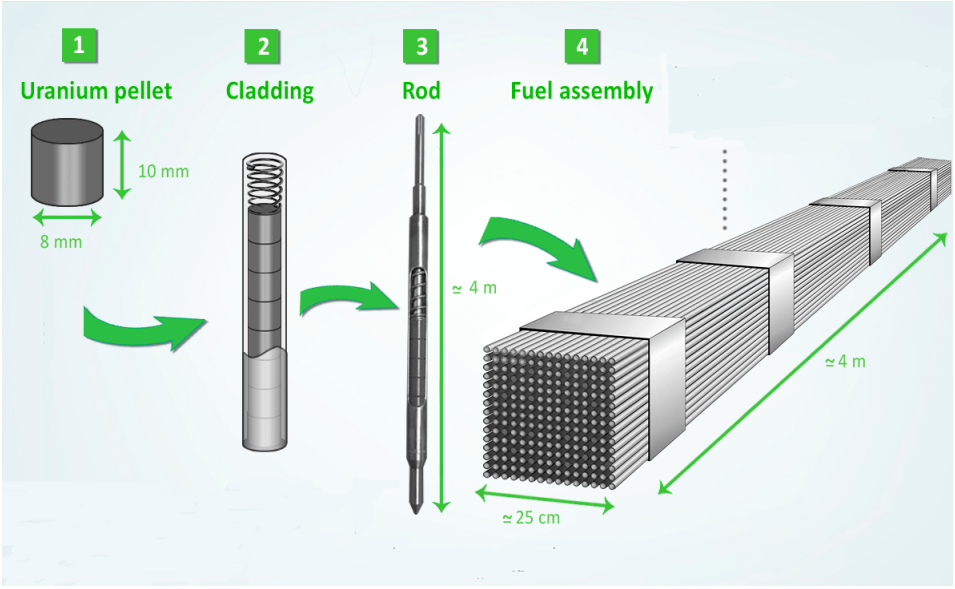

Figure 2.3: Fuel Assembly [22]

2. **Moderator**

   Moderator is the type of component in the core which slows down the fast neutrons discharged from fission so they can be more efficient in a fission chain reaction. Decelerate of this neutron will allow them to be readily consumed by other fissile nuclei, producing more fission events [23].

   The moderator should be able to slow down neutron speed while keeping a low neutron absorption cross-section. For this reason, most of the nuclear reactor tend to use light water (H_2O) as moderator because of its abundance and low-price. Heavy water (D_2O) and Graphite are also used as a moderator in some reactors [23].

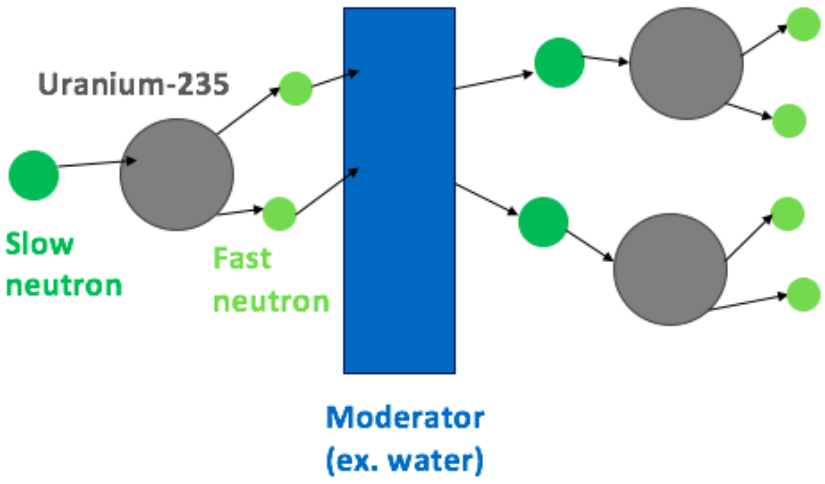

Figure 2.4: Moderator Slowing Neutron to Create more Fission Events [24]

3. **Control Rods**
   Control rod is an equipment that is used to consume neutrons so that the nuclear chain reaction taking place inside the core can be slowed down or stopped absolutely by injecting the rod ultimately or accelerated by pulling out slightly. On an average, 2.5 neutrons are released in fission of U-235, but only one neutron is adequate to continue the nuclear chain reaction at steady state. The control rod contains cadmium or boron material which absorbs these extra neutrons and can be used to alter the power output of the reactor [25].

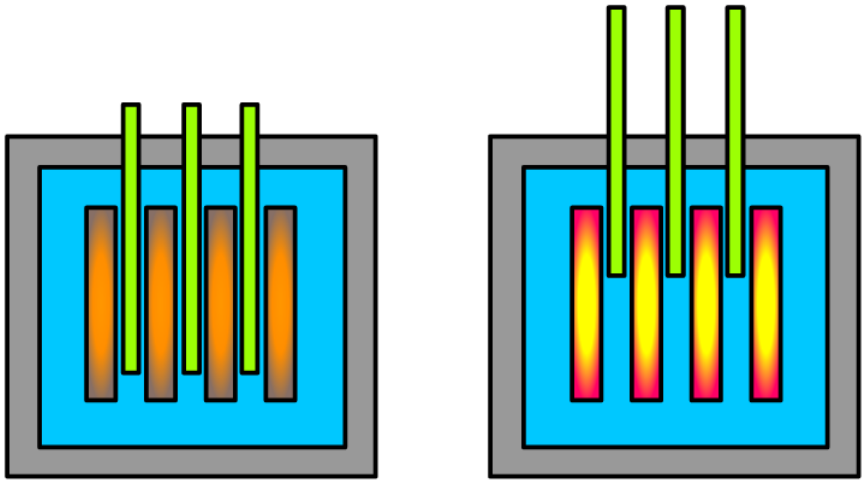

Figure 2.5: Schematic showing the change of power output about the position of control rod [26]

   When inserted in standard amount, control rod position is at critical, and the power output remains equal. In Figure 2.5 On the left, the control rods (shown in green) are inserted more than usual, reducing the number of neutrons which in turn reduces the power output of the reactor, and the reactor is below critical. On the right, the control rods are inserted less than usual, increasing the power output, and the system is beyond criticality [26].

4. **Coolant**
   Coolant extracts the heat from the fuel element in the reactor core and transfers it to the steam generator where the heat exchange process occurs. Later, steam is used to generate electricity in the power plant. A suitable coolant must be chemically stable, and it should not interfere with or be affected by the nuclear chain reaction. Light water (H_2O), carbon dioxide gas or liquid sodium are typically used as a coolant in the reactor. The advantage of using light water (H_2O) as a coolant in a reactor is that it can act both as a moderator and coolant simultaneously [27].

5. **Turbines**
   Steam produced in the boiler is passed to a turbine. The force of the steam makes the turbine to rotate converting heat energy into mechanical energy.

6. **Generator**
   The generator converts the kinetic energy of the turbine into electric energy. The turbine moves and causes change in magnetic flux which generates electricity. This electricity is later transmitted to electricity house or power lines [28] [15].

7. **Containment**
   Containment is a construction which surrounds the reactor pressure vessel. It is designed to protect reactor pressure vessel from surrounding interference and to protect outsides from the effects of radiation during a malfunction. It is a structure which is built with a metre-thick concrete and steel [29]. It is the dome structure that can be seen by a person from far in a nuclear facility, as seen in Figure 2.6.

Figure 2.6: Containment Building [30]

2.2.2 Types of Nuclear Reactor

There are many types of reactors based on different usage, but for this section, we can consider High Flux Reactor (HFR), and Molten Salt Reactor (MSR) briefly.

2.2.2.1 High Flux Reactor (HFR)

The HFR is a research reactor in Petten, the Netherlands. The design was based on the Oak Ridge research reactor in the United States of America. Development was contracted to the American Car and Foundry, Inc. Work commenced on 27 August 1957 and ended with the HFR's first criticality on 11 November 1961 [31]. HFR in Petten (operated by NRG) is one of the most dynamic multi-purpose research reactors which can be used for many experiments like fissile material testing, structural material testing, radioisotopes production, and training and education. HFR focused on the production of radioisotopes during last decade. Today HFR in Petten produces 20-25 percent of total world radioisotope medicine [32]. Isometric view of the HFR building in Petten is shown in Figure 2.7.

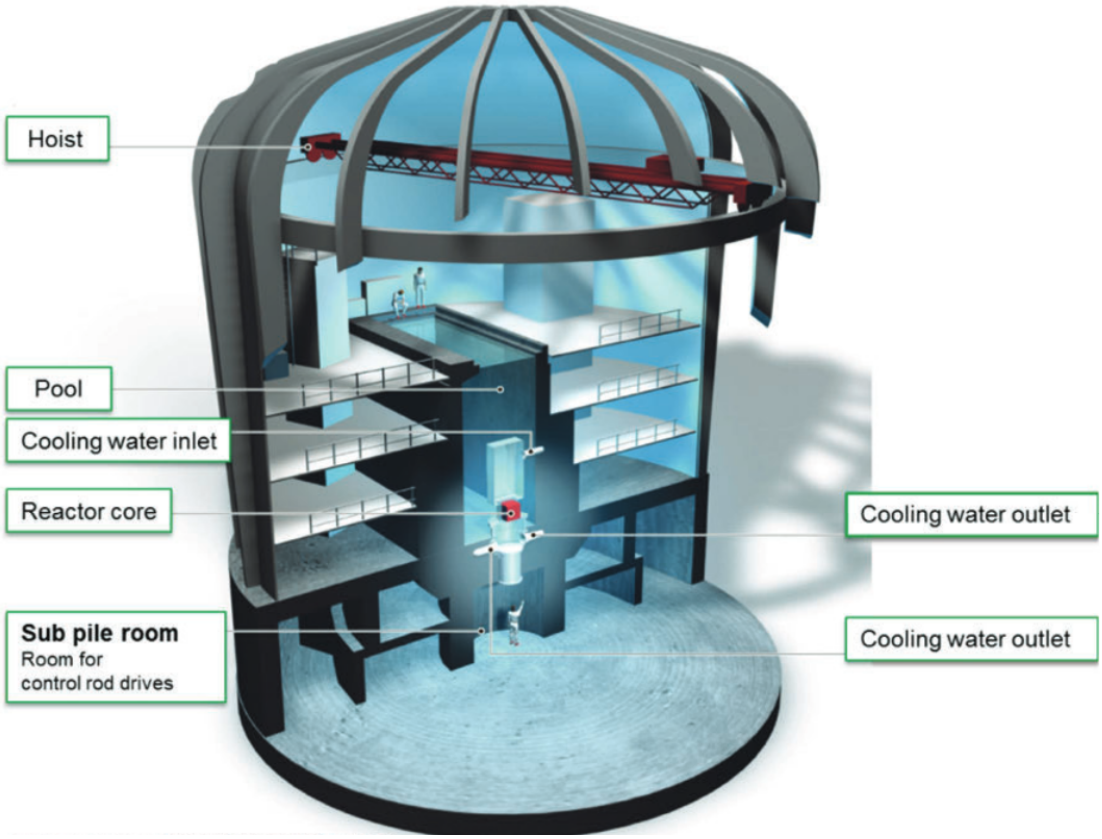

Figure 2.7: Isometric View of Petten High Flux Reactor [33] [34]

The HFR is light water cooled and moderated tank-in-pool type research reactor. The reactor core is housed in a sealed tank, which simultaneously with the circulation pumps and the heat exchangers forms the primary circuit. The reactor tank is immersed into a deep water-filled pool with thick concrete walls. The pool is covered with an aluminium liner. Low-enriched uranium is used as fuel. The regular operating thermal power of HFR is 45 MW [31]. The primary coolant's inlet and outlet temperature is 45 ^oC and 55 ^oC, respectively and the reactor is operated for more than 280 days/year [31].

2.2.2.2 Molten Salt Reactor (MSR)

The molten salt reactor is a class of nuclear fission reactor in which the primary nuclear reactor coolant is the salt which is heated above its melting mark to be as a fluid. Instead of fuel rod assembly like in the other types of reactors, MSR has fuel/fissile material dissolved and mixed in this molten salt. The salts used as primary coolant, are usually fluoride salts like lithium-beryllium fluoride and lithium fluoride, which remain liquid without pressurization. The fuel is a molten mix of lithium and beryllium fluoride (FLiBe) salts with dissolved low-enriched uranium (U-235 or U-233) fluorides (UF_4). The fuel flows around the graphite moderator which decelerates down the neutrons to support the reaction. This type of reactor has many advantages, but due to also technical research and development lag, MSR has not been commercialised [35].

2.2.3 Reactor Pressure Vessel (RPV)

The reactor pressure vessel is the pressure vessel enclosing reactor core, coolant, and other essential reactor internals. The RPV is designed to withstand high pressure. It is a structure placed inside the Containment and represents the first line of defence against a release of radiation in case of an accident [36]. A typically designed reactor pressure vessel is shown in the Figure 2.8

The RPV is cylindrical with a hemispherical bottom head, flanged and gasketed upper head. The bottom head is fused to the cylindrical shell while the top head is bolted to the cylindrical shell via the flanges. The top head is portable to allow for the refuelling of the reactor during prepared outages [36].

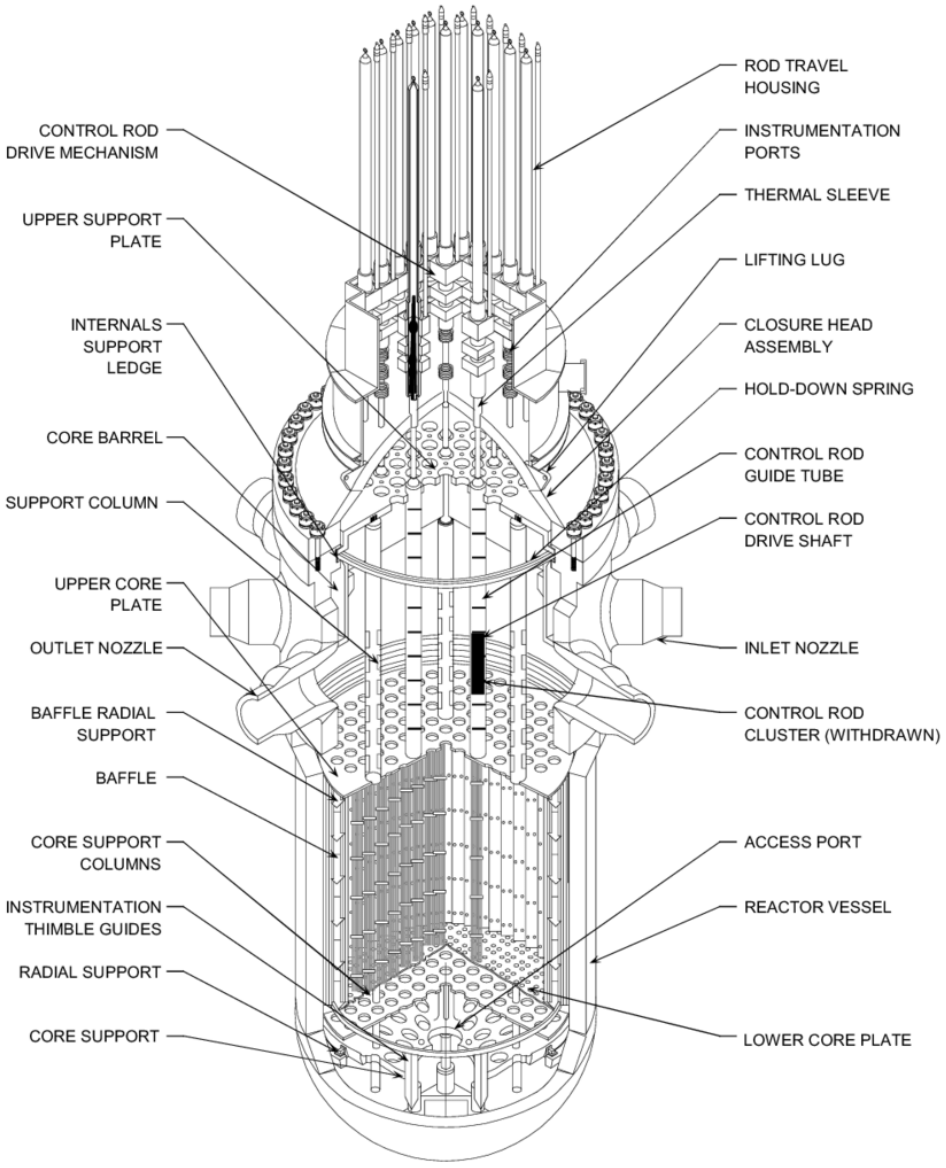

Figure 2.8: Reactor Pressure Vessel Internals [37]

There are one inlet (or cold leg) nozzle and one outlet (or hot leg) nozzle for each reactor coolant loop. The reactor coolant enters the reactor vessel at the inlet nozzle. It goes out the reactor from the upper region, where it is transmitted out the outlet nozzle into the hot leg of the primary circuit and travels on to the steam generator. The primary circuit of regular PWR is divided into four independent loops, each loop involves a steam generator and one coolant pump but can vary according to particular reactor design. Therefore, large inlet and outlet nozzles, as well as control rod drive tubes and instrumentation and safety injection nozzles penetrate the cylindrical shell. The total inlet and outlet nozzles is a function of the number of loops [38]. The RPV internal has a support assembly to tolerate the force due to weight, fuel assembly, control rods, vibration, and earthquake.

The support assembly is partitioned into lower core support and upper core support structures. The lead restraining and support member of the reactor internals is the lower core support structure, consisting of core baffle, the lower core plate, the thermal shield plates, the triangular fashioned core as seen in the figure 2.8. These support members are welded to the bottom head and the core support ring. Within the core-barrel are the axial baffles, which are secured to the core barrel wall and form the cage periphery of the assembled core. The lower core plate is located at the bottom level of the core below the baffle plates and provides support and orientation for the fuel assemblies and vertical downward load from the weight. The Bottom core plate is punctured and contains the locating pins for the fuel assemblies. The upper part support assembly consists of the upper support plate, upper core plate, support columns, and guide tube assemblies as seen in the figure 2.8. Similarly, support columns provide the spacing between the upper support plate, middle support plates and the upper core plate. The guide tube assemblies cover and guide the control rod drive shafts and control rods [39].

The flow path for the reactor coolant through the reactor vessel is shown in Figure 2.9.

The comparatively low temperature coolant enters the reactor vessel through the inlet nozzle and hits against the core barrel (shown in blue arrow). The core barrel drives the water to stream downward in the area between the reactor vessel wall and the core barrel; this area is usually recognised as the downcomer. From the bottom of the pressure vessel, the flow is overturned up through the core to pass through the fuel assemblies, where the coolant temperature rises as it passes through the fuel rods. Finally, the hotter coolant (shown in red arrow) enters the upper internal region, where it is routed out through the outlet nozzle and goes on to the steam generators. The body of the vessel is of low-alloy carbon steel. Surfaces with coolant contact are clad using 3 - 10 mm austenitic stainless steel to minimize corrosion [40].

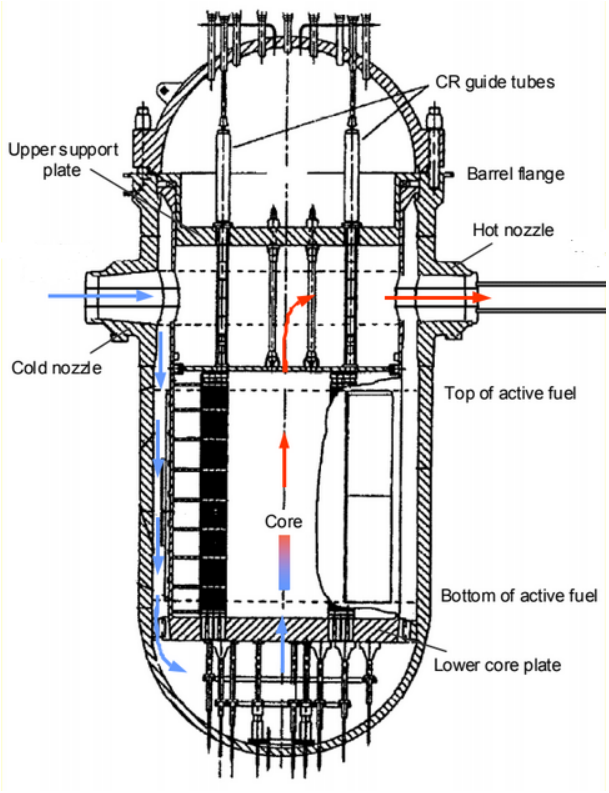

Figure 2.9: Coolant Flow Path in the reactor pressure vessel [37]

2.3 Theory for Pressurized Water Reactor

This section discusses some basic laws and constitutive equations which are relevant to the study of the pressurized water reactor.

2.3.1 Laminar and Turbulent flow

In fluid dynamics, laminar flow is described by smooth ordinary paths of molecules of the fluid. When a flow is laminar, the fluid flows in parallel layers, with no interruption between the layers. Therefore, laminar flow is also cited as a streamline or viscous flow. Turbulent flow is identified by the jerky movement of particles of the fluid. In turbulent flow, the lateral mixing is large, and there is a disruption between the fluid layers. In a turbulent flow, the acceleration of the fluid at a fixed point is continuously changing in magnitude and direction. The type of flow is influential in nuclear reactor channel to predict the heat removal capacity of coolant by considering the contact time and mass transfer of the coolant to the nuclear fuel assembly [41].

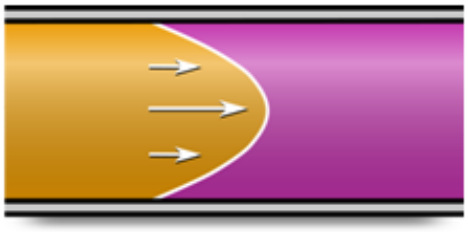

Figure 2.10: Laminar Flow [42]

Figure 2.11: Turbulent Flow [43]

2.3.2 Reynolds Number and Boundary layer

The Reynolds number is the ratio of inertial forces to viscous forces. The Reynolds number is a dimensionless number used to classify the fluids systems in which the effect of viscosity is necessary for handling the velocities or the flow pattern of a fluid. Mathematically, the Reynolds number, NRe, is represented as

$$N_{Re} = \frac{\rho v d}{\mu} \tag{2.3}$$

Where ρ is the density, v is the velocity, d is the diameter, and μ is the viscosity. The Reynolds number is utilized to determine whether the fluid is in a laminar or turbulent flow. It is considered that a Reynolds number lower than or equal to 2100 indicates laminar flow, and a Reynolds number higher than 2100 indicates turbulent flow [44]. The Reynolds number is used to calculate the type of coolant flow at the baffle in the reactor pressure vessel.

2.3.3 Conservation of Mass

The Law of conservation of mass is the essential principle of physics as described by Antoine Lavoisier in 1789. The principle of mass conservation signifies that matter is neither created nor destroyed. Overall volumetric mass in a process is fixed, but entities related to the mass may vary amid the process. For instance, consider the condensation of steam. In this process, water is initially in the gas state, but then it goes through a condensation process. In the final state, water is in the liquid phase. The conservation of mass requires that the mass of water at its original state (steam) be equal to the mass of liquid water after condensation [45]. The Law of conservation of mass is also relevant in nuclear reactors for its coolant.

(Rate of mass accumulation in reactor) = (Flow of mass into the reactor) - (Flow of mass from reactor)

Consider a moving fluid in the reactor. The mass is conserved as there is no depletion or accumulation of mass in the reactor. Hence the mass flow per unit area can be shown as follows:

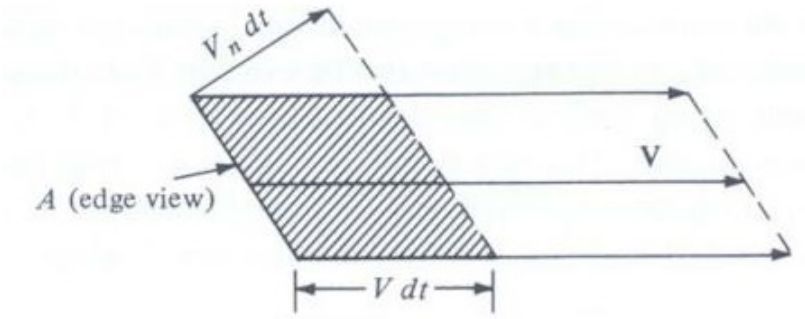

Figure 2.12: Sketch of mass flow through area A in a flow field

In Figure 2.12, edge view of area A can be seen. Let A be a small area with flow velocity V. In time dt after crossing A, the particle moved a distance of V dt. The volume and the mass are given by,

$$Volume = (V_n dt)A \tag{2.4}$$

$$Mass = \rho(V_n dt)A \tag{2.5}$$

V_n is the component of velocity normal to A. This mass has swept past A in time dt. Hence, the mass flow rate ($\dot{\mathbf{m}}$) is given by,

$$Q = AV_n \tag{2.6}$$

Where Q is Flow rate or Volumetric flow rate,

$$\dot{m} = \rho A V_n = \rho Q \tag{2.7}$$

Mass flux is given as the mass flow per unit area [46].

2.3.4 Convective Heat Transfer

Convective heat transfer is the transfer of heat from one place to another by the movement of fluids. It is the predominant form of energy transfer in gases and liquids. Occurs when the surface temperature differs from that of the surrounding fluid. Convection can be divided into two types; Forced convection where pumps or fans force the fluid for transfer of heat. Natural convection where the fluid motion is natural and caused by buoyancy and density change forces [47]. Natural convection occurs in PWR because hot water is less dense than cold water, due to low-density hot water rises in the PWR and go towards the outlet, while relativity cold water is at the bottom of the reactor.

Thermal analysis

Thermal analysis is used to determine the temperature distribution, heat flow, thermal gradient, and other different thermal entities in the process/structure. It can be divided into two types: a steady-state analysis where the thermal and boundary loading conditions does not change with time, and transient where the conditions change concerning time.

2.4 Finite Element Method Software: ANSYS

There are many sophisticated engineering questions for which we cannot attain perfect solutions. This inability to attain an exact solution may be associated with either the complicated nature of the governing equations or the complications that emerge from dealing with the boundary and initial conditions. To deal with such complications, we use numerical approximations. The universal class of numerical method is the finite element method. [48]

The finite element method is a numerical procedure that can be applied to have a result of a range of problems in engineering. Fluid, linear, nonlinear, thermal transfer, transient, and steady-state problems can be investigated with the finite element method. Finite element method was first developed and published in the 1940s. However, According to [49] finite element method was subsequently applied to thermal transfer and fluid flow issues in 1967. The benefit of finite element analysis lies in the capacity to solve arbitrarily complex problems for which analytical solutions are not accessible or which would be prohibitively time consuming and expensive to solve by hand. [48]

ANSYS is a global general-purpose finite element computer software started in 1970. The software can execute thermal transfer, structural, fluid flow, and coupled analyses. ANSYS has been a dominant finite element analysis program for over 40 years. Today, ANSYS is used in many engineering fields, including aerospace, automotive, electronics, and nuclear. However, to work in ANSYS, the end-user should understand the elemental concepts of finite element methods. [48]

ANSYS software provides a comprehensive range of simulation technologies like CFD, Finite Element Analysis (FEA). It has many thermal capabilities such as radiation, phase change, steady state, transient, conduction, convection, time-dependent boundary conditions, and temperature dependent materials. [50]

Since its initiation in the early 1970s, ANSYS FEA and CFD software has been the favoured engineering simulation software in the nuclear power industry, as it provides the FEA and CFD tools obligated to meet the precise design, engineering and regulatory challenges of the nuclear industry as well as includes standards such as American Society of Mechanical Engineering (ASME) Nuclear Quality Assurance - 1 (NQA-1), Quality Assurance Requirements for Nuclear Facility Applications, ASME Boiler Pressure Vessel Code Section III, Subsection NF and International Organization for Standardization (ISO-9001). [51]

ANSYS has many features or analysing process that can be used in different cases. Few of them are:

Steady-state analysis
ANSYS supports a range of steady-state and time-dependent analyses. It permits two forms of static analyses: single-step analyses where all loads are applied at the same time and multistep static analyses where various loads can be applied or removed with each load step. Multistep analyses allow various combinations of loads to be solved in a single run. They also allow loads to be applied increasingly in nonlinear analyses. [52]

Transient analysis
A transient analysis is applied to simulate the heat transfer circumstance in the presence of initial conditions and time-dependent boundary conditions. Along with boundary conditions, the user must

also consider several load steps, and time step size. Depending on the values of these quantities, results in the same problem may vary remarkably. According to [52], the solution is supposed to be more accurate as the time step size decreases (increased number of sub-steps). However, this may increase the cost of analysis significantly. [52]

ANSYS Parametric Design Language (APDL)

The ANSYS Parametric Design Language (APDL) is one of the most impressive features of ANSYS. It allows the user to describe some or all parts of the model (loads, material properties) as parameters and make the analysis more flexible. APDL also allows running logic operations (if, else, do) as ANSYS commands. [50] [52]

APDL incorporates several user-programmable features that support to organize a custom version of ANSYS. User-programmable components include customized commands, loading condition, elements, and material model. The merger of APDL, materials, and user-programmable features allows ANSYS users to develop custom applications. This makes it very flexible and powerful tools. [52]

ANSYS Workbench

In the 1990s, advancement emerged on a new user-friendly platform that was called as ANSYS Workbench. The workbench was designed to couple the strengths of existing ANSYS, Inc. technology with modern capabilities having improved solid modelling and better robust Computer-Aided Design (CAD) importation. New products and capabilities were integrated into the Workbench environment, and all ANSYS, Inc. products would interface with each other using Workbench.

ANSYS has three steps/phases to solve the problems:

- Pre-processing Phase
  In this stage, the solid model geometry is shaped, the element group and material properties are described, and the solid model geometry is meshed to create the finite element model. In ANSYS, these steps are performed in the Pre-processor (PREP7).
- Solution Phase
  In this phase, loads and constraints are applied, and a set of linear or nonlinear algebraic equations are solved to obtain nodal results, such as displacement or temperature at different nodes. These steps are performed in the Solution processor (SOL).
- Post Processing Phase
  After the solution is ready, the results are plotted, viewed, and exported in one of the post processors (POST1 or POST26), and exciting information is obtained.

There are many powerful programs for conducting finite element analysis. It is very complex to say which one is better. But let us discuss in brief why ANSYS was used for this assignment.

Pros of using ANSYS for the assignment

- ANSYS offers a powerful standalone interface and user friendly environment for pre-processing and post-processing, simplification, and advanced meshing.
- Transient analysis can be done economically [53].
- It has an integrated tool for both modelling and analysis.
- ANSYS is integrated with two standards; American National Standards Institute (ANSI) B31.1, and American Society of Mechanical Engineering (ASME) sections which are utilized to design the nuclear reactor [54].
- ANSYS modelling is convenient with more intuitive analysis results [54].
- ANSYS program has an advantage in the establishment of finite element model and result processing, the explicit kinetic simulation algorithm in integrated LS-DYNA program in ANSYS can quickly solve short-time, large deformation, dynamic problems [55] [56].
- Ansys is committed to the development of software tools, including Ansys Fluent and Ansys Mechanical, that follows the ASME's Nuclear Quality Assurance-1 (NQA-1) requirements as endorsed by the U.S. Nuclear Regulatory Commission (NRC) [57] [52].
- ANSYS.inc continues to make huge efforts to ensure that the program is backward compatible (i.e., that a newer version of the program can accept input generated by older versions of itself) which makes the program timeless, i.e. the program that is run today still incorporates code that was written in the 1970s [52]. This is the reason why ANSYS is preferred in energy industry.
- Using Mosaic-enabled meshing technology in Ansys Fluent, engineers can create a mesh for the complex solid model. The parallel meshing process produced a high-quality mesh eight times faster and with less user input [57].
- ANSYS allows relatively easy implementation of complex geometries, design domains, multiple load case, additive manufacturing, constraints, and coupled analysis [58].

Cons of using ANSYS

- Depending on how the ANSYS solved the equations, the time taken to perform the simulation could be shorter or longer. Generally, ANSYS takes a longer simulation time compared to ABAQUS [59].
- ANSYS lacks in efficiently solving non-linear analysis when compared to ABAQUS. Contact generation and behavior during and after deformation data can be extracted more realistically and near to exact solution with ABAQUS than ANSYS [60].
- ANSYS, Inc. products are dependent on product licenses. Each ANSYS license specifies which ANSYS products or capabilities can be used, the maximum number of elements that may be included in a model, and how many people can use the software at the same time [52].

- ANSYS APDL user-interface is outdated by 20 years when compared to user-interface of ABAQUS.

ANSYS has two essential features to build geometry; they are:

Nodes
A node is a coordinate location in a field where the Degrees of Freedom (DOF) are described. The DOFs for the point shows the possible movement of this point due to the loading of the structure. The DOFs also represent which forces and moments are moved from one element to the next.

Elements
An element is the primitive building block of finite element analysis. It is a mathematical relation that defines how the degree of freedom of node is related to the next node. There are several basic types of elements. These elements can be lines (trusses or beams), areas (2-D or 3-D plates) or solids (bricks or tetrahedral). Different element types are chosen based on the type of analysis which is going to be performed [61].

Chapter 3

Modelling and Thermal Analysis of the Pressurized Water Reactor

In this chapter, a systematic approach towards analysing and modelling of a pressurized water reactor is described. The base knowledge of the pressurized water reactor and reactor pressure vessel was necessary to deliver the process effectively.

Nuclear power plants today supply up to 7 percent of the world's primary electricity. The safe and reliable operation of nuclear power plants relies on many intertwined aspects involving technological and human factors. The reactor core is an important part which releases the energy for the generation of power using a turbine. These reactor core and turbine tends to failure due to many reasons, and one of the most important reason is due to thermal characteristics. Prediction of these thermal distributions in a nuclear power plant core is very much necessary to design and prevent the failure of the element in operating conditions. Hence, the main objective of this chapter is refining the reactor pressure vessel internal model of a pressurized water reactor and the prediction of the transient temperature distribution of reactor pressure vessel using ANSYS.

Transient analysis is an essential tool when designing nuclear reactors since they predict the behaviour of a reactor during changing conditions, such as a control-rod movement, induced by an operator, or an accident scenario, or start-up conditions. Transient simulation can be more comprehensive by predicting accurate estimates of the thermal distribution when compared to steady-state analysis because it computes the instantaneous values in each time interval for each quantity. Having a time-dependent thermal distribution results in the reactor core is extremely important in formulating safe procedures for the operation of nuclear facilities and the handling of irradiated fuel. With the rapid development of nuclear industry, simulating and analysing the reactor thermal distribution is of great significance for the nuclear safety because with these temperatures, thermo-mechanical calculations can be carried out. Moreover, these transient temperatures can be used to calculate the theoretical thermal heat capacity in the reactor core, which can be used for economic operations and to prevent accidents.

In this chapter, an attempt is made to find out the transient thermal analysis of a reactor pressure vessel internals in the operating condition of a nuclear power plant. All the modelling improvement is made with the help of ANSYS Workbench V19. The initial approach for this chapter is shown in the figure 3.1. For transient analysis, first, the working of the model made by AIS was understood with the

help of literature. Later, the model is refined for its mesh to have a balance between the quality of the mesh and computational time. Next, the boundary conditions for transient analysis were applied to the model, and the model was simulated to get the thermal distribution. At last, flow velocity and Reynolds number were calculated based on mass flow rate, to validate the simulated result for real-life nuclear thermal capacity.

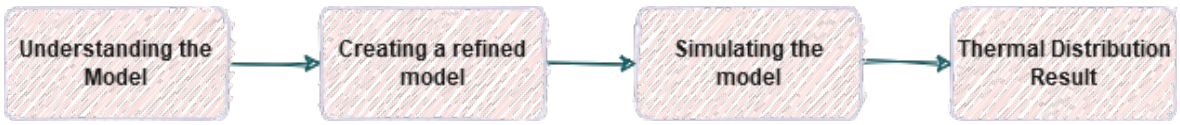

Figure 3.1: Initial Design Methodology

3.1 Model

AIS has modelled the Reactor Pressure Vessel (RPV) internal of pressurized water reactor for this section. The scope of parts to be considered in the RPV model is given by an internal management program [62]. The goal of this chapter is to carry out transient analysis and report the temperature in the reactor pressure vessel.

The design geometry of the RPV is shown in Figure 3.2

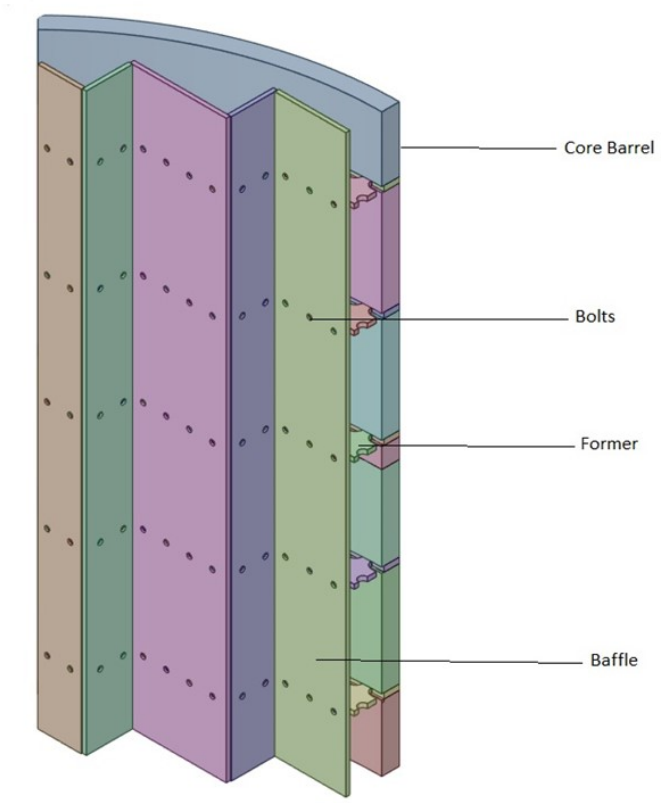

Figure 3.2: Geometry of RPV

Due to rotational symmetry $\frac{1}{8}th$ part of the whole RPV is used for analysis. If the whole model were prepared, the fuel assemblies would be placed inside and, in the middle, touching the inner surface of the baffle. All the individual parts will be shown with mesh in section 3.2. In Figure 3.2, the core barrel is the part which covers the fuel assembly and core in the RPV. The baffles are the innermost part of the RPV, which are near to the fuel assembly. The baffles act as a system to promote better flow of liquid for maximum efficiency in the RPV. The baffles are connected to the core barrel with the help of former and bolts. The contact between core barrel-former, former-bolt, and bolt-baffle are kept as bonded to avoid sliding or edge separation of the parts. Coolant flow through the inlet first hits the core barrel. As the core barrel is solid (without any gaps or holes), the only place for the coolant to flow is downwards. When coolant has reached the bottom, it crosses all the outer surfaces and reaches the inner surface of this model. The inner surface of this model has fuel assemblies. This fuel assembly heats the coolant, and the coolant flows towards the top of the RPV model and out through the outlet. This process is similar to the theory explained in Figure 2.9 but with the current modelled RPV. This flow in the RPV can be illustrated by viewing the flow path and temperature increase in Figure 3.18.

Parameters	Value
Diameter of inside surface of RPV	3.12 m [63]
Area of inner surface of RPV	7.64 m^3 [63]
Diameter of outside surface of RPV	3.29 m [63]
Area of outer surface of RPV	8.50 m^3 [63]
Design Pressure	16 MPa [64]

Table 3.1: Parameters for the PWR

3.2 Mesh

The meshing for the model was done in ANSYS Workbench V19. For the thermal calculations, 3-D higher-order SOLID90 elements are used for the model. It is used because of its geometric adaptability and smooth temperature variation results. SOLID90 is a higher-order version of the 3-D eight-node thermal element (SOLID70). The SOLID90 element has 20 nodes shown as dots in Figure 3.3, with a single degree of freedom and temperature at each node. The 20-node thermal element applies to a 3-D, steady-state or transient thermal analysis. If the model containing this element is also to be analysed structurally, the element should be replaced by the equivalent structural element such as SOLID186 [61]. However, for this chapter, we are considering thermal calculations; hence SOLID90 is used.

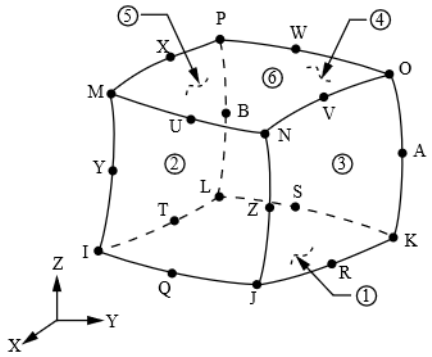

Figure 3.3: Nodes in SOLID90 Element

Meshing is an essential process of the finite element method where the model is broken into simple elements that can be used as discrete local approximations of the larger domain. The mesh biases the convergence, accuracy, and speed of the simulation. Moreover, since meshing often drains a significant portion of the time it takes to get simulation outcomes, the better and more automated the meshing tools, the time required to obtain the results will be faster [65]. Few common types of meshing are shown in Figure 3.4.

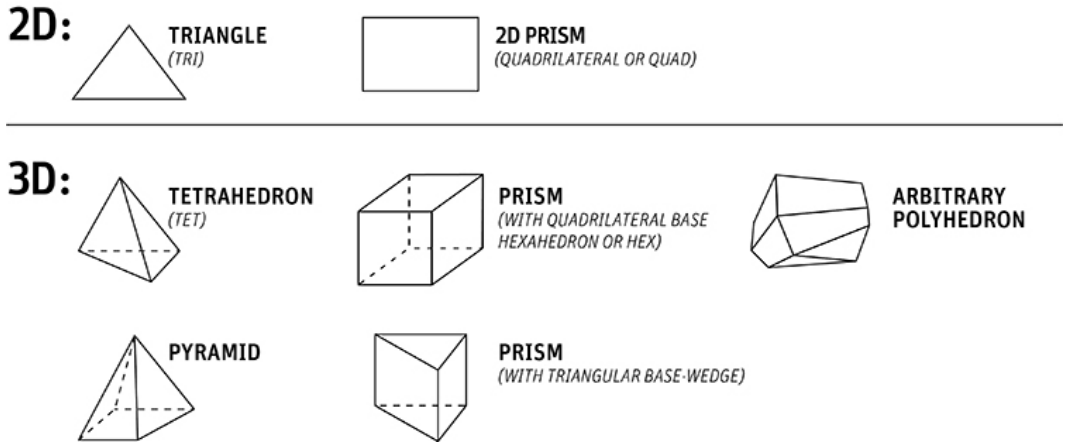

Figure 3.4: Common types of Meshing [Source: Ansys Inc]

Creating high-quality mesh is one of the crucial factors that must be considered for getting accurate results. A high-quality mesh should have an optimum balance between the simulation time and mesh size.

Ansys provides an intelligent meshing software to provide mesh for most of the geometries, but if the complexity of the geometry increases, the mesh will be broken into different types resulting in a low-quality mesh. The fineness of the mesh was increased at the baffle and former area by studying the mesh convergence; this led to having a balance between simulation time and quality. To check if the mesh quality in this model was good, skewness mesh metrics were used. According to [66], maximum skewness value should be less than 0.95; if the skewness average value after meshing

is zero then a perfect mesh has been achieved, if the skewness value is 1 then the mesh is of low quality. An average skewness value of 0.443 was found for this model after refining, which, according to skewness mesh metrics spectrum chart [66] is termed as “very good” mesh.

From Figure 3.5 to Figure 3.9, shows the mesh of all the parts in the model.

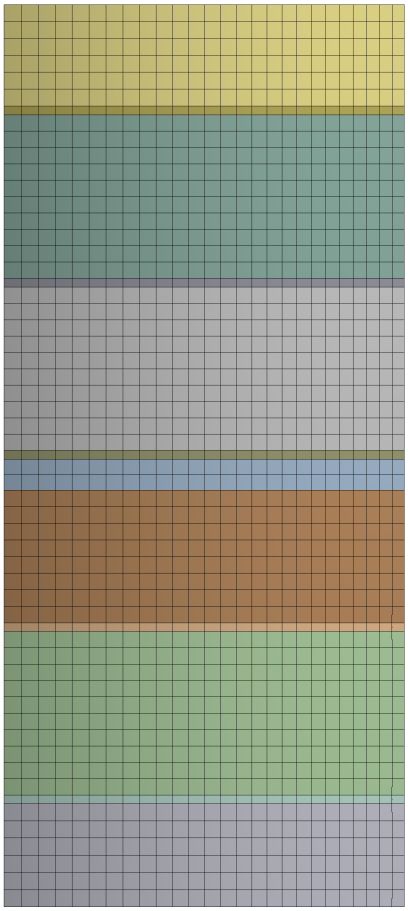

Figure 3.5: Mesh: Core Barrel (front view)

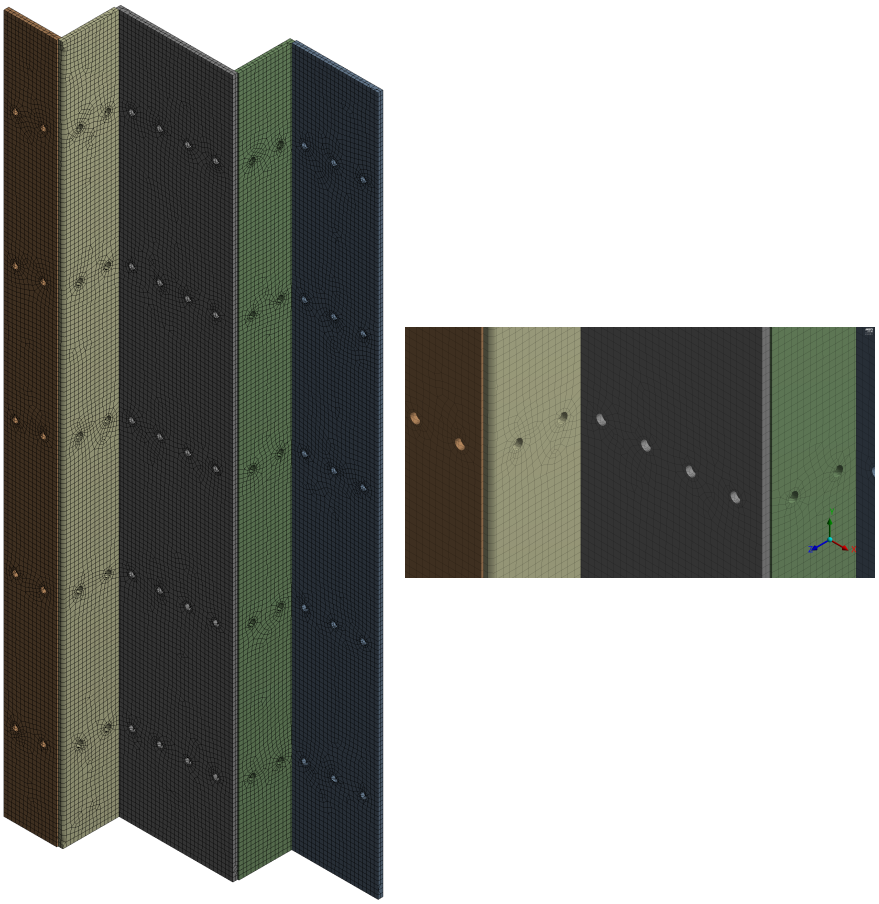

Figure 3.6: Mesh: Baffle

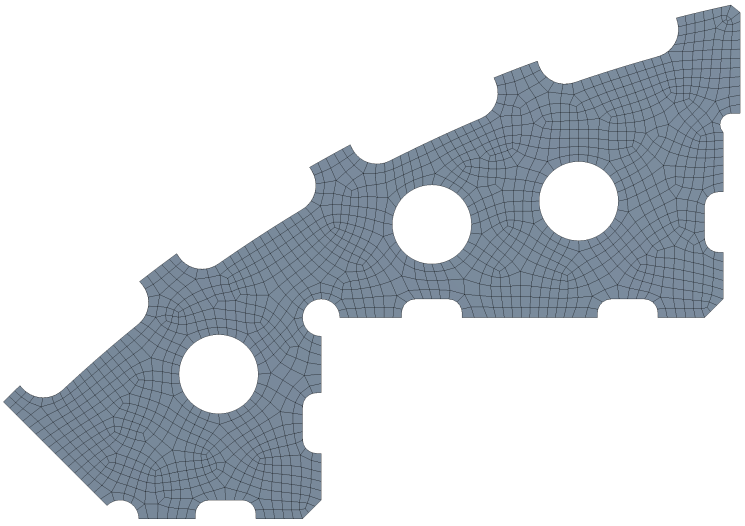

Figure 3.7: Mesh: Former (top view)

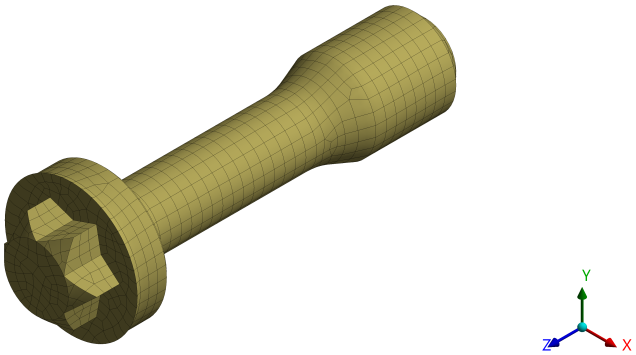

Figure 3.8: Mesh: M12 Bolt

Figure 3.9: Mesh for the Geometry

Table 3.2 gives a summary of the number of elements and nodes of parts in the model.

Model	Number of Elements	Number of Nodes
Core Barrel	3796	23058
Baffle	45988	188605
Former	46104	169164
Bolt	366877	1214256
Total Geometry	462765	1595083

Table 3.2: Mesh Details

3.3 Material

The materials were already defined, and used to model the RPV Internals they are as follows:

- 1.4550 (i.e. American Iron and Steel Institute (AISI 347)) for the former, baffle and core barrel. It is austenitic chromium-nickel stainless steel with titanium and niobium addition.
- 1.4571 (i.e. AISI 316Ti) for the bolts. It is austenitic titanium stabilized chromium-nickel molybdenum stainless steel.

The material property was taken from German safety standard Kerntechnischer Ausschuss (KTA) because the PWR is a German design. The reference to the material properties is given in Deutsches Institut für Normung (DIN) 17440 [67]. The material properties are shown below.

T (^oC)	E (GPa)	α (10^{-6} K^{-1})	k ($\frac{W}{mK}$)	ρ ($\frac{kg}{m^3}$)	C_p ($\frac{J}{kgK}$)
20	200	16	15	7930	470
100	194	16	16	7930	470
200	186	17	17	7930	490
300	179	17	19	7930	500
400	172	18	20	7930	520

Table 3.3: Temperature-dependent properties of AISI 347

T (^oC)	E (GPa)	α (10^{-6} K^{-1})	k ($\frac{W}{mK}$)	ρ ($\frac{kg}{m^3}$)	C_p ($\frac{J}{kgK}$)
20	200	16.5	15	7930	470
100	194	16.5	16	7930	470
200	186	17.5	17	7930	490
300	179	18.5	19	7930	500
400	172	18.5	20	7930	520

Table 3.4: Temperature-dependent properties of AISI 316Ti

Where ρ is the density, k is the thermal conductivity, α is the coefficient of thermal expansion, C_p is the specific heat capacity, E is the Young's modulus. According to [67], thermal analysis density of 7930 $\frac{kg}{m^3}$, Specific heat 500 $\frac{J}{kgK}$, and reference temperature properties are set to 20 ^oC.

3.4 Approach

The RPV internal model described above is solved with the approach, as shown in Figure 3.10.

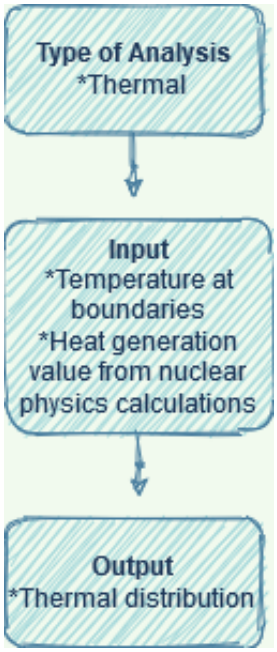

Figure 3.10: Approach to Model

First, transient thermal analysis was approached by having a time-dependent boundary conditions, which was the start-up condition of the reactor. This start-up loading conditions were supported with imported heat generation value and reference temperature. Finally, the thermal distribution in the reactor core was achieved. Along with thermal distribution, values of velocity, mass flow rate were calculated. These achieved thermal distribution was validated using the thermal heat capacity of the real-life pressurized water reactor.

3.5 Boundary Condition

The heat transfer coefficient and the temperature used as boundary condition are representative for real PWRs; German designed PWR [68], and the French CP0 PWR [69].

The thermal boundary conditions for the model is shown in Figure 3.11.

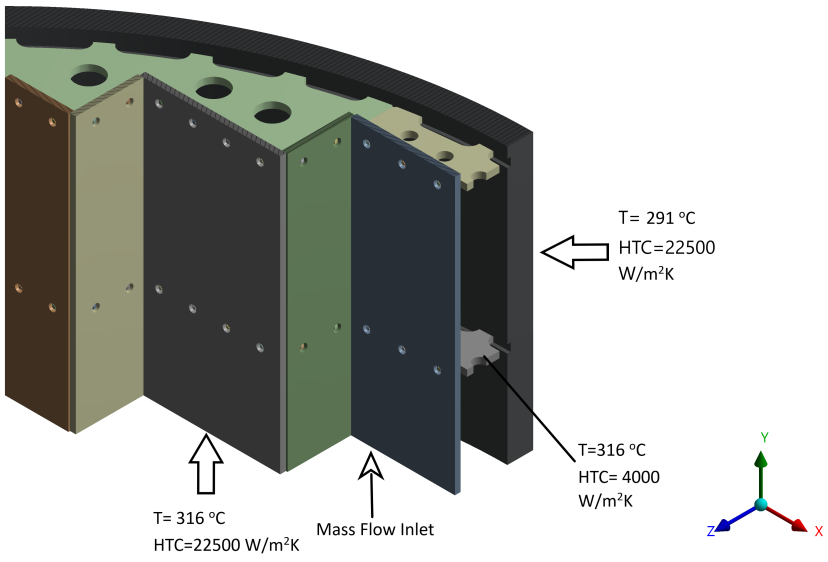

Figure 3.11: Thermal Boundary Conditions

Boundary Condition	Value
Heat Transfer Coefficient (HTC) for internal surface	22500 $\frac{W}{m^2K}$
HTC for external core barrel	22500 $\frac{W}{m^2K}$
HTC for former at the bottom	4000 $\frac{W}{m^2K}$
Reference temperature (T_{ref}) for External (Outer surface)	291 ^oC
Reference temperature (T_{ref}) for internal surface	291 to 316 ^oC (depending on the height of RPV)
Reference temperature for former	291 to 316 ^oC (depending on the height of RPV)
Body heat generation	Data from nuclear physics calculation

Table 3.5: Thermal Boundary Conditions

The RPV internal model is sectioned into small part to explain the boundary condition in the model. This sectioned model is the bottom part of the full RPV internal model. The heat transfer coefficient of 22500 $\frac{W}{m^2K}$ is applied to the outermost part of the RPV model (I.e. Outer surface of core barrel). The same heat transfer coefficient is applied to the innermost part of the model (i.e. inner surface of baffles). The heat transfer coefficient is kept at that constant value throughout the analysis. The reference temperature for the outer surface of the RPV model is given as 291 ^oC. The reference temperature for the inner part of the RPV model is dependent on height which ranges from 291 to 316 ^oC. As explained in section 3.1, the water hits the core barrel and goes down. Hence, Figure 3.11 shows the mass flow inlet, which is the water flowing inside the RPV. As the water flows from

bottom to the top (height) of RPV model the temperature increases due to heating, by this, we can say that the there is the different temperature at different height of the RPV. There is a pressure of 160 bar inside the reactor core due to this pressure the boiling point of water becomes 346 ^oC. All the boundary conditions in Table 3.5, are current real-life data of the PWR and is found in NRG internal reports [68] [64].

Body heat deposition data are values of heat deposition in the steel and in $\frac{W}{g}$. The heat deposition depends on the number of neutrons escaping the core region, so it depends on the fluence in the structures surrounding the core. The number of neutrons leaking from the core region depends on fuel distribution. Currently, the PWR has a low-leakage core. This data was already calculated by Monte Carlo N-Particle Transport Code (MCNP) and has been imported to perform transient analysis as a boundary condition [70]. The MCNP data was provided in a format suitable to be read by the FE software, which is an American Standard Code for Information Interchange (ASCII) table format, as shown in Figure 3.12. The data were converted from $\frac{W}{g}$ to $\frac{W}{m^3}$, so it was multiplied by the density value in $\frac{g}{m^3}$. Later, this data in table format is applied to the whole RPV model in the form of boundary condition, and heat generation in the RPV is obtained, as shown in Figure 3.13.

heat_steel_mclist_check	X (m)	Y (m)	Z (m)
361.916	-0.925536593	0.001063425	-0.978834441
361.916	-0.925756686	0.000983264	-0.978837375
361.916	-0.925696356	0.001072791	-0.978836917
377.6	-0.935122178	0.01560371	-0.97883891
377.6	-0.934991735	0.015764774	-0.978839224
377.6	-0.934855348	0.015927051	-0.978835998
377.6	-0.934715465	0.015996207	-0.978839023
377.6	-0.934726048	0.01611367	-0.978838508
377.6	-0.934562803	0.016277789	-0.978846805
377.6	-0.934866848	0.015835921	-0.978916234
377.6	-0.933932476	0.016776392	-0.978836189
377.6	-0.93390142	0.016933005	-0.978841491
377.6	-0.933728544	0.017074927	-0.978840378
377.6	-0.933558856	0.017200517	-0.978840739
375.587	-0.932823213	0.017735537	-0.978840528

Figure 3.12: Part of 3D ASCII table in excel

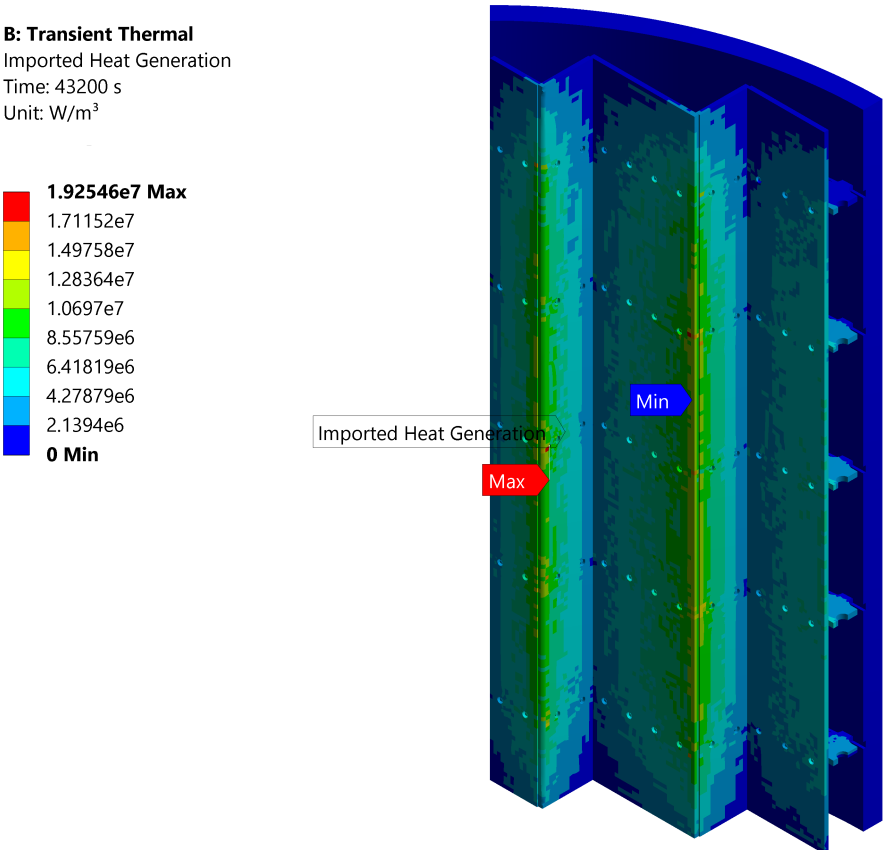

Figure 3.13: Imported Heat Generation

To replicate a real-life scenario with transient analysis in the RPV. The start-up nuclear reactor loads were considered. The graph for a nuclear reactor start-up contains time and temperature. The PWR start-up is shown through the graph in Figure 3.14.

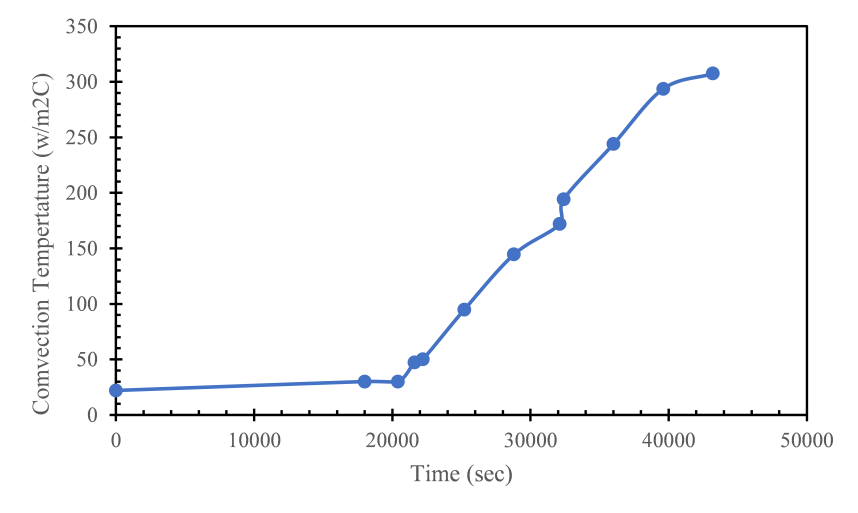

Figure 3.14: PWR Start-Up Condition Graph

	Steps	Time [s]	[B] Convection (Temperature) [°C]
1	1	0.	22.
2	1	18000	30.
3	2	20400	30.
4	3	21600	47.1
5	4	22200	50.
6	5	25200	94.7
7	6	28800	144.5
8	7	32100	171.8
9	8	32400	194.2
10	9	36000	243.9
11	10	39600	293.6
12	11	43200	307.4

Figure 3.15: PWR Start-Up condition in ANSYS Tabular Data

The start-up loads for the PWR is found in [63], which is a German report found in archives of NRG. In general, the refuelling is done every 12 to 18 months, some of the fuel – commonly one third or one-quarter of the core – is transferred to the spent fuel pool. At the same time, the rest is reorganized to an area in the core better suited to its remaining level of enrichment. After refuelling and core alternation, a physics test is necessary to verify that the reactor is operating as per its pre-calculated core design. This process may take several days or months because of safety checks on all the operating systems inside the nuclear core, and the usage of heat from nuclear chain reaction is prohibited initially due to safety reasons. Reactor start-up after refuelling is a start-up from a cold condition since refuelling requires the Reactor Coolant System (RCS) to be cooled down and depressurized. The initial conditions are the Nuclear Steam Supply System (NSSS) is in the "cold shutdown" mode, that means T_{avg} = 30^0C and pressure are equal to near atmospheric. In Figure 3.15, the time between zero to 18000 seconds is where the NSSS heats up from Cold Shutdown to Hot Standby. This hot standby is performed by reactor coolant pumps working together with a decay heat left behind in the core during shutdown and can be used for heating the primary coolant. This heating from decay heat process is taken slow. After reaching the 18000 seconds mark the heat up rate is limited to about 30 ^oC per hour initially to minimize internal stress in the material of the pressure vessel, primary piping, and other components. This limitation will linearly increase the start-up temperature of the reactor. The plant is brought to near operating temperature (T=293 ^oC) after 11 hours of an initial start-up with a reactor coolant pump because the usage of heat from nuclear chain reaction is prohibited initially. At 12 hours, the reactor reaches the target/operating value, and the start-up is finished. Later the temperature of the coolant is maintained throughout balance use of the reactor. Hence, this is the balanced-out stage of PWR; all the transient analyses are done for a total time of 43200 seconds (12 hours). Due to safety reasons and to prevent internal stresses, the temperature in the start-up condition of the reactor is limited initially. This start-up temperature in the core should increases linearly at a slow speed. However, in the figure 3.14 and figure 3.15 it can be seen that the temperature increases suddenly from 171.8 ^oC to 194.2 ^oC in a concise amount of time. This phenomenon occurs because the reactor has a negative void coefficient. Water boiling at those temperature leads to voids (steam bubbles) inside the reactor. The number of voids inside the reactor can affect the reactivity of the reactor. There is a sudden pressure rise at that interval this will result

in decrease in void content. The sudden increased pressure will cause some of the steam bubbles to collapse. This void collapse will give out additional energy in the form of heat. Hence, due to the additional heat given out by the voids, there is a sudden increase in temperature at that short interval of time.

The tabular data shown in Figure 3.15 is applied as the convection boundary condition to the exterior wall of the core barrel in the model, as seen in Figure 3.16. This convection boundary condition is defined by reference temperature and heat transfer coefficient. The heat transfer coefficient was held at a constant value of 22500 $\frac{W}{m^2K}$ as a function of time, while the reference temperature was varied with time, from the Figure 3.14.

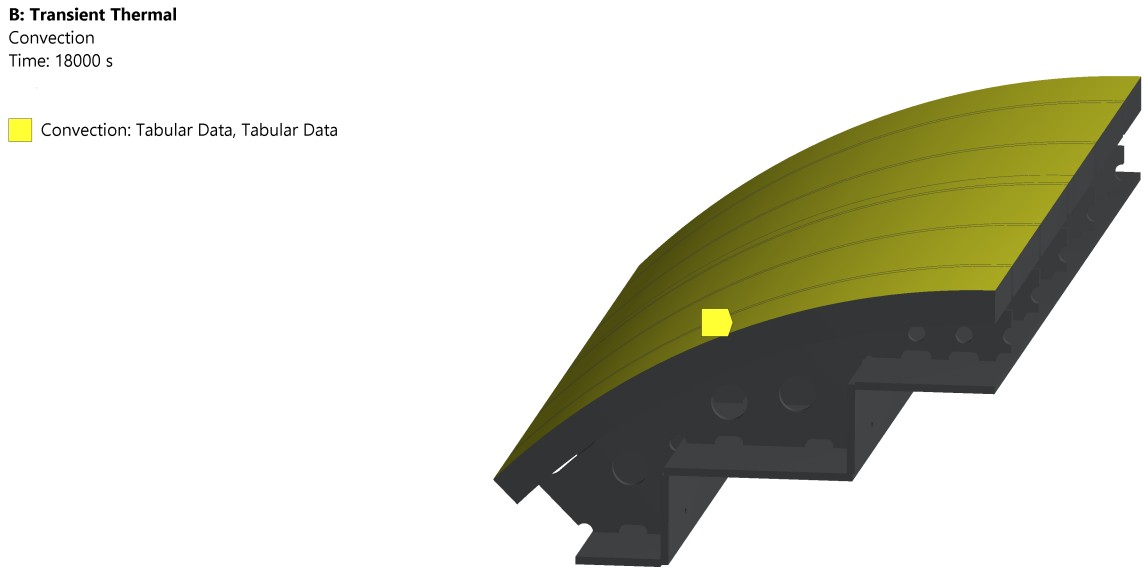

Figure 3.16: Convection Boundary on Core Barrel

From the above paragraph, we can say that convection based on real-time (transient) is given to the outside surface of the core barrel. Now inner part, i.e. baffle, should also be given convection based on time, to make it a real-life start-up loading phase of the reactor.

To give boundary condition to baffle, we consider the height of the model, the time, and the reference temperature. Consider the conditions of a start-up from Figure 3.15 and reference temperature for the internal surface from Table 3.5. According to [68], the temperature difference between the top part of RPV and bottom part of RPV in the PWR at any given point of time during start-up is 20.26 ^oC. Now we can combine all the information given in this paragraph to form a tabular data which gives us the boundary condition for the baffles. The tabular data is shown in Figure 3.17.

Y	TIME								
		1.8e+04	2.04e+04	2.16e+04	2.22e+04	2.52e+04	2.88e+04	3.21e+04	3.24e+04	3.6e+04
	-0.3	30	30	47.1	50	94.7	144.5	171.8	194.2	243.9
	2.32	50.26	50.26	67.36	70.26	114.96	164.76	192.06	214.46	264.16

Figure 3.17: Temperature as a function of time and height boundary condition for baffle

The distance reference co-ordinates in the model was placed 0.3 metres from the bottom-most part of the RPV. So, in Figure 3.17 , the height of the bottom part of the RPV has a negative sign (-0.3). The height of the top part is 2.32 metres. The height of the RPV model is described in [68]. According to [68], there is a temperature difference of 20.26 ^oC. To explain the Figure 3.17, consider the start-up time 18000 seconds, at this time the temperature at the bottom-most part of the reactor will be 30 ^oC [Figure 3.15] and top-most part of the reactor will be 50.26 ^oC [68]. These temperatures are illustrated in Figure 3.18. In Ansys Workbench all the three components, i.e. height, temperature and time could not be defined using workbench function. Hence, an APDL command was written and added to the workbench to give a boundary condition to the baffles. The code is shown in the appendix A.

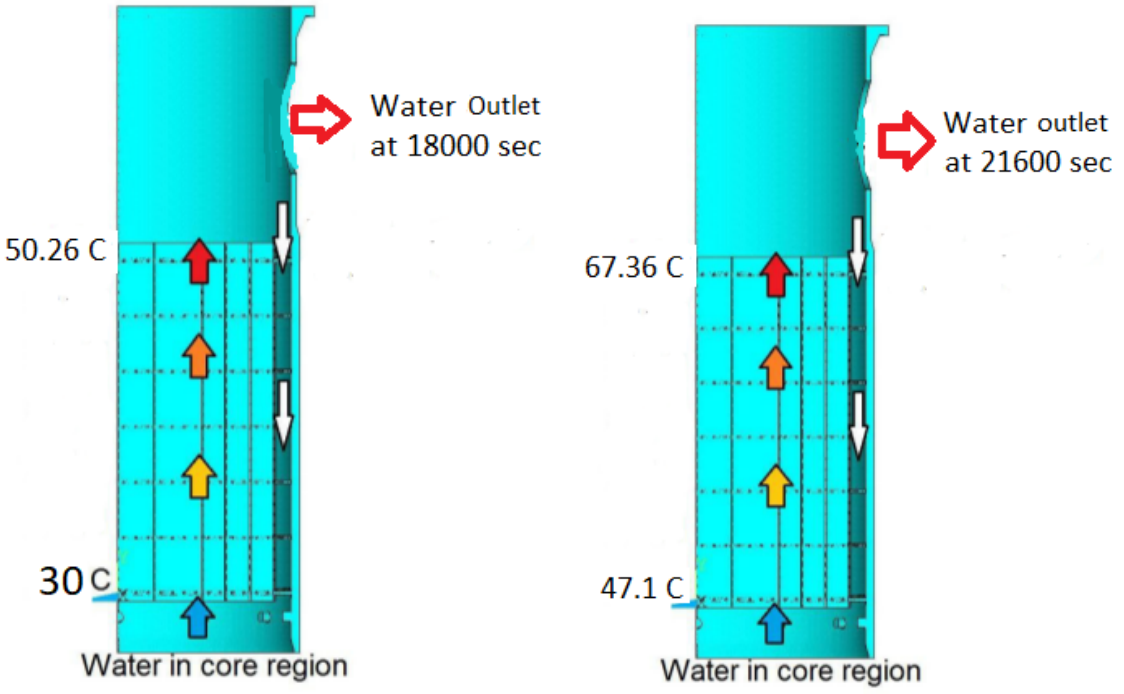

Figure 3.18: Representation of boundary condition for baffle

3.6 Results

This section shows the thermal results for FE analysis. Temperature distribution of the RPV internal model is shown in Figure 3.19.

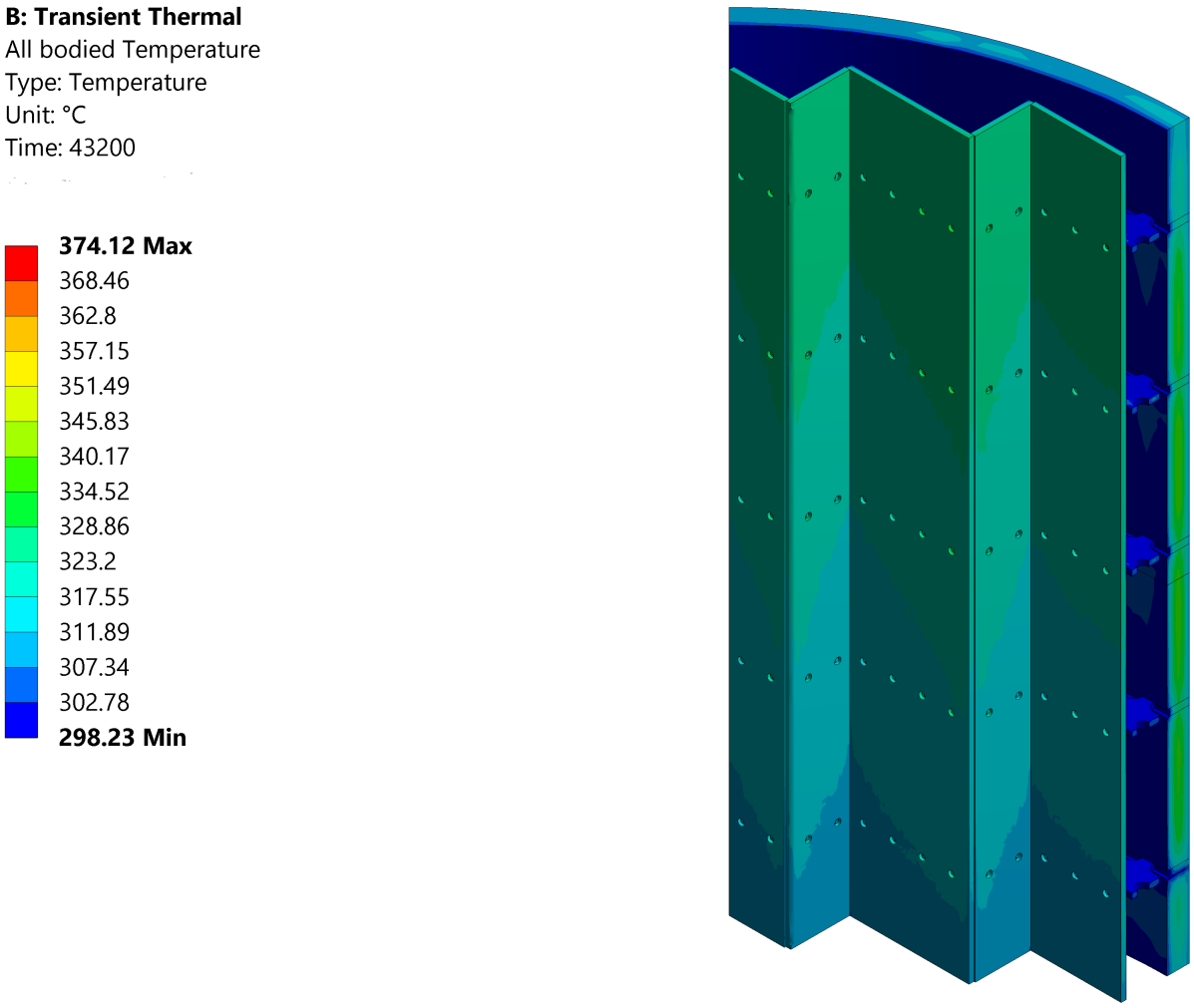

Figure 3.19: Temperature Distribution of the Model

Temperature distribution for individual parts is shown in figure 3.20 to figure 3.23.

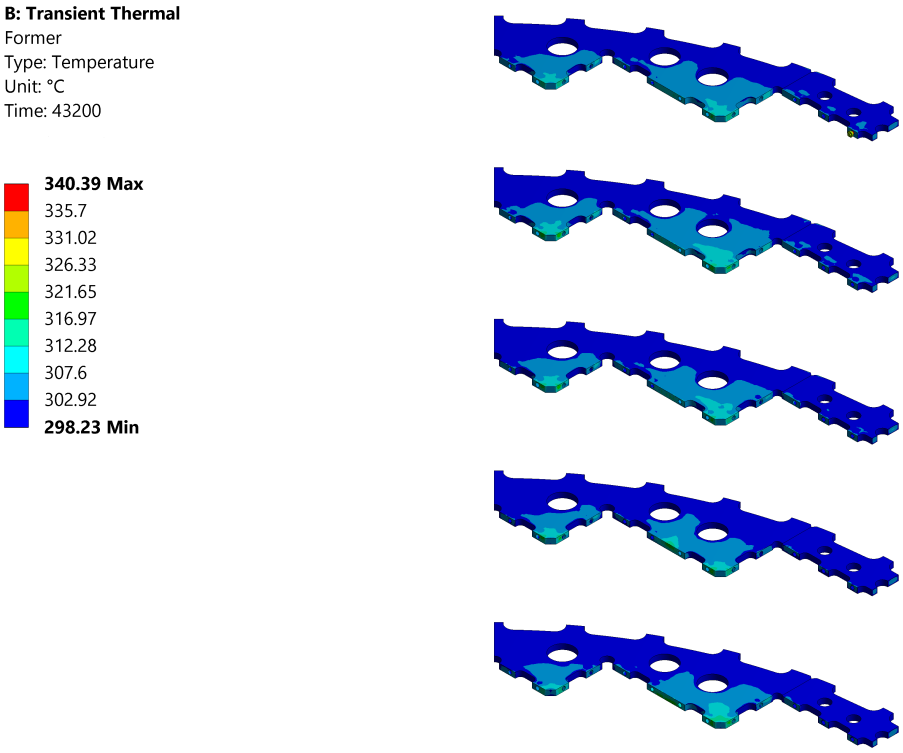

Figure 3.20: Temperature distribution of formers

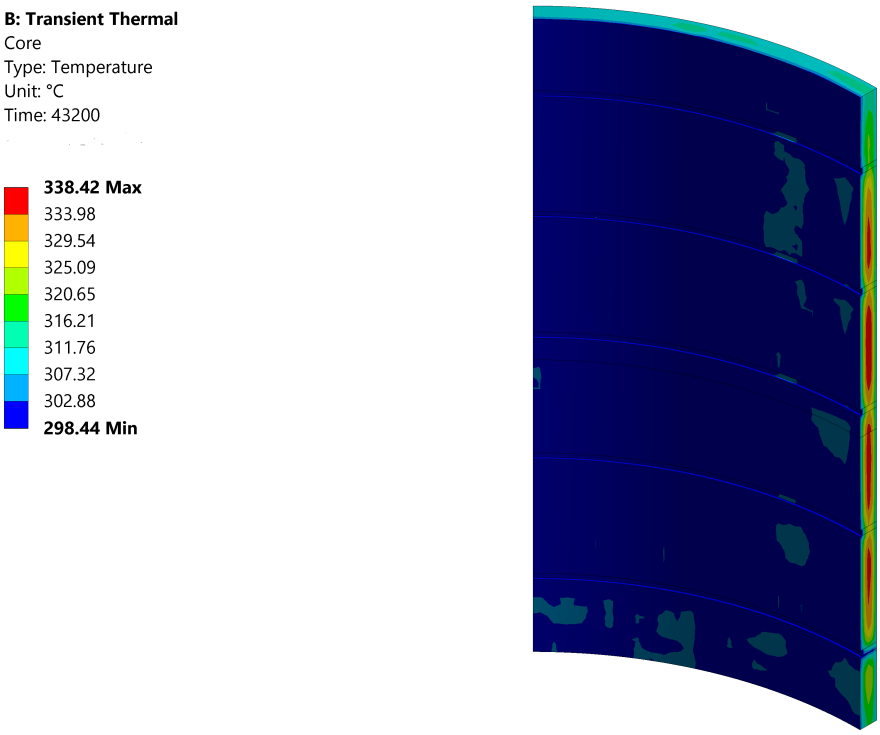

Figure 3.21: Temperature distribution of Core Barrel

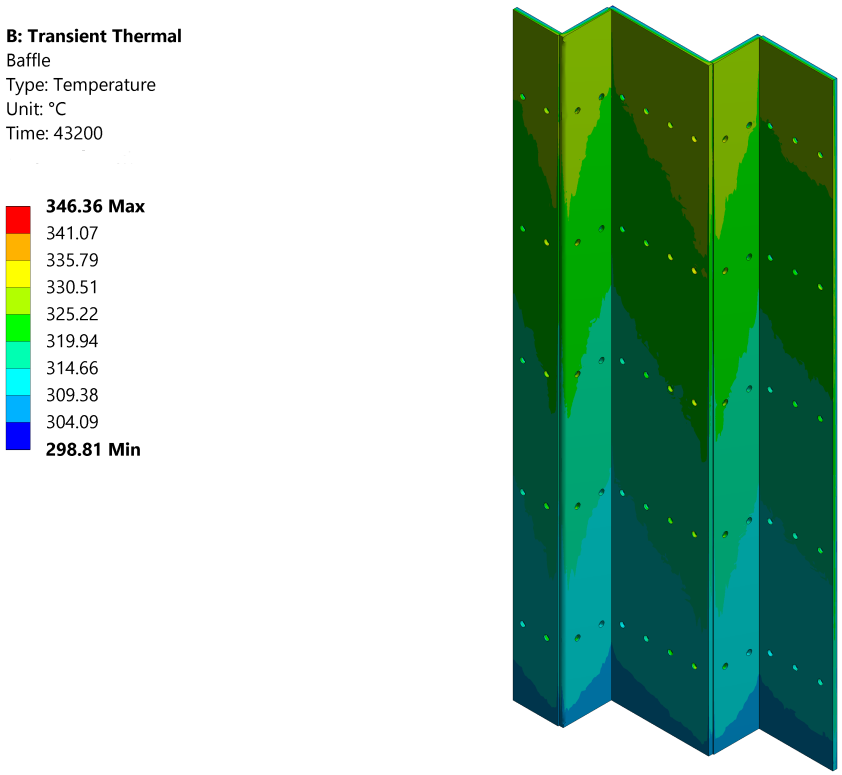

Figure 3.22: Temperature distribution of baffle

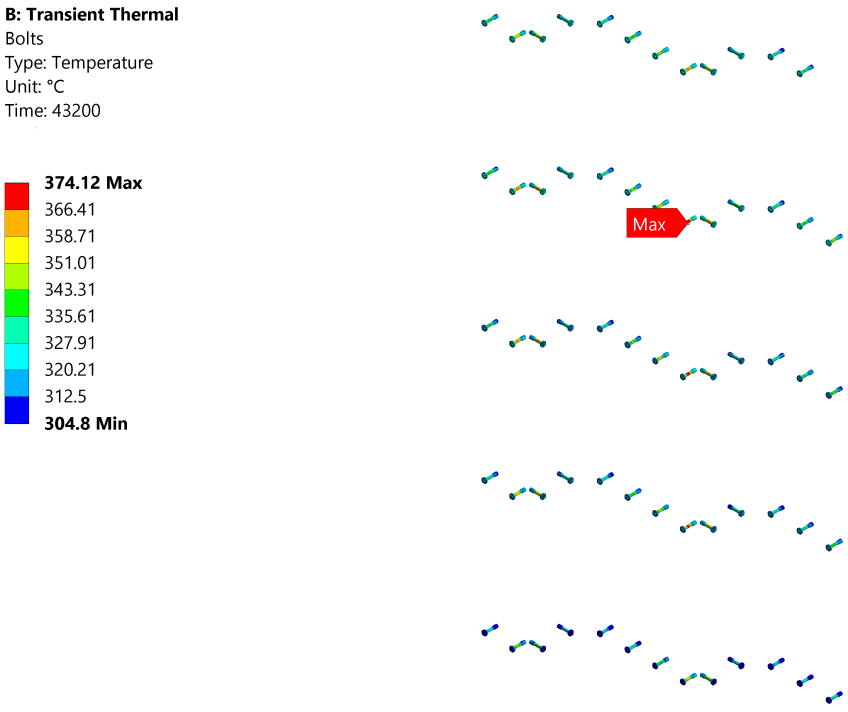

Figure 3.23: Temperature distribution of bolts

The temperature of the RPV internals is increasing from bottom to top, as seen in the figure 3.19. This increase is due to the increase in reference temperature with the height of the RPV internal model. The lowest temperature in the model is 298.23 ^oC and is located on the core barrel. The highest temperature is 374.12 ^oC which is in the central bolts.

The inner part of the former is connected to the baffle is seen as the hot surface in the figure 3.20, and the slight behind part which is in contact with the core barrel is seen having a lower temperature.

The core barrel has the lowest temperature seen in the figure 3.21 because this part receives the lowest amount of heat deposition and is exposed to the lowest reference temperature of 291 ^oC.

The temperature increases from bottom to the top part of the baffle seen in the figure 3.22 because of imported heat generation.

As seen from figure 3.23, the central bolts have the maximum temperature in the model because this region experiences the highest amount of heat generation, from figure 3.13. Every bolt, subject to heat deposition, tends to expand according to the thermal expansion coefficient of the material and, if the expansion is constrained, thermal stresses develop. The bolt has a higher value of expansion coefficient than the baffle and the former [Table 3.4]. The area where the temperature is the highest in the bolt is small [seen in Figure 3.24], this maximum temperature only occurs at a particular single bolt. It does not much affect the overall temperature distribution of the model.

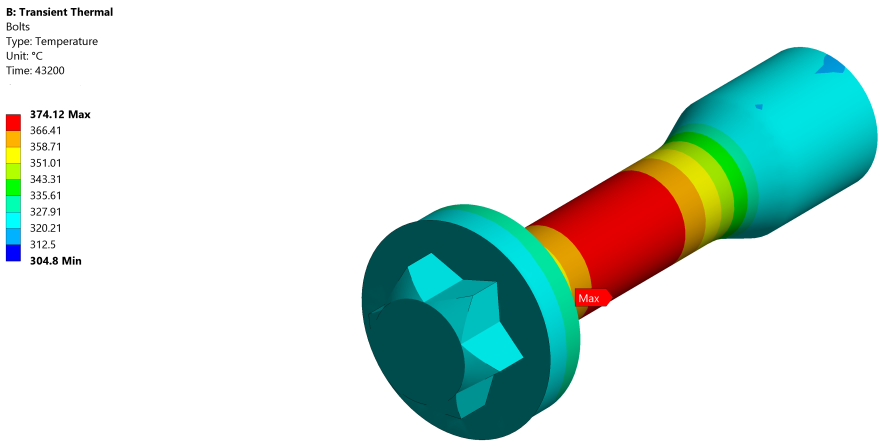

Figure 3.24: Maximum temperature distribution in a single bolt.

In the analysed model, if a node/element is selected on a specific spot on the height of the model, then the temperature at that specific height can be known. For example, the total height from the bottom of the RPV model (not from 0.3 m reference point) is 2.62 meters [Y in Figure 3.17]. If this height is considered, then the accurate temperature at that height can be found by the analysed model, which is 317.55 ^oC [see in Figure 3.19]. With this transient analysis of RPV internal model, an estimate temperature distribution of the real-life scenario of start-up load of that PWR is reported.

3.6.1 Result Validation

To validate if the analysed temperatures distribution is correct. We must calculate velocity inside the core. According to [68], the mass flow rate ($\dot{m}$) inside the core is 11000 kg/s. According to 2.3.3 , the mass rate of coolant flowing inside the reactor should be equal to mass rate flowing out of the reactor. By using the equation (2.7), we must find the velocity. For this temperature on the top-most part of the RPV internal model is used, which is 317.55 ^oC because this is the temperature with which the coolant from top-most part goes out of RPV through the outlet valve/leg. Equation (2.7), requires a density of coolant (water) at 317.55 ^oC and the pressure of 156 bar. Hence, the density of water in this situation is 673.8 $\frac{Kg}{m^3}$ [71]. The area of the inner surface of the RPV is 7.64 m3 [Table 3.1]. By solving the equation, we get

$$V_{innercore} = 2.14\frac{m}{s} \tag{3.1}$$

Using equation (2.6), we also get

$$Q = 7.64 \times 2.14 = 16.35\frac{m^3}{s} = 981000\frac{L}{min} \tag{3.2}$$

Using the above velocity, we can calculate the Reynolds number. For this, we use equation (2.3),

$$R_e = \frac{2.14 \times 3.12}{0.001057} = 6316.74 \tag{3.3}$$

From equation (3.3), the Reynolds number is 6316.74. If the Reynolds number is above 4000, then the flow is said to be turbulent [72]. According to this, we can say that the flow inside the core is turbulent.

To find the thermal heat capacity of the nuclear power plant [73], we use,

$$Q = \frac{\rho \times Q \times C_p \times \Delta T}{60} \times SF \tag{3.4}$$

Where ρ is the density of coolant in $\frac{Kg}{m^3}$ (at 317.55 ^oC), Q is the volumetric flow ($\frac{L}{min}$), C_p is the specific heat capacity of fluid ($\frac{kJ}{KgK}$) at 317.55 ^oC, ΔT is a difference in temperature at the outlet (317.55 ^oC) and inlet (298.23 ^oC). SF is the safety factor. Substituting all the values in equation (3.4), we get,

$$Q = \frac{673.8 \times 981000 \times 6.17 \times (317.55 - 298.23)}{60} \times 1 \tag{3.5}$$

According to the analysed values from the RPV internal model, the thermal load capacity of the German designed PWR is,

$$Q = 1313.23MWt \tag{3.6}$$

According to [74] [68] [64], The real working thermal heat capacity of German designed PWR is,

$$Q = 1366MWt \tag{3.7}$$

Comparing equation (3.6) and (3.7), we can say that the transient analysed temperature distribution in RPV internal model is almost accurately estimated to real PWR.

Chapter 4

Convergence in SALIENT Experiment Model

In this chapter, a pool-type research High Flux Reactor (HFR) in Petten, operated by NRG is considered from section 2.2.2.1. First details of salient experiments in HFR and modelling of the experiment is explained to understand the problem entirely. Later limitation of the current model is explained, and finally, some potential tried solutions are elaborated.

4.1 SALIENT Experiment Model

Before considering the model, let us understand what salient experiments mean in the HFR. In 2015 NRG started together with the European Joint Research Centre (JRC) in Karlsruhe a series of nuclear fuel irradiation experiments to support the development of Molten Salt Reactor technology. Such experiments were not performed since the '60s when the Oak Ridge National Lab carried out a large-scale investigation. The first experiment in the series named SALIENT-01 was irradiated in Petten's High Flux Reactor. Some of the challenges faced by the Molten Salt Reactor (MSR) is that it is too complicated and multidisciplinary. Research should be done to solve technological challenges and make MSR economical and less time-consuming. With its facilities available like the HFR in Petten and its experience, NRG can significantly contribute to undertaking the challenges of MSR by researching molten salt fuel interactions. In view for long term future of MSR technology, NRG has commenced on MSR research and development based on government-supported programs. The SALIENT experiment is one of the supported experiments to contribute to MSR research. This program is called "the Dutch molten-salt program". The SALIENT experiment comes as a project under the Dutch molten-salt program. These experiments are conducted to get the knowledge or to research about salt-metal interaction in MSR.

The type of irradiation facility in the HFR is adapted to the project needs in terms of specimen type and size, target dose and temperature, and situation. In this assignment, the HFR experiment facility is tailored to act as an environment of MSR.

All these experiments need an irradiation device to be placed in and experimented. These irradiation devices are called rigs. In a multipurpose research reactor, it is recommended to standardize

the experimental facilities as much as possible. There are three standardised irradiation rigs in HFR seen in Figure 4.1 [33].

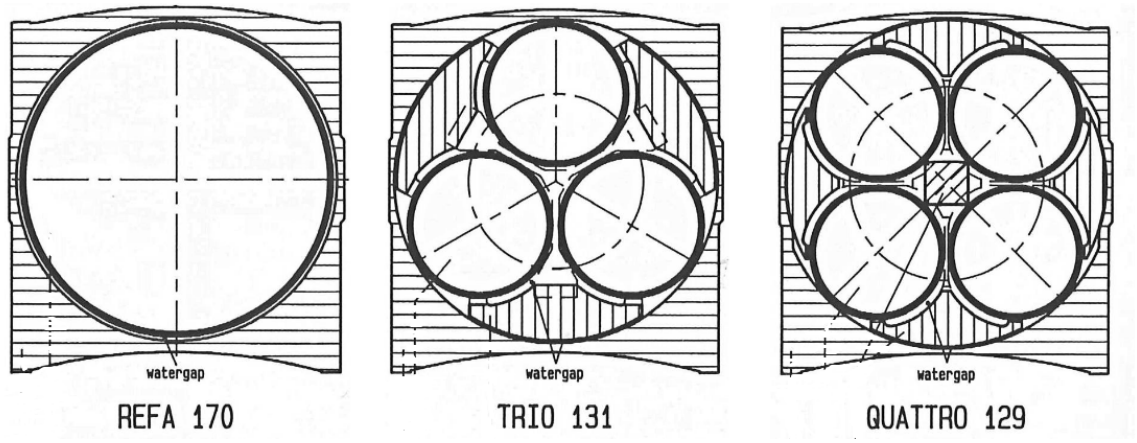

Figure 4.1: Three main configurations for in-core irradiation channel at the HFR [75]

The SALIENT experiment modelled in this assignment, TRIO-131 has been used as the irradiation rig, seen in Figure 4.1. A TRIO-131 capsule (consisting of 3 irradiation channels) has each of its irradiation channels filled with a different experiment material to be tested. Filling all three of rig channels depends upon the requirement of the experiment. They are placed parallel to each other in the in-core facility, as seen in Figure 4.2.

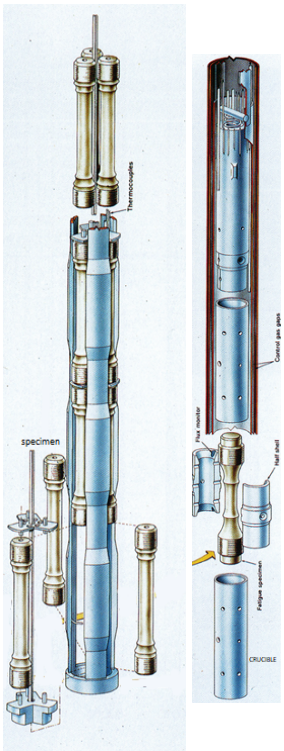

Figure 4.2: TRIO-131 set up in the in-core facility for the experiment [76] [32]

Figure 4.2 represents the isometric drawing form and the TRIO-131 set-up in the in-core facility. They are set up as three channels by using a pin to align them as TRIO-131. Rigs are generally instrumented with 12 to 24 thermocouples to find the temperature rise due to fuel (molten salt). This set-up seen in Figure 4.2 containing the molten salt (fuel) is placed in irradiation facility and is considered as an experimental setup.

SALIENT Experiment Design

These set of experiments are operated to build up experience with molten salt fuel irradiation and to research the molten salt-metal interaction. SALIENT experiments are coined as the world's first thorium molten salt experiment in over 40 years. Currently, phase 3 of these experiments are being conducted (SALIENT-03). To model, we first consider the design of SALIENT-03 experiment in-core facility. This design is placed inside the HFR for irradiation experiments. The view of the design setup of the SALIENT-03 is shown in Figure 4.3.

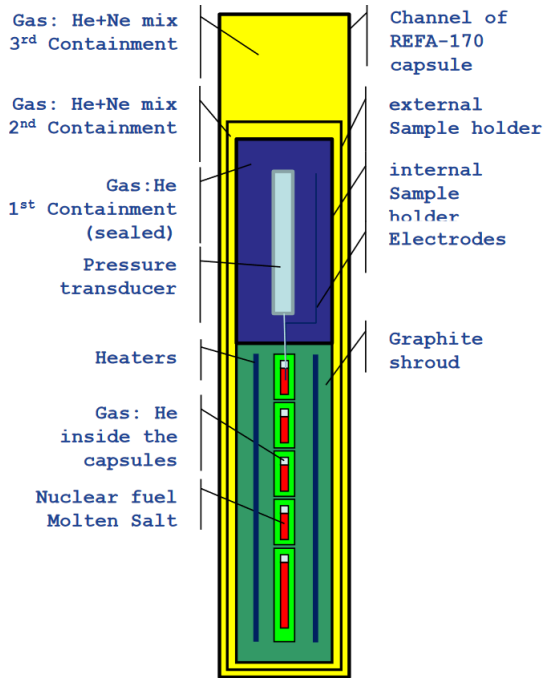

Figure 4.3: SALIENT-03 experiment setup design [75]

Figure 4.3 shows the section front-view of the SALIENT-03 setup. Heaters are introduced in this experiment to avoid radiolysis during HFR downtime. It has welded Alloy N rod and a pressure transducer to measure pressure during irradiation [33]. Thermocouples are installed to measure the temperature gradient due to fission reaction by molten salt. The radiation emitted from the core (fuel) is transferred into the materials causing internal heating of testing materials. A graphite shroud is surrounded the nuclear fuel molten salt to act as moderator enhancing the reaction. There is a total of 3 containments in the setup. The testing samples are held inside the 1st containment. The outermost containment of the setup is REFA-170. For this specific experiment, the outer surface of REFA-170 is the only part, which is in contact with the reactor coolant water, rest all the other parts inside the core is cooled/heat transferred by an inert gas like He, Ne through gas gaps. The heat generated in the

experiments is removed by water that is forced through the facilities. The irradiation facilities distribute cooling water over the outer wall of each of the irradiation channels. Due to the large amount of water forced through the facilities, the water itself is not heated signs along the way. The temperature of the samples themselves is controlled utilizing the multiple gas gaps that are present between them and the coolant.

A 2D version of SALIENT-03 experiment setup design was modelled in ANSYS APDL by AIS with the same dimension as of the experiment setup, shown in Figure 4.4. This model is precisely based on the design setup explained in the above paragraph.

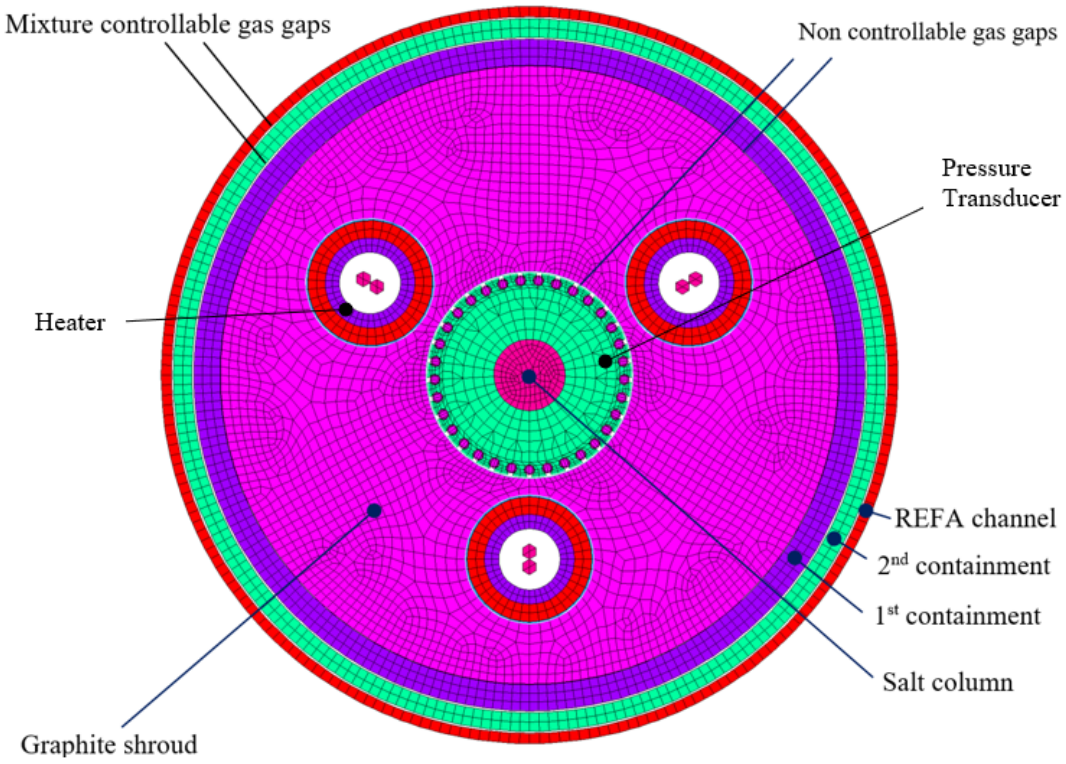

Figure 4.4: Transverse model of SALIENT-03 experiment [76]

All the gas gaps with gas gap numbers are shown magnified in the Figure 4.5. The molten salt is placed in the middle as seen in the Figure 4.4 The heaters are placed beside the fuel but and surrounded by graphite shroud. The first gas gap is placed between the graphite shroud and pressure transducer. The second gas gap is situated between graphite shroud and first containment as seen in the figure 4.5. The outer wall of REFA channel is the place where there is a flow of reactor water coolant as seen in the figure 4.4. The size of all the gas gaps are minimal and is fixed for all experiments.

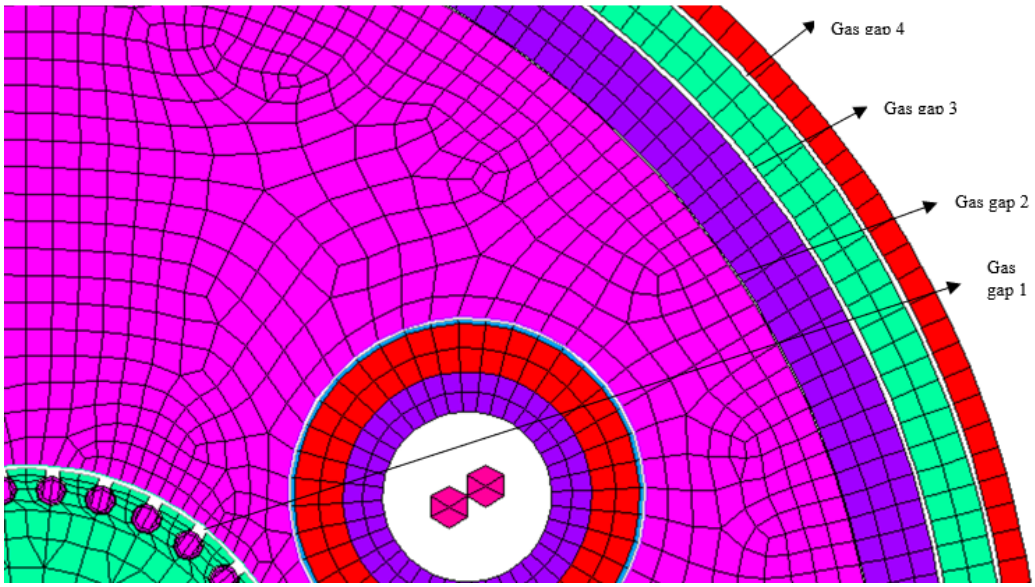

Figure 4.5: Position of Gas Gaps [76]

Boundary Conditions and material properties

All the boundary conditions and material properties were predefined for the model because of pre-existing data of experiments conducted in Oak Ridge research reactor [33]. There are many materials like helium and neon, which are used for these experiments.

The nuclear fission produces the heat in the model in the salt column. This heat is calculated by a thermocouple placed in the facility. A nuclear heating table which contains heat generation values is given to the salt column in the model. A heat transfer coefficient of 30000 $\frac{W}{m^2K}$ is given to the outer surface of REFA channel because of convection, and the temperature of the coolant is given as 45 ^oC. The output obtained from this boundary condition is the temperature distribution in the model.

In Figure 4.3, the model created by AIS has a full geometry because of the usage of professional ANSYS license of NRG. However, the later worked model has 1/3rd of the geometry because of the limitation of ANSYS student license. The 1/3rd geometry of the model worked on ANSYS is shown in Figure 4.6.

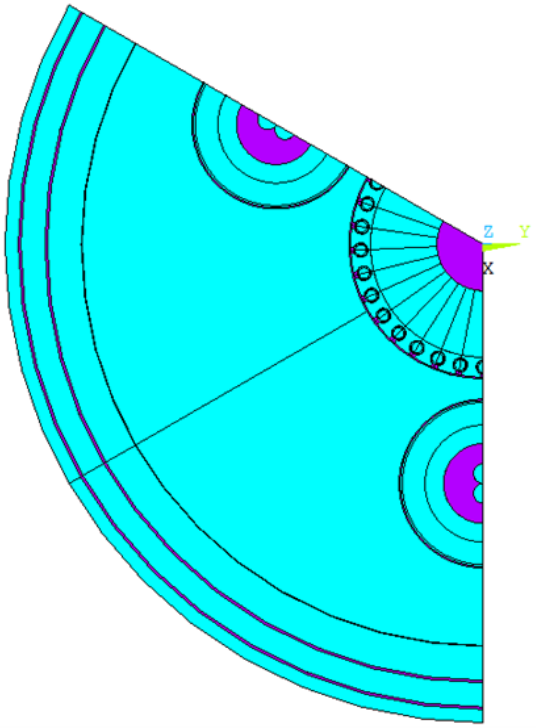

Figure 4.6: 1/3rd of the whole model

4.2 Limitation in the current model

The setup modelling and boundary conditions were predefined for this experiment, but there is a limitation to this model, it does not converge with the latest version of ANSYS APDL. In this analysis, by 'does not converge' it means that the algorithm inside the solver is unable to find an accurate and stable solution to this problem. The only limitation of this model is that it does not converge in the higher version of ANSYS APDL. This section gives a detailed explanation about limitation in SALIENT-03 model.

The model is analysed using direct-coupled field analysis in ANSYS MAPDL. The direct-coupled field is used to solve models in Multiphysics. By Multiphysics, it means that the model can examine fluid-structural interaction where the program determines each physics by itself and carries the resulting values from one physics as a load on the next physics. This type of analysis requires a solution of each physics for every step in the solving process, till points converge [77].

There are many different types of elements in ANSYS that can be used to create the geometry. For a 2D modelling PLANE elements are used. In this Direct-coupled field analysis, the element type PLANE223 has been used. Let us know what PLANE223 element is? PLANE223 is a 2D 8-node couple field solid element, as shown in Figure 4.7. The element has eight nodes with up to five degrees of freedom per node. This element can be used in thermal-structural or couple field analysis and is a quadratic element.

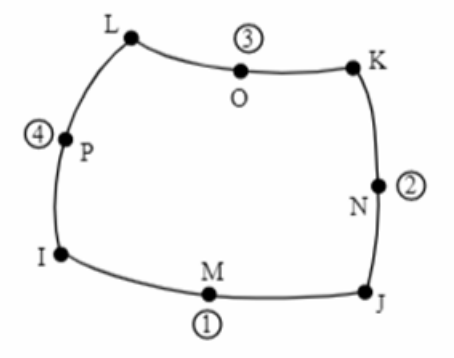

Figure 4.7: PLANE223 Element [77]

This PLANE223 were used to build the SALIENT-03 model in ANSYS MAPDL. However, the problem is that this model with PLANE223 elements only converges in ANSYS MAPDL software which is below Version 16, If the same model is tried to analyse in the latest version of ANSYS APDL then the solution does not converge to give accurate results. The reason why the model does not converge is, consider the SALIENT model in the Figure 4.5, the gas gap in between the components consists of solid PLANE223 elements, just like the components themselves (Gas elements are unselected in that figures shown, the voids are filled with elements in the models). The stiffness of the gas elements in the model is minimal (1000 Pa) when compared stiffness of steel TRIO rigs (200 GPa) in the same model. As the type of analysis is a direct-coupled field, it considers all the multi-physics. In older versions (versions below 16), the gas elements would be able to withstand significant deformation due to stiffness difference without causing convergence issues. The solution convergence was possible because, in older versions of ANSYS APDL, there was an option to turn off the stress stiffening condition during analysis manually. However, in the latest versions of APDL, there is the automatic activation of stress stiffening feature during analysis and the toggle to turn it off (SSTIF, OFF) is also removed. Due to these issue in the latest version, the solution does not converge and give accurate results.

One might ask what this has to do with the PLANE223 elements? PLANE223 element is a quadratic element type, which means that it retains mid-side nodes on elements created in the part or body. The mid-side nodes [M, N, O, and P] can be seen in Figure 4.7. Although using a quadratic element type increases the number of degrees of freedom and accuracy of the analysed results. Nevertheless, in later versions of APDL, due to automatic activation of stress stiffening feature, the mid-side nodes in this quadratic element are shifted away from the shape of the geometry. This type of elements is called as highly distorted elements. Due to this shifting of nodes, the APDL solver cannot relate and solve the equations required to reach an accurate result. An illustration is shown in Figure 4.8. Hence, the solution is said not to be converging at that shifted node; in-turn does not converge the overall solution. We can say that, in this case, automatic activation of stiffness and usage of PLANE223 element type together contribute to the solution not to converge.

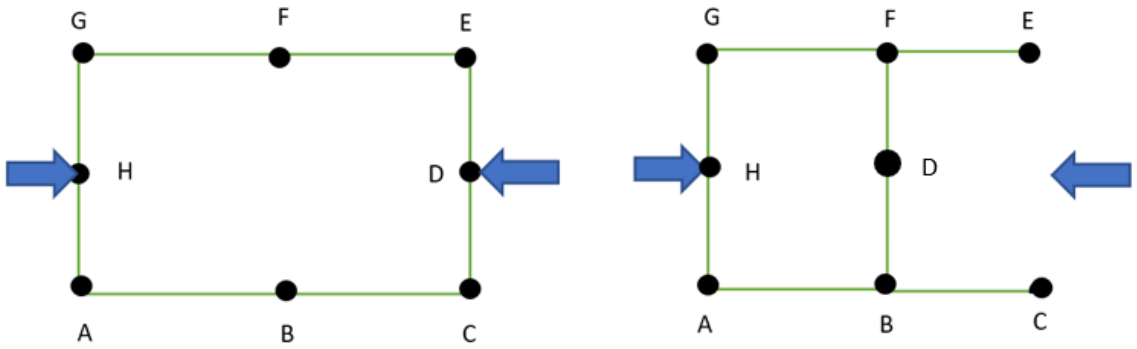

Figure 4.8: Mid-side PLANE223 nodes: a) Aligned b) misaligned (highly distorted) during analysis in higher version of APDL

4.2.1 Requirements for the solution

After knowing the limitation of the current model, the necessary steps should be taken to propose a new solution. There are few requirements for the new solution to have, they are:

1. The newly proposed solution should be able to improve in converging the solution in higher version of ANSYS APDL.
2. The newly proposed solution should have almost the same result accuracy in the higher version of APDL as compared to the older versions.
3. The new solution should apply to all model which have gap gaps

Why is the model to be converged in higher version of ANSYS APDL? To answer this, NRG desires to upgrade and improve in technology by using the latest software of ANSYS. This model successfully converges up to ANSYS version 16, and above that the solution fails in converging. To improve their modelling capabilities and to take advantage of new features in the latest version of ANSYS, the company wants the solution to be converged in the latest/higher version of ANSYS. The next section shows some tried hypothesis to converge the solution in higher version of APDL.

4.3 Tried Hypothesis and Results to Solve for Convergence

The estimated accurate temperature distribution results, at the end of the analyses, will show us if the solution has been converged. The focus in this section is to try and solve the convergence issue of the highly distorted elements in the gas gap by researching different techniques which can be incorporated in APDL. To begin, let us see how temperature distribution of converged and not converged solution of the model looks like in ANSYS APDL Version 14 (V14) and APDL V20 R1 respectively.

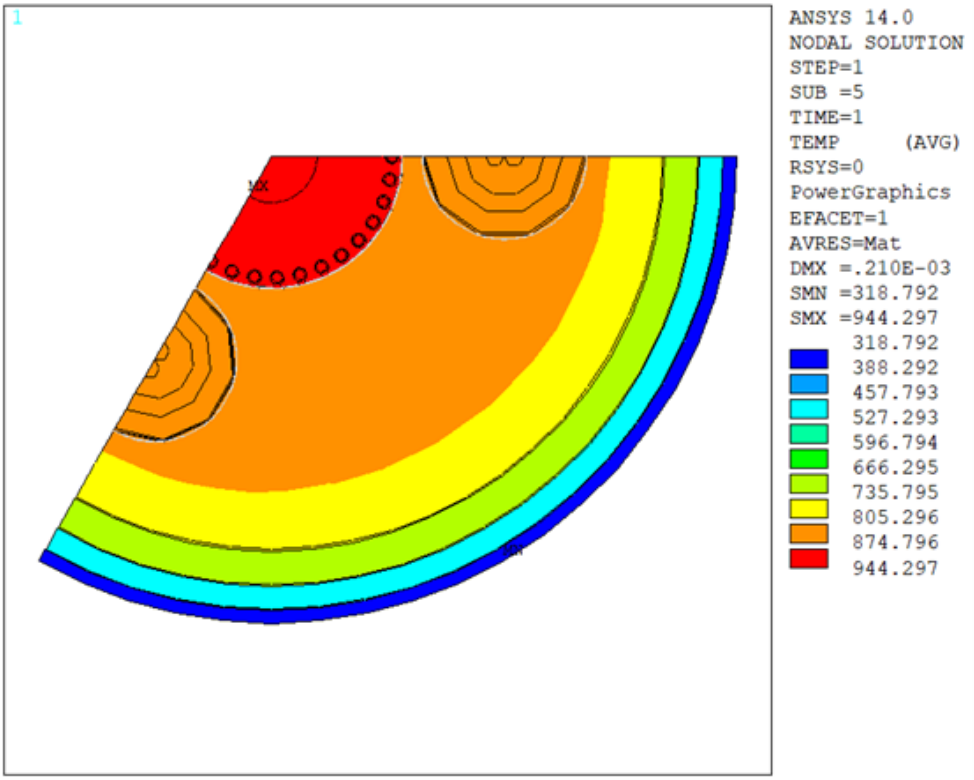

Figure 4.9: A converged solution in ANSYS APDL V14 (lower version) using PLANE223

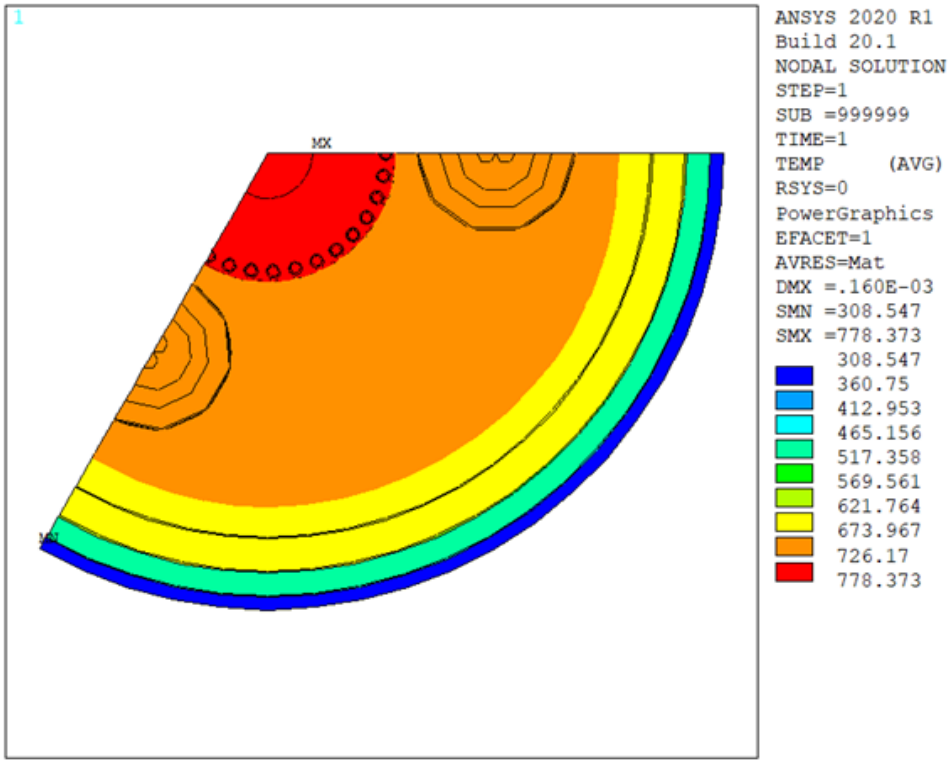

Figure 4.10: Not converged solution in ANSYS APDL V20 (latest version) using PLANE223

Figure 4.9 shows the estimated accurate temperature distribution in the SALIENT-03 model. One of the easy methods to know if the solution is not converged is in Figure 4.10, one can see 'SUB=999999' in the legend. If this type of number is displayed in the number of steps section that means the solution is not converged during analysis, results of such analysis are not to be trusted. As we do not know which technique will work for the highly distorted element convergence problem, below are the things which were tested for the gas gap.

4.3.1 Manual Mesh Rezoning

In a large-deformation investigation, mesh distortion in the elements lowers simulation certainty, creates convergence complications, and can ultimately abort an investigation. The rezoning grants the user to rebuild the distorted mesh and continue the simulation. Rezoning can be performed many times in an analysis. The term manual rezoning means that the user determines when to use rezoning, then a new mesh is generated in that region. During the rezoning process, ANSYS transfers boundary conditions and loads from the original mesh to new mesh.

In order to find on the region to apply manual mesh rezoning, we first consider the SALIENT-03 model (Figure 4.6) in the latest version (V20) of ANSYS APDL. The analyses time is set to 1 (TIME=1). However, during analysis, the solution does not converge at TIME=0.603, as shown from the APDL command image in Figure 4.11. If we see Figure 4.11 at 67th sub-step (i.e. TIME=0.602) the solution converges and goes to the next point, but at TIME=0.603, the solution stops, and SUB=999999 is displayed. The temperature distribution increases initially and stops at TIME=0.603, due to divergence

in the model, as shown in Figure 4.12. After a study, it is found that the element number 752 (ELEMENT=752) is the element which is highly distorted inside the gas gap 2 in the model [refer Figure 4.5], because of the highly distorted ELEMENT=752 the solution does not converge at TIME=0.603. In the complete analysis, this element number 752 is the first point where the solution fails to converge. If the ELEMENT=752 is removed from the analysis, then the next element in gas gap two, i.e., ELEMENT= 758 does not converge. With this, we can say that it would be efficient if the whole area of gas gap two is considered for rezoning.

```
67 0.60264          1          67         888
68 0.60314          1          68         903
69  1.0000          1      999999         907
```

Figure 4.11: The time point where the solution does not converge in higher version of ANSYS APDL

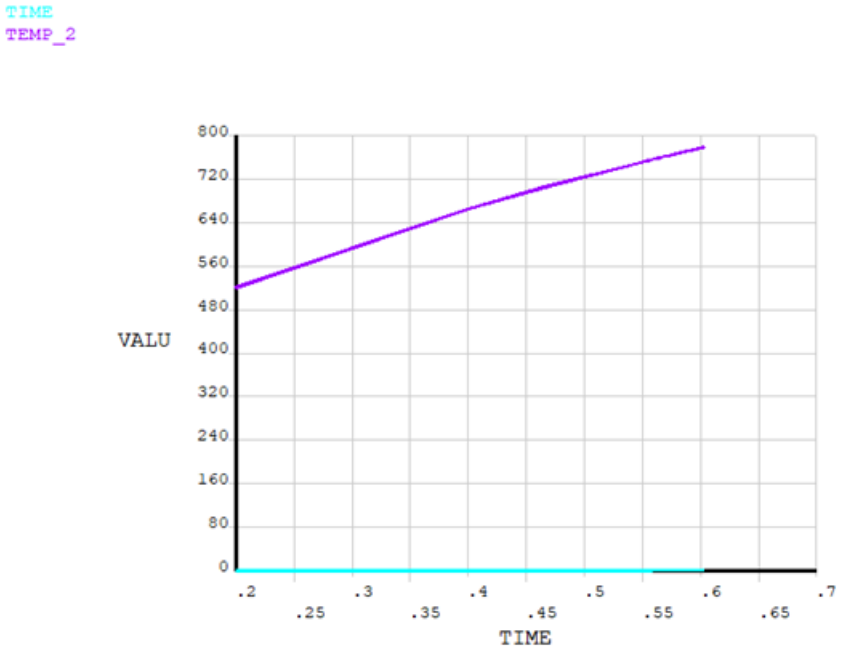

Figure 4.12: The time and temperature value at the point of not converged solution in higher version of APDL

So, the manual rezoning was applied to the ELEMENT=752 and whole area of gas gap 2. After rezoning the convergence in the ELEMENT=752 was solved, but it gave rise to a new distorted element in the model. Now the solution passes TIME=0.603 mark and goes up-to TIME=0.706, but at that time, it again does not converges due to another distorted element as shown in iteration plot of APDL in Figure 4.13. If this is continued, it will create a loop where other elements were distorted after solving one, and the individual rezoning process for the element would be time-consuming. So, all the possible gas gaps containing distorted elements were selected at once for manual rezoning. After rezoning the whole gas gaps, the solution does not converge fully in this model. It may be because initially the model was constructed by AIS, using the professional license of ANSYS in NRG. However, due to licensing limitation, 1/3rd portion of the model is used in the student ANSYS version, this model was not intact for the rezoning. The contacts at the sides of the model were open, which interfered

in the manual rezoning process. Nevertheless, using this method, the solution of this model in the higher version of ANSYS APDL was partially converged 18 percent more with regards to convergence time, than the previous regular analysis, this can be seen in Figure 4.14 where the temperature result is increased from 778.37 ^oC(from figure 4.10) to 797.93 ^oC and getting close to converged solution results in Figure 4.9.

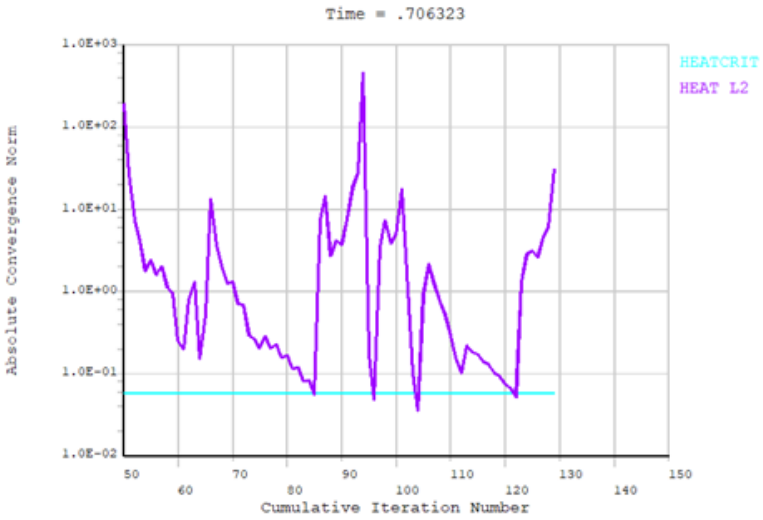

Figure 4.13: Iteration time, and convergence after rezoning (TIME=0.706)

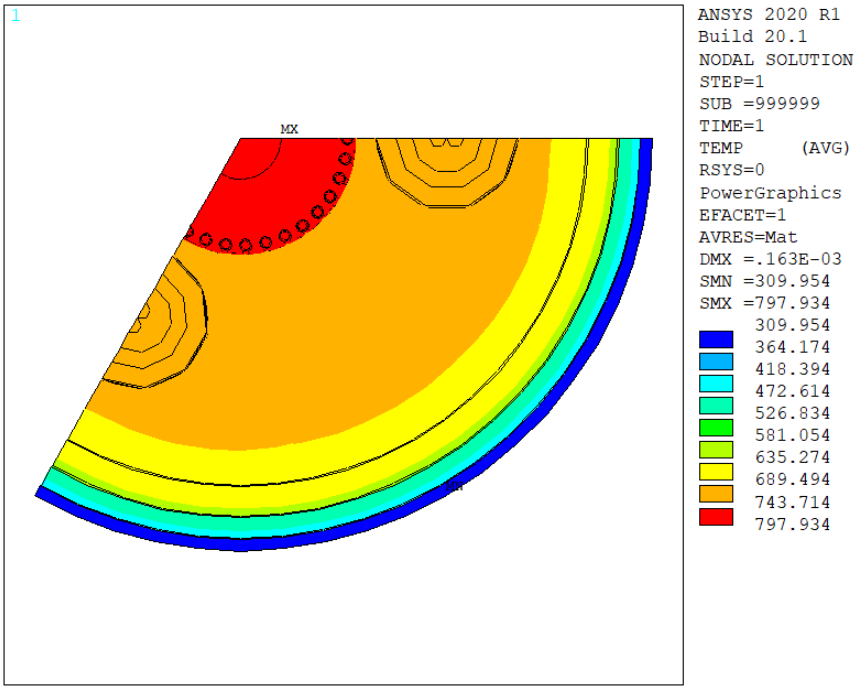

Figure 4.14: Partial convergence plot at TIME=0.706

As open ends of the 1/3rd portion of the model were causing hindrance in manual rezoning. It was decided to test this hypothesis of manual rezoning works for gas gap elements. The intent to check this manual rezoning hypothesis on another model is to know whether the solution would converge, and rezoning method would create a rezoned mesh in the gas gap during analysis. To apply this hypothesis, a model created by infinite was used, which had three fully closed solids and a gas gap in between them, as shown in Figure 4.15. This model was analysed in a higher version of ANSYS APDL. For analysing to see if rezoning work in the gas gap, a higher displacement value was given to solid one seen in Figure 4.15.

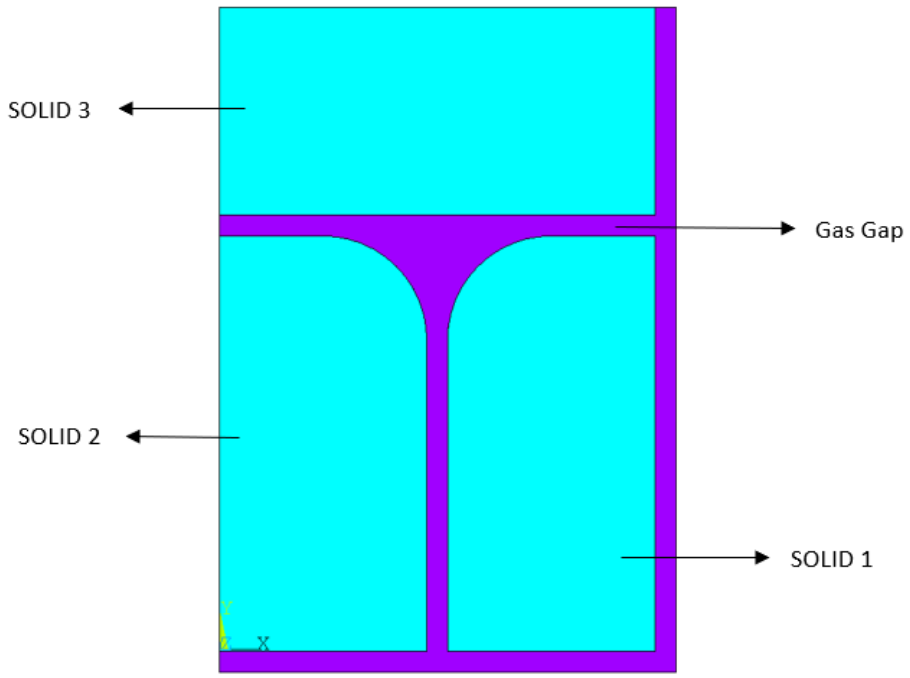

Figure 4.15: A solid model containing gas gaps in between

Along with the displacement, a heat generation table was given to gas gaps, and the analysis was carried out. The first analysis was done without using rezoning, and it was found that the solution does not converge in the gas gaps with PLANE223 in higher version of APDL as seen in the Figure 4.16. However, later in another analysis, the manual rezoning was applied to the whole gas gap, this time, the solution converged in higher version of APDL as shown in Figure 4.17. We can see the difference in the initial mesh and final mesh of the analysis with manual rezoning in Figure 4.18 and Figure 4.19.

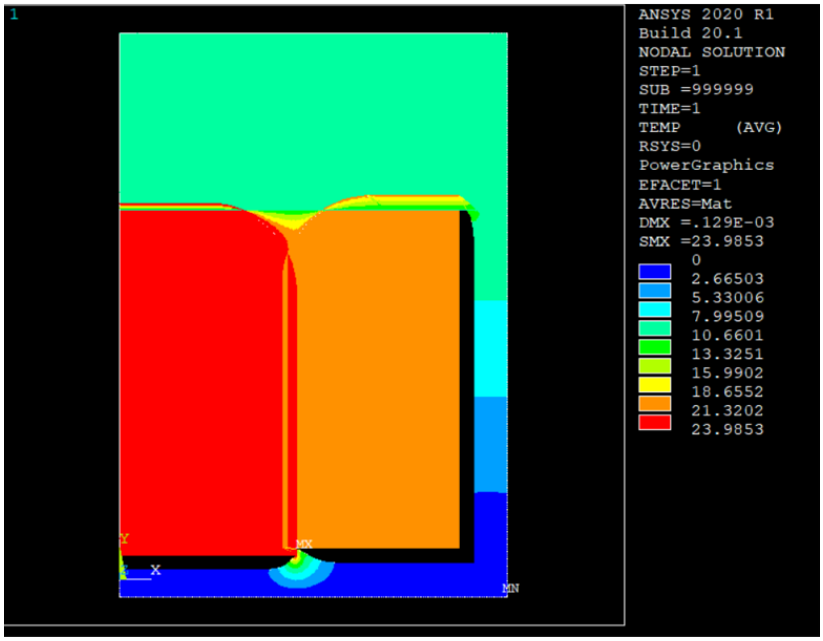

Figure 4.16: Not converged results of the model before manual mesh rezoning

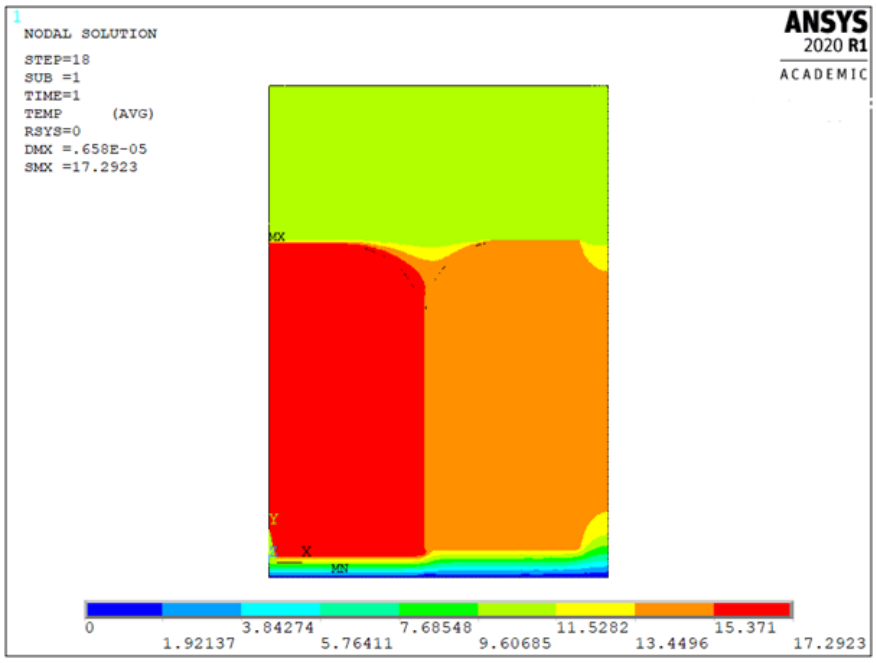

Figure 4.17: Converged solid model after rezoning in higher version of APDL with gas gaps

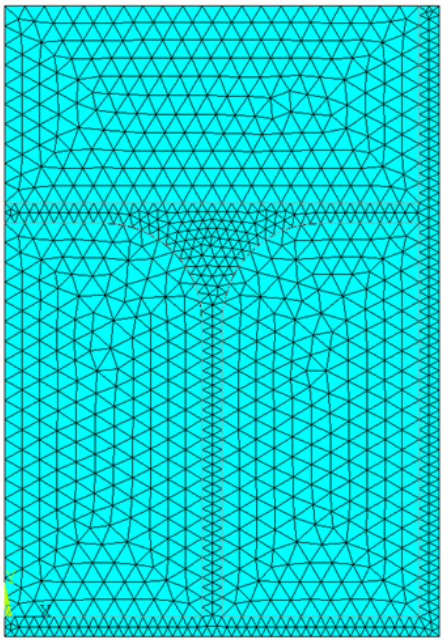

Figure 4.18: Initial mesh during analysis

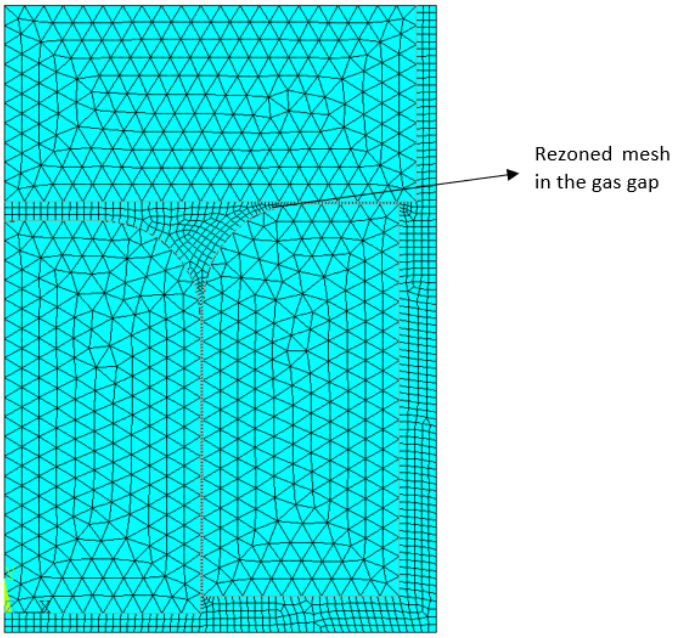

Figure 4.19: Final mesh after rezoning

With this analysis, we can say that it is possible to apply manual rezoning in the gas gap, which creates full rezoned mesh during analysis. The only thing necessary for this hypothesis to work is to have an entirely solid model with all the contacts bonded and intact. Based on this analysis, we can say that this hypothesis could be tried and used on the whole geometry of the SALIENT-03 model, and this may help to converge the solution in higher version of ANSYS APDL.

4.3.2 Mesh Adaptability

The ANSYS program provides predicted techniques for estimating mesh discretization error for definite sorts of analyses. Apart from using the mesh rezoning, this mesh adaptability hypothesis is also tested for the gas gaps. By adopting this type of technique, the program can then detect if an appropriate mesh is sufficient enough. If not, the program will automatically refine the mesh so that the measurement error will decrease and the solution can proceed- this process of automatically evaluating mesh discretization error and refining the mesh, called adaptive meshing.

This technique was used in ANSYS Workbench but not in ANSYS APDL because to try to widen the analyse solution area of the SALIENT-03 model and to see if this type of analysis works in another format of the software. As it is technically not possible to directly open the SALIENT-03 APDL model in ANSYS Workbench. So, a model was constructed in workbench, which resembles SALIENT-03 functions and with a gas gap, as shown in Figure 4.20. As the SALIENT-03 model was a 2D model, a 2D model in the workbench is considered to try this technique. The model in the workbench is made to have the same boundary conditions as in SALIENT-03 model with the same amount of nuclear heat generation.

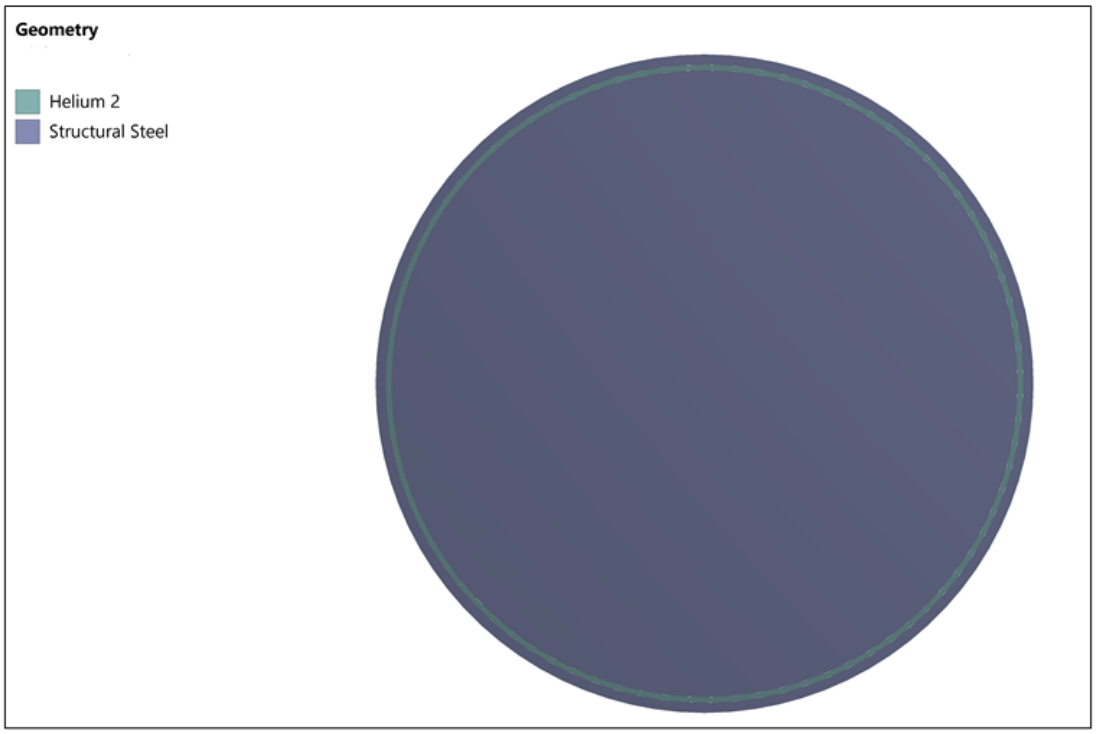

Figure 4.20: 2D Geometry in workbench

Figure 4.20 is like SALIENT-03 model; there are two surfaces which are dived by helium gas. There is a gap between the steel structure, which is assigned with helium properties to consider the gas as a gas gap. This model is relatively simple; it has one surface inside which resembles the salt column in the SALIENT-03 model and one outer surface which is in contact with reactor coolant. Nuclear heating table with heat generation value of 20000000 $\frac{W}{m^3}$ is given to the central part of this model. This heating value is a bit higher than the SALIENT-03 heat generation value, i.e. 17761312.8 $\frac{W}{m^3}$, to have some tolerance due to shape. Convection of 30000 $\frac{W}{m^2K}$ and ambient coolant temperature of 45 ^oC is applied to the outer surface of the workbench model. The mesh adaptability setting is turned on and is applied to the single gas gap. With all these conditions, the analyses are carried, and this model converges and produces converged results in ANSYS Workbench, as shown in Figure 4.21.

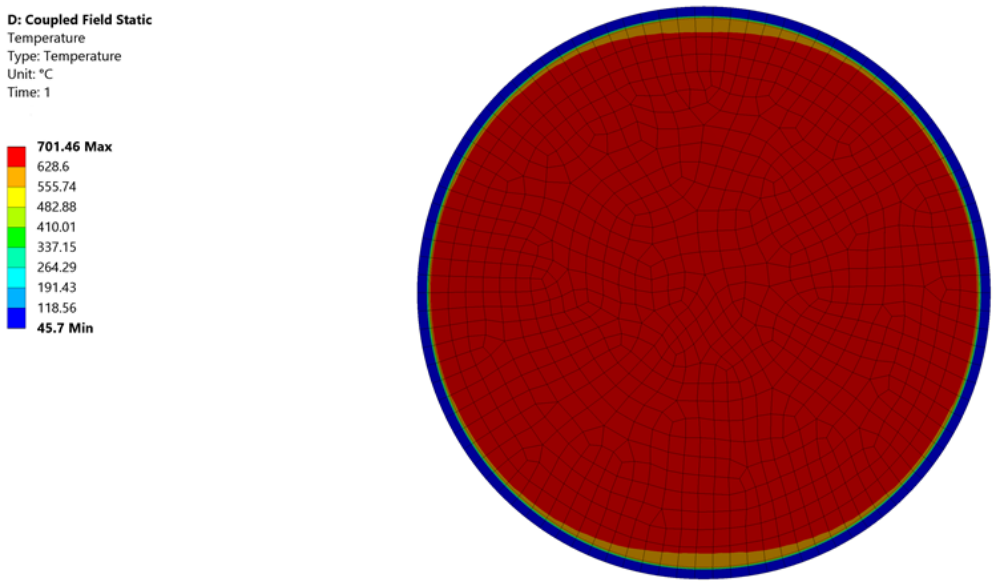

Figure 4.21: Converged solution in workbench

This technique is useful as it gets the solution to converge but to be applied to SALIENT-03, the model needs to be recreated in workbench. The SALIENT-03 solution could be converged in workbench, but there are few limitations to use the workbench for this model, which will be discussed in chapter 5.

4.3.3 Transient Analysis

All the previous hypothesis were based on either static or static-thermal analysis (couple field). To try to solve the SALIENT-03 model in higher version of APDL, we will now consider the transient analysis in APDL. A transient thermal analysis is where the applied load is a function of time. To specify time-dependent loads, we first divide the load-versus-time curve into load steps. To transient analyse the SALIENT-03 model in APDL V20, we have divided the load cycle into five steps, and the analysis is done for TIME= 3600 sec with all the same features of SALIENT-03 such as same boundary conditions as previous and same element types (PLANE223). As the SALIENT-03 model had many open contacts inside the model, hence, there was no proper separation of elements. So, all the element contact in the model are separated and later bonded together in a better way. In Figure 4.22, the red colour shows the elements are in full contact, and orange shows sliding contact and yellow shows near contact elements. To transient analyse the model, the contacts were improved, leaving only a few far open contacts elements as seen in Figure 4.22.

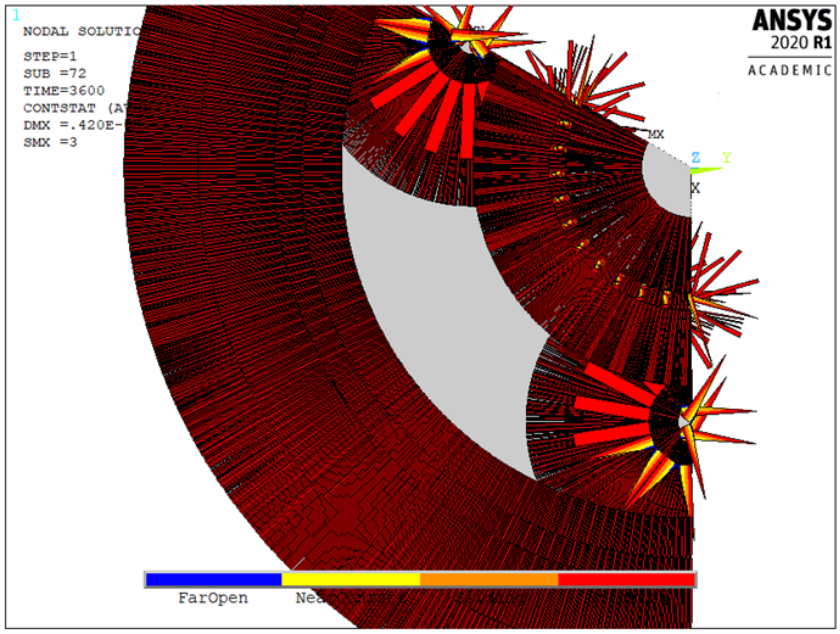

Figure 4.22: Contact in between elements

After the contact improvement, the transient analyses were carried out in the higher version of APDL (V20). The final solution converged for the SALIENT-03 model with original element type PLANE223, as seen in Figure 4.23.

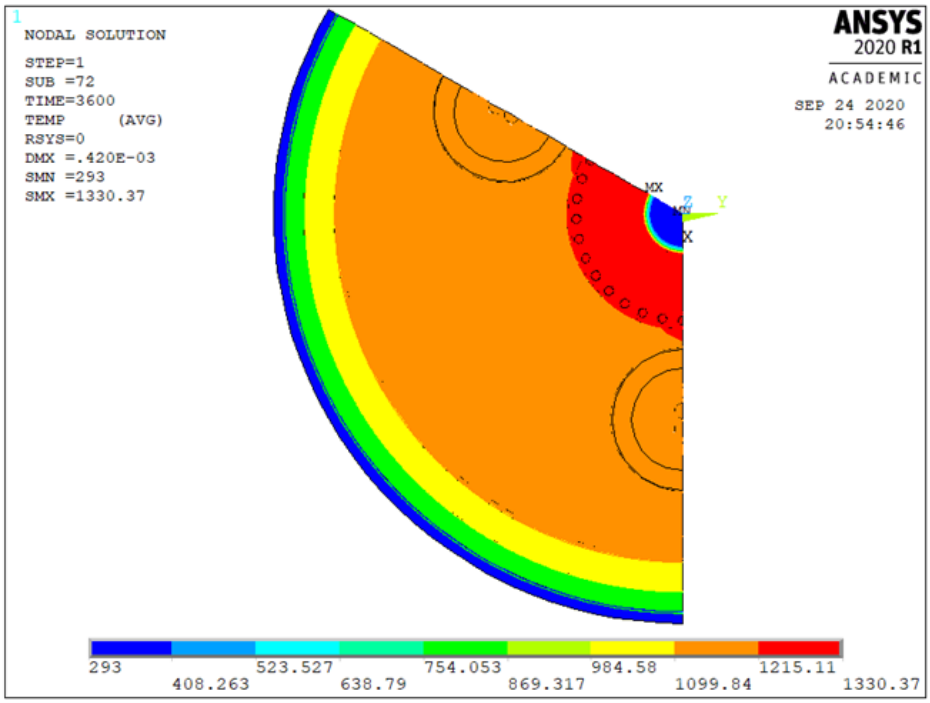

Figure 4.23: The converged solution of transient analysis of SALIENT-03 model in APDL V20

A thermal transient analysis could be used to calculate the temperature distribution in the SALIENT-03 model. But there are also limitiation to this hypothesis which will be discussed in chapter 5.

4.3.4 Element type PLANE222

The SALIENT-03 model is made up of the element type PLANE223, which is a quadratic element. However, what if we use element type PLANE222? First let us see, what is element type PLANE222?

PLANE222 is a 2D 4-Node Coupled field solid element, as shown in Figure 4.24. It is a four-node element with up to three degrees of freedom. This element type can also be used for both couple-field and structural-thermal analysis. PLANE222 is a linear element.

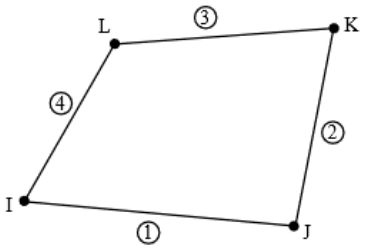

Figure 4.24: PLANE222 element type [77]

The difference between element type PLANE223 and PLANE222 is the former is quadratic, and the latter is a linear element. Linear element is the one which does not have any mid-side nodes as compared to quadratic, as seen in Figure 4.24. Due to the missing of mid-side nodes, the linear element PLANE222 has a smaller number of degrees of freedom compare to quadratic element PLANE223.

Suppose the SALIENT-03 model is built with the element type PLANE222 instead of PLANE223. In that case, the solution of the whole model converges in any version of ANSYS APDL without applying any techniques or hypothesis. Now one can ask how PLANE222 will converge? The answer is the same as in Figure 4.8, but considering PLANE222, this element type has only 4-nodes at each one of the nodes is placed at the corner. Hence, there is significantly less chance of an intact corner node to be misaligned or distorted during analysis, unlike in the case of PLANE223 where there is high probability of mid-side element to be displaced or distorted.

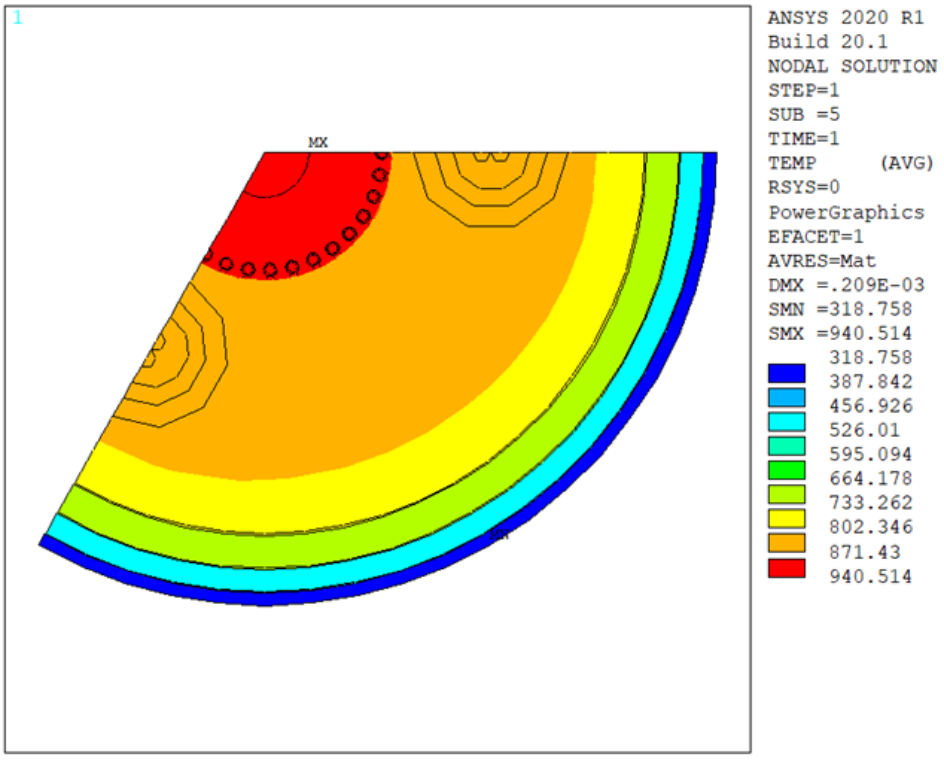

Figure 4.25: The converged solution in V20 just by changing from PLANE223 to PLANE222

Although element type PLANE222 is the easy solution to converge the model in any version of ANSYS APDL, there are a few downsides to it. The major downside is that the PLANE222 is a linear element which has 4-nodes, which means the number of nodes in the element will be less and because of less number of nodes the accuracy of the results will also be slightly less when compared with 8-node element solutions. As PLANE222 has 4-nodes and three degrees of freedom, it is less flexible at the corners. In Figure 4.25 and Figure 4.9 are compared, we can see that the former results are slightly less accurate because of the usage of PLANE222 in the former. However, in general, if PLANE222 elements are used, then the SALIENT-03 model will converge in any ANSYS APDL versions without any additional technique/hypothesis.

Chapter 5

Discussion

This chapter discusses the outcome of the results reported in Chapter 3 and Chapter 4. It will be discussed accordingly.

5.1 Modelling and thermal analysis of the PWR

1. Average skewness value of the model before refinement was 0.547, but after refinement, the average skewness value was found to be 0.443. In the skewness mesh metrics, it is defined that the closer the average skewness value is to zero, the better the mesh. Hence, there was 23.47 percent increase in quality of the mesh.
2. Initially, an automatic mesh feature of ANSYS Workbench was used in the reactor pressure model. The time required to simulate the solution was two days and nine hours using an iterative solver type. Later the automatic generated mesh was refined to remove unnecessary elements in the baffle and formers, and make a smooth quadratic mesh by adding methods like body sizing, sweep method and multizone. After refining, a direct solver was used for the transient thermal analysis because of its efficient memory requirement. The simulation time was reduced to 1 hour 20 min.
3. The thermal distribution results highly depend upon the imported heat generation from MCNP neutronic calculation and on the applied boundary conditions.
4. To validate the simulated thermal distribution, the thermal capacity in the real-life reactor core of a nuclear power plant is considered. This validation is highly dependent on the mass flow rate of the feedwater, velocity of the feedwater inside the RPV. The validation of the simulation results are still affected by errors whose origins can be attributed to several reasons as, approximations in the numerical solution, and imperfect knowledge of boundary and initial conditions.

5.2 Convergence in SALIENT Experiment Model

1. After analysis in higher version of ANSYS APDL, it was found that the highly distorted elements that hinder the convergence of the solution were situated in gas gap 2 counted from inside of

the SALIENT model (refer figure 4.5).

2. Suppose the code of the model which is converged in the lower version of ANSYS APDL (example APDL version 14) is used and simulated in the higher version of ANSYS APDL (version 20) without any functional addition to the code. In that case, it converges until TIME=0.603 sec. If manual mesh rezoning function is added to the model, then it converges until TIME=0.706 sec in higher versions. This rezoning gives 18 percent improvement with respect to convergence time of the model when compared to the previous model.

3. The gas gap model was created by AIS team at NRG using a professional ANSYS license, but due to limitations of ANSYS student license 1/3rd part of the model was considered for analysis. Due to the usage of the 1/3rd part of the model, there were open ends at the corner of the model. The manual rezoning could not be applied at those open ends. Hence, manual rezoning only could improve 18 percent convergence. A further study can be done to apply manual rezoning on the whole model and to check if the solution may converge.

4. The requirements of the new solution stated that the solution could be applied to any gas gap model. It was decided that the manual rezoning hypothesis be tested on a gas gap in a different model (refer figure 4.15). This manual rezoning hypothesis was successfully converged on this whole model in higher ANSYS versions.

5. By using the technique described in section 4.3.2, this SALIENT model could be created in Ansys Workbench, and the solution can be converged. Workbench does not give flexibility to the user to do certain things which are not predefined by ANSYS.inc in the software program. However, the main limitation that was found out after creating and analysing this model described in section 4.3.2 was that the solution would converge for a gas gap but with the limited value of heat generation. The convergence of the gas gap model fails if the heating value increases above 2E+08 $\frac{W}{m^3}$. The heating value for the SALIENT experiment model was 1.7E+07 $\frac{W}{m^3}$ which was well below the limit for the model in section 4.3.2. Hence, the solution was converged, but a further in-depth study must be done on this analysis before implying to the whole SALIENT experiment models.

6. The temperature in the transient analysis, as seen in figure 4.23 is much higher compared to figure 4.9. It is because figure 4.9 is a steady-state analysis, while figure 4.23 is a transient analysis. The steady-state solves the problem by considering time as infinite, while transient analysis considers a specific time given to the analysis by the user. In section 4.3.3, the time that was given to the transient analysis was 3600 seconds. It should be known that at this specific time, i.e., 3600 seconds, the temperature is high as compared to steady-state. However, eventually, at the time nearing to infinite, the transient state analysis results will be equal to the steady-state analysis results. With this, we can say that the transient temperature is higher at 3600 seconds when compared to steady-state temperatures, but eventually with time, for example, say if the analysis is run until 86400 seconds then maybe the transient temperatures will be near equal to the steady-state. This model was also checked for 61000 second, but still at that point of time the solution slightly improves but does not reach the temperatures similar to temperatures as seen in figure 4.9 (steady-state). Moreover, the time where the transient analysis reaches steady state will be different for different gas gap models, if exact time inputs

are unknown for the specific model then it will be a lengthy task to apply transient analysis. As this part of work is limited, a detailed transient study for the experimental model should be carried to exactly know the limitations to be applied to SALIENT models.

7. In the section 4.3.4, the thermal distribution results are slightly less accurate as seen in the figure 4.25 because of using linear PLANE222 element when compared to results in the figure 4.9 which uses quadratic PLANE223 element type. The results are less accurate while using PLANE222 element because it has four nodes (refer figure 4.24) with up to three degrees of freedom per node when compared to PLANE223 which has eight nodes with up to five degrees of freedom per node. DOF associated with PLANE222 has less possibility to move in defined direction, and carry less information about thermal temperatures. Hence, the results are slightly less accurate.

Chapter 6

Conclusions and recommendations

In this chapter, the conclusions and recommendations that are drawn from the work presented in this thesis are reported.

6.1 Conclusions

The main objective of this thesis was to develop and improve the modelling capabilities of reactor vessel internals. This goal was achieved for Nuclear Research and Consultancy Group (NRG) using ANSYS Workbench and Mechanical APDL. The work started with research and understanding the concept and process of nuclear energy and various nuclear reactor types. The configurations and working of a pressurized water reactor model created by AIS was refined with mesh to have an overview of the real-time thermal distribution in the vessel internals. Due to working from home situation, the work was slightly shifted to develop and improve the SALIENT experiment model, which is a facility/experiments that are radiated inside the reactor core to help in developing a new type of reactor. Therefore, each research question was answered separately in the previous chapters. Therefore, the conclusion will not be expressed in values but in achievements, and can be summarized as follows,

- The transient analysis is highly dependent on the time, temperature, and boundary conditions, i.e. the start-up loading conditions and the reference temperature of a nuclear reactor.
- Thermal transient temperature distribution in the reactor pressure vessel of a PWR was successfully implemented, and the results of analysis depict almost real-life scenario of that specific pressurized water reactor.
- Many potential solutions to converge the molten salt experiment model were studied and tested in higher versions of ANSYS MAPDL, which are described in Chapter 4. These potential solutions moderately help to improve the model capacity of SALIENT experiments.
- Some of the potential solutions converge partially on the SALIENT-03 model, and some other converge totally, which are described in Chapter 4. A further research for some of the hypothesis is necessary to successfully implement it to the model.

In conclusion, all these findings and results tend to develop and improve the modelling capacity and capability of the pressure vessel. These improvements in the modelling capabilities will help to efficiently use the pressure vessel and to develop a new type of reactor. An initial study to converge the molten salt model was done which would indirectly be used in the research conducted by the Dutch Molten Salt Program. Furthermore, detailed research and integration of different techniques described in Chapter 4 should be conducted to implement it to the SALIENT-03 model successfully.

6.2 Recommendations

The thesis work is a part of broad research in the nuclear industry. Although the thesis deals with thermal temperature distribution and convergence in the model. A few recommendations can be made,

- The transient simulation results for the reactor vessel were validated for the real-life nuclear power plant. Hence, this data can be used in the future analysis of the specific nuclear power plant.
- The mass flow rate and velocity of feedwater for the reactor vessel were updated and should be carefully examined and applied if necessary in future analysis.
- The mesh quality and computational time were balanced. Hence, the RPV model can be used further in future analysis.
- Although the results of rezoning for the molten salt experiment model were partially converged, a further study on manual mesh rezoning is recommended to be applied to the whole SALIENT model.
- Creating the molten salt model in ANSYS workbench has a few limitations based on the flexibility of the software. Although the results converge for this molten salt experiment model, an in-depth study is needed to check its applicability for gas gap model with high heat generation.
- The PLANE 223 element in the molten experiment model can be changed to PLANE 222 to converge in the higher version of APDL because, in this particular molten salt model, the difference in accuracy is slight. Hence, this can be applied while considered some percentage of error in the model.

6.2.1 Recommendations based on literature

- ANSYS has many advantages for its usage in energy industry, but ABAQUS could be used for non-linear analysis as it performs better in that specific field. This will make the company more diversified in the usage of analysing softwares.

Bibliography

[1] R. L. Murray and K. E. Holbert, “Nuclear energy: An introduction to the concepts, systems, and applications of nuclear processes: Seventh edition.” Elsevier Inc., 2014, pp. 1–550.

[2] World Nuclear Association, “World Nuclear Performance Report 2018,” Tech. Rep., 2018. [Online]. Available: http://www.world-nuclear.org/getmedia/b392d1cd-f7d2-4d54-9355-9a65f71a3419/performance-report.pdf.aspx

[3] J. Conca, “Is Nuclear Power A Renewable Or A Sustainable Energy Source?” vol. 15, pp. 1–6, 2016. [Online]. Available: https://www.forbes.com/sites/jamesconca/2016/03/24/is-nuclear-power-a-renewable-or-a-sustainable-energy-source/#59bd4c6f656e

[4] Foro de la Industria Nuclear Española, “What are the new reactors of the future?” n.d. [Online]. Available: https://www.foronuclear.org/en/updates/in-depth/what-are-the-new-reactors-of-the-future

[5] NRG, “NRG and PALLAS appoint Bertholt Leeftink (CEO) and Gerrit Zalm,” 2020. [Online]. Available: https://www.nrg.eu/en/news/nrg-and-pallas-appoint-bertholt-leeftink-ceo-and-gerrit-zalm

[6] E. D’Agata, C. Ohms *et al.*, “Operation and Utilisation of the High Flux Reactor EUR 27340 EN,” 2015.

[7] NRG, “World Leader in Medical Research,” 2020. [Online]. Available: https://www.nrg.eu/en/research-development/medical-research

[8] P. Y. Thro, J. Pierre *et al.*, “European Research Reactor Position Paper for DGE Energy - 2018 report,” Tech. Rep., 2018.

[9] Tetzemann, “Petten Forschungs reaktor,” 2019. [Online]. Available: https://en.wikipedia.org/wiki/Petten_nuclear_reactor#/media/File:Petten_Forschungsreaktor.jpg

[10] Union of Concerned Scientists, “How Nuclear Power Works,” 2014. [Online]. Available: https://www.ucsusa.org/nuclear-power/nuclear-power-technology/how-nuclear-power-works

[11] A. Potsi, “The Capability Approach and Early Childhood Education Curricula,” 2016.

[12] B. Priddy, “What Is the Safest Energy Source?” 2017. [Online]. Available: https://sciencing.com/what-is-the-safest-energy-source-13637377.html

[13] Danny, “Nuclear Fission Stock Illustrations,” Dreamstime. [Online]. Available: https://www.dreamstime.com/illustration/nuclear-fission.html

[14] Foro de la Industria Nuclear Española, “How does a nuclear power plant work?” September 2007. [Online]. Available: https://www.foronuclear.org/en/nuclear-power/how-does-a-nuclear-power-plant-work/

[15] P. K. Kanti and N. Sanathkumar, “A Review Paper on Nuclear Power Plant and Its Importance in Indian Economy,” *International Journal of Engineering Trends and Technology*, pp. 244–247, 2016.

[16] G. Choppin, J.-O. Liljenzin *et al.*, “Principles of Nuclear Power,” in *Radiochemistry and Nuclear Chemistry*, 2013, pp. 595–653.

[17] World Nuclear Association, “How does a nuclear reactor works,” n.d. [Online]. Available: https://www.world-nuclear.org/nuclear-essentials/how-does-a-nuclear-reactor-work.aspx

[18] R. Nave, “NUCLEAR BINDING ENERGY,” *School Science and Mathematics*, vol. 74, no. 5, pp. 436–436, 1974. [Online]. Available: http://hyperphysics.phy-astr.gsu.edu/hbase/NucEne/nucbin.html

[19] Mux’s blog, “Fission reactors,” 2017. [Online]. Available: https://ssj3gohan.tweakblogs.net/blog/15349/lets-look-at-nuclear-power-part-3-fission-reactors

[20] OpenStax, “Carnot’s Perfect Heat Engine: The Second Law of Thermodynamics Restated,” 2011. [Online]. Available: https://courses.lumenlearning.com/physics/chapter/15-4-carnots-perfect-heat-engine-the-second-law-of-thermodynamics-restated/

[21] “Nuclear Fuel,” Nuclear Power, 2020. [Online]. Available: https://www.nuclear-power.net/nuclear-power-plant/nuclear-fuel/

[22] Foro de la Industria Nuclear Española, “Infographics - Foro Nuclear,” n.d. [Online]. Available: https://www.foronuclear.org/en/resources/infographics/

[23] J. C. Bryan, *Introduction to Nuclear Science*, 3rd ed. CRC Press, 2018.

[24] B. Afework, J. Hanania *et al.*, “Neutron Moderator,” *Energy Education University of Calgary*, 2018.

[25] Ian Hore-Lacy, *Nuclear Energy in the 21st Century*, 1st ed. USA: Elsevier Inc, 2018.

[26] B. Afework, J. Hanania *et al.*, “Control rod,” University of Calgary Energy Education, 2018. [Online]. Available: https://energyeducation.ca/encyclopedia/Control_rod#cite_ref-RE1_2-2

[27] A. Singh, “Study of Functioning of Nuclear Power Reactors,” *International Research Journal of Engineering and Technology*, June 2020.

[28] World Nuclear Association, “Nuclear Power Reactors,” 2020. [Online]. Available: https://www.world-nuclear.org/information-library/nuclear-fuel-cycle/nuclear-power-reactors/nuclear-power-reactors.aspx

[29] “Safety of Nuclear Power Reactors,” World Nuclear Association, 2019. [Online]. Available: https://www.world-nuclear.org/information-library/safety-and-security/safety-of-plants/safety-of-nuclear-power-reactors.aspx

[30] Coast News wire services, “County extends agreement on shuttered San Onofre nuclear plant,” The Coast News Group, June 2020. [Online]. Available: https://thecoastnews.com/county-extends-agreement-on-shuttered-san-onofre-nuclear-plant/

[31] International Atomic Energy Agency, “Utilisation related design features of research reactors: a compendium,” Vienna, Tech. Rep. 87–100, 2007.

[32] European Comission, “High Flux Reactor (HFR) Petten, Characteristics of the installation and the irradiation facilities,” p. 196, 1993.

[33] P. R. Hania, “The Salient Fluoride Fuel Salt Irradiations,” p. 19, 2016. [Online]. Available: https://public.ornl.gov/conferences/MSR2016/docs/Presentations/MSR2016-day1-17-Ralph-Hania-The-SALIENT-Fluoride-Fuel-Salt-Irradiations.pdf

[34] G. Zwartsenberg, “‘Petten’ has started world’s first MSR-specific thorium fuel irradiation experiments in 45 years,” 2017. [Online]. Available: https://www.thmsr.com/wp-content/uploads/2020/05/20170810-SALIENT-for-thmsr-inp-april-3-processed.pdf

[35] World Nuclear Association, “Molten Salt Reactors,” 2018. [Online]. Available: https://www.world-nuclear.org/information-library/current-and-future-generation/molten-salt-reactors.aspx

[36] R. K. Nanstad and W. Server, “Reactor Pressure Vessel Task of Light Water Reactor Sustainability Program: Assessment of High Value Surveillance Materials,” Oak Ridge National Laboratory, Tech. Rep., June 2011.

[37] Westinghouse, “Reactor Vessel and Internals,” Westinghouse Technology Systems Manual, n.d. [Online]. Available: https://www.nrc.gov/docs/ML1122/ML11223A212.pdf

[38] Nuclear Power, “Reactor Pressure Vessel,” 2003. [Online]. Available: https://www.nuclear-power.net/nuclear-power-plant/nuclear-reactor/reactor-pressure-vessel/

[39] J. M. Collado, “Design of the reactor pressure vessel and internals of the IRIS integrated nuclear system,” in *International Congress on Advances in Nuclear Power Plants - Proceedings of ICAPP*, 2003.

[40] International Atomic Energy Agency, “Integrity of Reactor Pressure Vessels in Nuclear Power Plants: Assessment of Irradiation Embrittlement Effects in Reactor Pressure Vessel Steels,” IAEA Nuclear Energy Series, Vienna, Tech. Rep., 2009.

[41] G. Harold, “Laminar Flow vs. Turbulent Flow,” Reactor Physics, 2019. [Online]. Available: https://www.reactor-physics.com/engineering/fluid-dynamics/laminar-flow-vs-turbulent-flow/

[42] R. Skilton, “New Applications of Flow Chemistry in Industry and Academia,” Tech. Rep., 2006. [Online]. Available: https://www.vapourtec.com/wp-content/uploads/2017/07/Advanced-Flow-Chemistry-NiceFlow-2017.pdf

[43] R. Skilton, “Laminar and turbulent flow,” Vapourtec, 2020. [Online]. Available: https://www.vapourtec.com/flow-chemistry/laminar-turbulent/

[44] B. Rehm, D. Consultant *et al.*, “Situational Problems in managed pressure drilling,” in *Managed Pressure Drilling*. Elsevier Science, january 2013, pp. 39–80.

[45] Y. Haseli, “Fundamental concepts,” in *Entropy Analysis in Thermal Engineering Systems*. Academic Press Elsevier, January 2019, pp. 1–11.

[46] John D. Anderson, *Fundamentals of Aerodynamics*, 4th ed. Singapore: Mcgraw-Hill Series in Aeronautical and Aerospace Engineering, 2005.

[47] n.d, “Convective heat transfer,” Wikipedia, 2020. [Online]. Available: https://en.wikipedia.org/wiki/Convective_heat_transfer

[48] S. Moaveni, *Finite element analysis — theory and application with ANSYS*, 4th ed. Essex, England: Pearson education limited, 2015. [Online]. Available: https://www.academia.edu/44041523/Finite_Element_Analysis_Theory_and_Application_with_ANSYS_Global_Edition

[49] O. Zienkiewicz and Y. Cheung, “The Finite Element in Structural and Continuum Mechanics,” *McGraw-Hill Publishing Coy Ltd, London*, p. 148, 1967.

[50] E. Madenci and I. Guven, *The Finite Element Method and Applications in Engineering Using ANSYS®*, 2nd, Ed. Boston, USA: Springer US, 2015. [Online]. Available: http://link.springer.com/10.1007/978-1-4899-7550-8

[51] SimuTech Group, “Nuclear Power Generation,” 2020. [Online]. Available: https://www.simutechgroup.com/fea-cfd-nuclear-power-generation

[52] T. M. Kathryn and T. John, *ANSYS Mechanical APDL for Finite Element Analysis*. Butterworth-Heinemann, Elsevier, 2017.

[53] K. M. Pandey and A. Sarkar, “Structural Analysis of Nuclear Fuel Element with Ansys Software,” *International Journal of Engineering and Technology*, vol. 3, no. 2, pp. 187–192, 2011.

[54] F. Liu, X.-J. Liu *et al.*, “Study on the Seismic Behavior of Nuclear Pipes by Using FEM,” *Advances in Engineering Research (AER). 3rd Annual International Conference on Mechanics and Mechanical Engineering (MME 2016)*, vol. 105, pp. 0–5, 2017.

[55] V. H. S. Souza, A. A. R. Santos *et al.*, “Evaluation of the interaction between a harvester rod and a coffee branch based on finite element analysis,” *Computers and Electronics in Agriculture*, vol. 150, pp. 476–483, july 2018.

[56] Y. Meng, J. Wei *et al.*, “An ANSYS/LS-DYNA simulation and experimental study of circular saw blade cutting system of mulberry cutting machine,” *Computers and Electronics in Agriculture*, vol. 157, pp. 38–48, feb 2019.

[57] F. S. Sarikurt, “Simulating a Salt-Cooled Reactor for Safety,” 2020. [Online]. Available: https://www.ansys.com/about-ansys/advantage-magazine/volume-xiv-issue-1-2020/simulation-salt-cooled-reactor

[58] D. Jankovics, H. Gohari *et al.*, “Developing Topology Optimization with Additive Manufacturing Constraints in ANSYS,” *ScienceDirect*, vol. 51, no. 11, pp. 1359–1364, 2018. [Online]. Available: https://doi.org/10.1016/j.ifacol.2018.08.340

[59] L. O. Alcalá, “Comparision between ANSYS and ABAQUS using ultrasonic guided waves,” Ph.D. dissertation, École de Téchnologie Supérieure, Montréal, Canada, July 2014. [Online]. Available: https://core.ac.uk/download/pdf/41816196.pdf

[60] E. Hansen, N. Ehlers *et al.*, “Developing an Interface between ANSYS and Abaqus to Simulate Blast Effects on High Security Vehicles,” *The Eighth International Conference on Advances in System Simulati*, pp. 73–76, 2016.

[61] ANSYS Inc., “Theory Reference for the Mechanical APDL and Mechanical Applications - Release 12.0,” pp. 1–1226, April 2009.

[62] R. Kilian and R. Keim, “Ageing Management review to support Long-term operation for KCB reactor pressure vessel internals,” *NRG Internal Report*, 2011.

[63] Oswald, “Festigkeitsnachweis der Kernumfassungsschrauben im geraden Bereich infolge mechanischer Belastungen fur den Austausch der Inconel-Schrauben durch Austenit-Schrauben,” *NRG Internal Report Archive*, 1986.

[64] F.J.Blom, “Studie binnenwerk reactorvat KCB,” *NRG Internal Report 21747/06.75689C*, 2006.

[65] Ansys Inc., “Ansys Meshing Solutions,” 2020. [Online]. Available: https://www.ansys.com/products/platform/ansys-meshing

[66] ANSYS Inc., “Mesh Quality and Advance Topics - Release 15.0,” *ANSYS Manual 2015*, p. 14, December 2015. [Online]. Available: http://200.19.248.10:8002/professores/mauro/Curso%20Ansys/Meshing_CD_16/lectures_trainee/Mesh-Intro_16.0_L07_Mesh_Quality_and_Advanced_Topics.pdf

[67] DIN 17440, “Technische Lieferbedingungen für Blech, Warmband, Walzdraht, gezogenen Draht, Stabstahl, Schmiedestücke und Halbzeug,” *NRG Internal Report*, July 1985.

[68] W. V. Maaren and W.de Koning, “Spannings analyse reactorvatflens German PWR,” *NRG Internal Report EPZ report Z 0142753 002 01*, 1985.

[69] I. Rupp, C. Peniguel, and M. Tommy Martin, “Large scale finite element thermal analysis of the bolts of a French PWR core internal baffle structure,” *Nuclear Engineering and Technology*, vol. 41, 2008.

[70] F. F. Charpin-Jacobs and S. C. van der Marck, “Neutronics calculations for the project German designed PWR bouten,” *NRG Internal Report 23329/13/122160 I&D/FC/LD*, 2013.

[71] The Engineering Toolbox, “Water - Density, Specific Weight and Thermal Expansion Coefficient,” 2003. [Online]. Available: https://www.engineeringtoolbox.com/water-density-specific-weight-d_595.html

[72] MIT, “Reynolds Number & Pipe Flow,” *MIT course on mechanical engineering*, 2002. [Online]. Available: http://ocw.mit.edu/courses/mechanical-engineering/2-000-how-and-why-machines-work-spring-2002/study-materials/TurbulentFlow.pdf

[73] M. Howard, “Six Methods for Calculating Application Thermal/Heat Load,” Applied Thermal Control, United Kingdom, Tech. Rep., 2018.

[74] Power Reactor Information System (PRIS), “PWR, Netherlands,” International Atomic Energy Agency, 2020.

[75] P. Hania, “MSR IRRADIATION PROGRAM AT NRG PETTEN,” *MSR Workshop, ORNL, US*, p. 28, 2018. [Online]. Available: https://msrworkshop.ornl.gov/wp-content/uploads/2018/10/MSR2018-presentation-Hania-NRGEU.pdf

[76] P.J. Baas, “Introduction- High deformed elements,” *NRG Report Archive*, 2019.

[77] ANSYS.inc, “ANSYS advanced analysis techniques guide,” *Ansys Help*, pp. 724–746, 2007.

[78] S. Birnie and J. K. Lamonby, “Pressurised water reactor operation,” *Federal Ministry for the Environment, Nature Conservation and Nuclear Safety (BMU)*, vol. 28, pp. 74–76, 1997.

[79] World Nuclear Association, “Research Reactors,” 2020. [Online]. Available: https://www.world-nuclear.org/information-library/non-power-nuclear-applications/radioisotopes-research/research-reactors.aspx

[80] International Atomic Energy Agency, “The applications of research reactors,” *Nuclear Energy Series*, p. 115, 2014.

[81] P. Ageron and G. Denielou, “Swimming-pool nuclear reactor,” Nuclear Science Abstact Series, july 1966.

[82] J. Ahlf, “The High Flux Reactor Petten, Present Status and Prospects,” Institute for Advanced Materials Joint Research Centre, Petten, The Netherlands, Tech. Rep., 1990. [Online]. Available: https://inis.iaea.org/collection/NCLCollectionStore/_Public/36/023/36023802.pdf?r=1&r=1

[83] World Nuclear News, “Molten salt irradiation test completed at Petten,” 2019. [Online]. Available: https://www.world-nuclear-news.org/Articles/Molten-salt-irradiation-test-completed-at-Petten

[84] Lam S.K., “Pressurized Water Reactor Simulator Manual,” International Atomic Energy Agency, Vienna, Tech. Rep., 2005. [Online]. Available: https://www-pub.iaea.org/MTCD/Publications/PDF/TCS-22_2nd_web.pdf

[85] John Edward Akin, *Finite element analysis concepts: via solidworks*, illustrated ed. Wspc, 2010.

[86] Sarah Harman, “NUCLEAR 101: How Does a Nuclear Reactor Work?” office of Nuclear Energy, May 2020. [Online]. Available: https://www.energy.gov/ne/articles/nuclear-101-how-does-nuclear-reactor-work

Appendix A

Snippet Code

```
!   Commands inserted into this file will be executed just prior to the ANSYS SOLVE command.
!   These commands may supersede command settings set by Workbench.

!   Active UNIT system in Workbench when this object was created:  Metric (m, kg, N, s, V, A)
!   NOTE:  Any data that requires units (such as mass) is assumed to be in the consistent solver unit system.
!               See Solving Units in the help system for more information.


*DIM,convection_TABLE,TABLE,2,11,,y,time,,0
*SET,convection_TABLE(1,0,1),-0.3,2.32,                ! Y
*SET,convection_TABLE(0,1,1),18000, 30,50.26,          ! Y and Time 1st case
*SET,convection_TABLE(0,2,1),20400,30,50.26,           ! Y and Time 2 case
*SET,convection_TABLE(0,3,1),21600, 47.1, 67.36,       ! Y and Time 3 case
*SET,convection_TABLE(0,4,1),22200,50,70.26,           ! Y and Time 4 case
*SET,convection_TABLE(0,5,1),25200,94.7,114.96,        ! Y and Time 5 case
*SET,convection_TABLE(0,6,1),28800,144.5,164.76,       ! Y and Time 6 case
*SET,convection_TABLE(0,7,1),32100,171.8,192.06,       ! Y and Time 7 case
*SET,convection_TABLE(0,8,1),32400,194.2,  214.46,     ! Y and Time 8 case
*SET,convection_TABLE(0,9,1),36000, 243.9,264.16,      ! Y and Time 9 case
*SET,convection_TABLE(0,10,1),39600,293.6, 313.86,     ! Y and Time 10 case
*SET,convection_TABLE(0,11,1),43200, 307.4,  327.66,   ! Y and Time 11 case


SHPP,ON



SF,SELECTION,CONV,22500,%convection_TABLE%

SF,BAFFLE,CONV,22500,%convection_TABLE%
```

Figure A.1: Snippet code for height, time, and temperature

Appendix B

Pressurized Water Reactor (PWR)

PWRs are the most common type of reactor accounting for two-third of current equipped nuclear generating capacity worldwide. It was originated as a submarine power plant and used water as coolant and moderator. The research and development work was performed by the Knolls Atomic Power Laboratory and the Westinghouse Bettis Laboratory. As a result of this research and development work, commercial PWRs were designed and developed for nuclear power plant applications [84]. Eventually, several commercial PWR suppliers emerged such as Westinghouse, Siemens in Germany, and Framatome in France. A PWR has fuel assemblies of 200-300 rods each, arranged vertically in the core, and a large reactor may have about 150-250 fuel assemblies with 80-100 tonnes of uranium [27]. The PWR design has two separate circulation arrangements for the turbine and the reactor: the primary and the secondary coolant circuits. The primary circuit transfers the water (coolant) through the reactor core. In the core, fuel rods transfer the energy released by fission, heating the water from 291 ^oC to 325 ^oC as it a closed loop. The reason why water does not boil at this temperature is that the core is kept pressurised to about 157 atm, and the steam maintains the pressure in a pressure tank [78].

The heated water then flows from the core into the tubes of the steam generator. The heat is transferred to the water around the tubes in the secondary system. After the heat is transferred in the steam generator, the cooled water in the primary system is pumped back into the core. As the pressure on the secondary circuit is only around 64.5 bar, the feedwater evaporates here at around 280.5 ^oC. This evaporation produces steam, which is then passed to the turbines. These turbines are connected to a generator that converts the kinetic energy (rotational energy) into electricity. Coldwater, flowing through the tubes in the condenser, removes excess heat from the steam, which allows it to condense. The water is then pumped back into the primary circuit for reuse, and the process is repeated. The main reason to have two circuits (primary and secondary) in PWR is to separate the water that is boiled in the steam generator from the fission process, and so it does not become radioactive. Some plants use water from the river, lakes to cool the system, while others use tall cooling towers [78]. Schematic view of a pressurized water reactor is shown in Figure B.1.

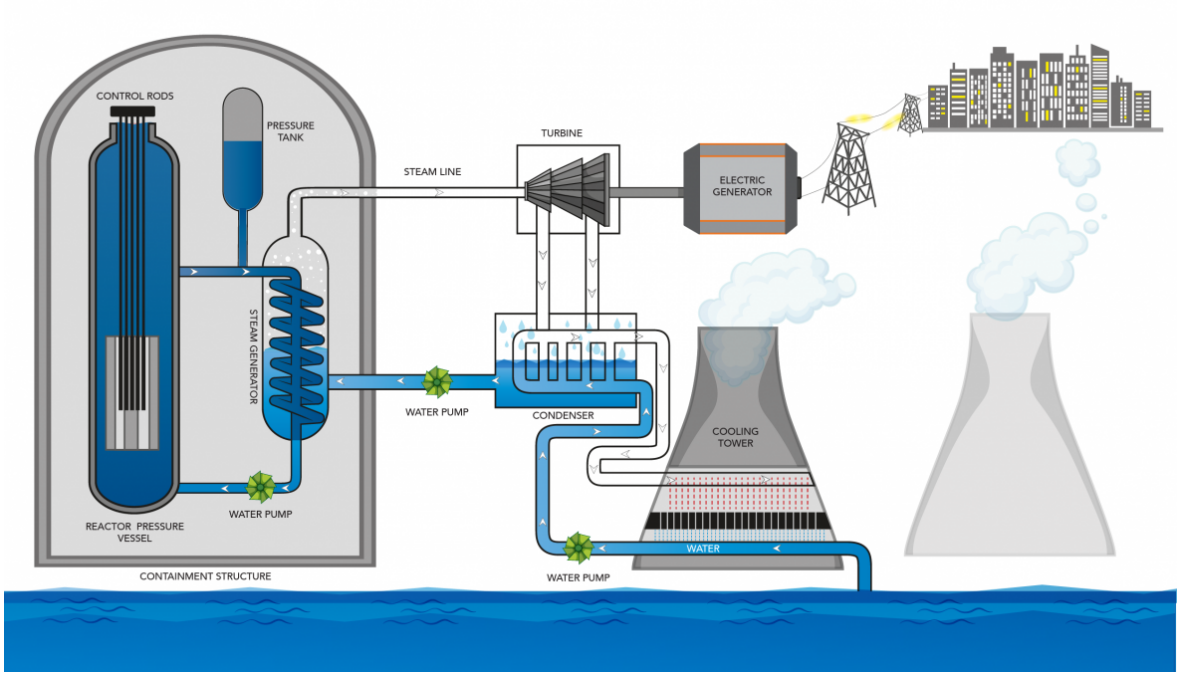

Figure B.1: Pressurised Water Reactor [86]

Appendix C

Small Portion of Code for Manual Mesh Rezoning

```
!!!!Adaptive settings!!!!!!!

esel,s,type,,2
cm,cm222,elem
allsel

cnvtol,f,,1e-3
cnvtol,u,-1
cnvtol,heat,,1e-3

nlad,cm222,add,mesh,shape,145  !nlad with mesh-quality-based criterion
nlad,cm222,add,energy,mean,1
nlad,cm222,on,,,1,0,1

nlmesh,nlay,100                !no. of sculpting layers
nlmesh,grad,0                  !option for mesh gradient control
nlmesh,srat,1                  !control global sizing of new mesh
```

Figure C.1: Portion of Mechanical APDL code